Cape Peninsula
University of Technology

Process design for the up-scale zeolite synthesis from South African coal fly ash

By

P.W Du Plessis

Dissertation submitted in fulfilment of requirements for the degree

Master of Technology: Chemical Engineering

In the FACULTY OF ENGINEERING

At the Cape Peninsula University of Technology

Supervisor: Ass. Prof. T.V. Ojumu

Co-supervisor: Ass. Prof. L.F Petrik

Cape Town Campus

March 2014

DECLERATION

I, Pieter Wynand du Plessis, declare that the contents of this thesis represent my own unaided work, and that the thesis has not previously been submitted for academic examination towards any qualification. Furthermore, it represents my own opinions and not necessarily those of the Cape Peninsula University of Technology.

Signed_____ **Date**_____

ABSTRACT

In South Africa only 5% of the coal fly ash produced annually by power stations finds use. Due to the high quantities of Si and Al in the coal fly ash researchers have explored the opportunity to use the fly ash as a feedstock in zeolite synthesis. Two principal methods have been successfully employed on a micro scale namely the 2-step method and fusion assisted method. However, in order to scale-up these processes some fundamental process design changes are required. Fly ash contains various elements including highly toxic elements such as As, Pb and Hg. The fate of these elements during the synthesis processes is not known. Both these processes generate large quantities of liquid supernatant waste. Disposal of these wastes would be expensive and environmentally harmful, thus making these processes industrially unfeasible. The well known fusion assisted process, contains an energy intensive fusion step operating at 550 °C. Construction and operation of a furnace to implement fusion would be too expensive on an industrial scale. The 2-step method has a time consuming pre-hydrothermal treatment step (aging step). In order to improve the feasibility of the 2-step process the processing time of the aging step needs to be reduced. In order to breach the scale gap between micro and pilot plant scale a principal reactor design has been suggested. However, to date, no consideration has been given to the safety and operational reliability of this design. A HAZOP study is required to prevent costly incidents from occurring during the operation of this reactor. The aim of this study formed part of the overall initiative to scale-up the synthesis of zeolites to pilot and ultimately do at industrial scale. The aim of this study specifically was to perform some principal process design activities in order to prepare these processes for scale-up. The objectives were to perform material balances on the two principals synthesis approaches in order to determine the distributional fate of elements. Secondly, to make critical process design changes and develop protocols whereby the supernatant waste resulting from these processes can be minimised. Thirdly, to replace the fusion step (used in the fusion assisted process) and the aging step (used in the 2-step process) with a short high intensity sonochemical treatment step. Lastly, to perform a HAZOP study on the principal bench scale reactor design, and make design changes based on the outcome of the study.

Material balances illustrated that most of the elements originating from the coal fly ash (Fe, Mn, Mg, Ca, Ti, Ba, Ce, Co, Cu, Nb, Ni, Pb, Rb, Sr, Y and Zn) do not leach out into solution during either of the two synthesis approaches. This was due to the CaO content in the ash retarding the mobility of these elements. This meant that during the 2-step process these elements reported to the overall zeolite product but did not form part of the zeolite crystal structure. On

the other hand, during the fusion assisted process these elements reported to the solid residue waste. The yield efficiency of the fusion assisted process was found to be poor with only 19.6% of the Si and 21.6% Al reporting to the zeolite A product. The 2-step process on the other hand incorporated 72.2% of the Si and 81.5% Al into the zeolite product. However, the 2-step process produced a mixed phase zeolite product while the fusion assisted process produced a pure phase zeolite A product. Therefore there is a trade-off between yield efficiency and product purity. It was found that the liquid supernatant waste produced during both the synthesis processes contained toxic elements such as As, Pb, Hg, Al and Nb. This highlighted the importance to minimise the liquid supernatant waste generated. The waste minimisation studies illustrated that the liquid supernatant waste can be recycled while still producing highly crystalline zeolite products, in both the synthesis approaches. During the 2-step process the supernatant waste was recycled as a source of NaOH. By recycling the waste it was found that 40% of the supernatant could be recycled. However, by making a minor process design change a protocol was developed whereby 100% of the supernatant waste could be recycled. Also, by recycling the liquid waste, zeolite analcime became the dominant phase due to the accumulation of Si in the waste. In the fusion assisted process, protocols were developed whereby the liquid supernatant waste was recycled as a source of water. It was found that 100% of the supernatant could be recycled without compromising the relative crystallinity and purity of the zeolite A product. Both the fusion step (used in the fusion assisted approach) and the 48 hr aging step (used in the 2-step process) could be replaced with 10 min of sonochemical treatment. It was found in both cases that the introduction of ultrasound, during the pre-hydrothermal stage, increased the rate of crystal formation during the hydrothermal treatment step. It was also found that by replacing the high temperature fusion step, in the fusion assisted process, the required hydrothermal treatment temperature could be reduced to 90 °C. By introducing sonochemical treatment in these two synthesis approaches their synthesis time and energy demands could be reduced successfully. A HAZOP study on the principal bench scale reactor design enabled design changes to be made preventing future loss during operation. A final optimised reactor design was proposed based on the outcome of the HAZOP study. This study effectively prepared both zeolite synthesis approaches for up-scale operation. Scale-up of this process will reduce disposal of coal fly ash offering relief to the financial and environmental strain caused to the country.

DEDICATION

This thesis is dedicated to my four closest family members for their support throughout my tertiary education:

- Ruth du Plessis (Mother)
- Lisel Dryden (Sister)
- Sean Dryden (Brother in law)
- Desiree du Plessis (Sister)

ACKNOWLEDGEMENTS

I would like to thank the following parties who contributed towards the completion of my thesis:

- My supervisor, Professor T.V Ojumu, for his continues support and insight throughout my research. Also for the opportunities he has provided me to present my research on an international level. I would like to acknowledge his excellent supervisory knowledge, support, insight, assistance, advice and guidance.

- My co-supervisor, Professor L.F Petrik, for her support and guidance throughout the duration of my MTech research. For her prompt responses to queries and questions. Lastly, for all her critical input to my thesis and research work.

- Dakalo Mainganye for his help in analysis, guidance, mentoring and valuable advice.

- Dineo Kadi for her assistance in lab work, data acquisition and analysis.

- Joseph Kapala for his help in lab work.

- Hannalene Small for her assistance in ordering chemicals and equipment. Also for her valuable advice, support and motivation.

- Alwyn Bester for his help in fabrication of equipment and maintenance work. Also for his advice, support and motivation.

- Ilse Wells from UWC (ENS department) for performing ICP-AES analysis on all my liquid samples.

- Tanya Dreyer from UCT (Geology department), for her help on XRD analysis. Also, for her quick replies on queries, this made XRD analysis quick and efficient.

- Miranda Waldron from UCT (Physics department) for her help in SEM analysis.

- Nicholas Musyoka for his input and guidance.

- My close family for their love, support, patience, motivation and guidance. For always believing in me and inspiring me.

- The ENS group at UWC for their friendly welcome into their group and their support.

- J.E Hums for his valuable advice and guidance.

- All my postgraduate colleagues for their support, motivation and friendship.

- CPUT and ESKOM for the funding provided towards this research.

- Lastly, to my friend, Jules Lind. For his inspiration, motivation, friendship and support the past 7 years. For his “never give up’ attitude which helped me throughout my studies.

TABLE OF CONTENTS

LIST OFFIGURES

LIST OF TABLES

LIST OF EQUATIONS

LIST OF SYMBOLS AND ABBREVIATIONS

Symbol	Description	Units
English symbols		
d	Inter-planar spacing	nm
Greek symbols		
η	Integer	-
γ	X-ray wavelength	nm
θ	X-ray wave incident angle	Degrees
Abbreviation Meaning		
Å	Angstrom	
A	Zeolite A	
Al	Aluminium	
AMD	Acid Mine Drainage	
Ana	Analcime	
As	Arsenic	
ATR	Attenuated total reflectance	
Ba	Barium	
Be	Beryllium	
Ca	Calcium	
cm	Centimetre	
CMW	Cirumneutral mine water	
Cd	Cadmium	

Ce	Cerium
Co	Cobalt
Cr	Chromium
Cu	Copper
FA	Fly ash
Fe	Iron
FTIR	Fourier transform infrared spectroscopy
Hr	Hour
H	Hematite
Hg	Mercury
HS	Hydroxysodalite
HT	Hydrothermal treatment
ICP-AES	Inductively coupled plasma atomic emission spectrometry
IZA	International zeolite association
JCPDS	Joint Committee on Powder Diffraction KOH Potassium hydroxide
K	Potassium
Li	Lithium
LOI	Loss on ignition
M	Mullite
Mag	Magnetite
Mg	Magnesium
Mn	Manganese

Mo	Molybdenum
NaOH	Sodium hydroxide
Nb	Niobium
Ni	Nickel
O	Oxygen
P	Zeolite Na-P1
Pb	Lead
PBU	Primary building units
ppm	Parts per million
Q	Quartz
Rb	Rubidium
rpm	Revolutions per minute
SBU	Secondary building units
SEM	Scanning electron microscope
Si	Silicon
Sr	Strontium
Th	Thallium
Ti	Titanium
V	Vanadium
Y	Yttrium
Zn	Zinc
Zr	Zicronium

CHAPTER 1

1 Introduction

1.1 Background

South Africa is still in a developing stage and naturally the country's decisions and core operations are focused on economic growth. Sustainability and environmental considerations receive attention. However, in the modern world economic growth cannot be separated from the environment. South Africa is largely dependent on coal as energy source. Statistics indicated that during 2009 South Africa consumed 170.5 Mt of coal (NationMaster, 2011). Coal, in South Africa, is mainly used in the generation of electricity (Eskom, 2011b). Other than heat, the combustion of coal generates incombustible products known as coal combustion by-products. Of these products, fly ash are among the finer particles that are entrained in the flue gas of the boilers and collected in electrostatic precipitators (Hower *et al.*, 1996; Scheetz and Earle, 1998). With focus placed on economic growth the country exports high grade coals and use low grade coal in the generation of electricity. The low grade coal has a significantly higher ash content which results in the production of enormous amounts of fly ash each year. On average 36 Mt of fly ash is generated by Eskom (Eskom, 2011a), South Africa's main power utility supplier. This waste product needs to be disposed safely in ash dams or dumps, which requires large vacant land. With the country's increasing energy demands this is becoming an increasingly expensive operation placing severe economic strain on the country. Currently only 5% of coal fly ash generated annually is utilized (Eskom, 2011a). This 5% is mainly used in the building industry which in turn depends solely on industrial and residential expansion. For this reason alternative uses for this waste product has been investigated.

Due to the high Al and Si content of coal fly ash, increasing focus has been placed on the synthesis of zeolites from fly ash (Yang and Yang, 1998). Zeolites are alumina-silicate crystalline structures consisting of AlO_4 and SiO_4tetrahedrally linked together by oxygen atoms (Auerbach *et al.*, 2003b; Molina and Poole, 2004). What makes zeolites so valuable is their vast amount of uses due to their unique properties such as high cation exchange capacity, uniform pore sizes, their ability to sieve molecules of certain sizes and their ability to act as catalyst (Querol *et al.*, 2007; Querol *et al.*, 2002; Somerset *et al.*, 2004). The process of synthesizing zeolites is complex and numerous studies proved that the synthesis conditions greatly affect the type and purity of zeolites formed (Auerbach *et al.*, 2003b; Bebon *et al.*, 2002; Cundy and Cox,

2005; Pfenninger, 1999). Most studies to date have been performed on microscale. The composition of fly ash differs with varying combustion conditions (Bebon *et al.*, 2002). For this reason the first step in the scale-up of zeolite synthesis is to optimize the conditions on a micro scale. In 2012 Mainganye illustrated that the mineralogy of South African fly ash is inconsistent (Mainganye, 2012). In recent studies South African coal fly ash was successfully converted into zeolites A, Na-P1, X and sodalite(Musyoka *et al.*, 2012b; Musyoka *et al.*, 2011a; Musyoka *et al.*, 2012c). The authors used two principal processing routes to obtain these zeolite products namely the 2-step process and the fusion assisted method. The process conditions for these synthesis routes were successfully optimized by the authors on a micro scale. The 2-step process consists of an aging step operated at 47 °C for 48 hours followed by hydrothermal treatment at 140 °C. In the fusion assisted process however, fly ash is first fused with NaOH at 550 °C after which Si and Al is extracted from the fused ash followed by hydrothermal treatment. Design of a pilot and/or industrial scale processes to produce these valued products is important to the development of this country.

Before these two synthesis routes can be scaled up, fundamental process design engineering activities need to be performed. The first activity is to perform a material balance which is critical to sizing the required scale-up reactor. Fly ash contains various elements originating from the raw coal including toxic elements such as As, Pb and Hg. An elemental balance is required to determine the distributional fate of these elements. This is vital information since disposal of waste is closely monitored and governed by legislation.

Both synthesis routes suffer the same fate with respect to waste generation. The large amounts of liquid waste produced during the synthesis of zeolites would require disposal. This makes these processes environmentally problematic and disposal would require costly pre-treatment. This contradicts the purpose of the zeolite synthesis system i.e. reduce the cost of waste disposal. Before an upscale system can be considered, the waste generated during synthesis should be minimised dramatically to make the process feasible.

The fusion assisted process makes use of an electrical furnace operating at 550 °C. This energy intensive process would be likely very expensive to operate on an industrial scale. Other than the energy needs it creates, the construction of a purpose built furnace would also likely be too expensive and space consuming to Eskom. Process design changes are required to replace this energy intensive step. In a recent study, sonochemical treatment was employed in the synthesis of cancrinite from coal fly ash (Musyoka, 2012). In light of the success of this study it

was deemed fit to make process changes whereby the fusion step could be replaced with sonochemical treatment. The 2-step process suffers from a similar fate as the fusion assisted method. The pre-hydrothermal treatment step (aging) continues for 48 hours. Although it does not operate at such a high temperature, its processing time is 46.5 hours longer. The opportunity to replace this step with high intensity sonochemical treatment needs to be investigated.

To bridge the gap between micro scale operation and pilot scale, a principal reactor design was suggested. However, the safety and operational soundness of this design has not been assessed. Before this reactor design could be fabricated, a hazard and operability study (HAZOP) was required on the principal design. A HAZOP study is critical to ensure safe and reliable operation of this bench scale design.

This study investigated some of the core process design aspects of the synthesis of zeolites from South African coal fly ash. It attempted to improve the feasibility of the process design while providing vital process data required for environmental legislation purposes. It also attempted to provide an optimized reactor design whereby the gap between micro and pilot scale can be closed.

1.2 Problem statement

With South Africa's growing economy the country's energy demands has risen to unprecedented levels. Therefore, finding alternative uses for the large volumes of coal fly ash generated need to be investigated before it becomes too expensive to dispose. Two synthesis routes, whereby fly ash is converted into zeolitic products, have been successfully employed on micro scale namely the 2-step method and fusion assisted process. The problem however, with both these processes, is that enormous volumes of liquid waste are generated during these processes. The fusion assisted process also makes use of an energy intensive step which is not economically sound for scale-up purposes. The 2-step process suffers from a time consuming aging step which needs to be shortened in order to promote its feasibility. Fly ash contains various elements; the distribution of these elements between the zeolite products and wastes is not known. It is vital that the destination of these elements is known for disposal considerations, which is governed by South African law. Lastly, a preliminary reactor design was suggested for a bench scale operation in order to close the operational gap between micro scale and pilot scale synthesis. However, no consideration has been given to the safety and operational reliability of the design.

1.3 Objectives and research questions

This study forms part of the overall initiative to study the scale-up opportunity of the synthesis of zeolites from South African coal fly ash. The aim of the initiative is to scale-up the process to pilot plant scale and ultimately industrial scale. The aim of this study was to apply the fundamental process design engineering principals to the processes with the view to developing a database necessary for design of scale-up operation. The objectives of this study were to:

- Perform a material balance on both the 2-step and fusion assisted synthesis process to determine the distributional fate of elements originating from fly ash.
- Make process design changes and develop protocols whereby the liquid supernatant waste, resulting from the 2-step process, can be minimised.
- Develop waste minimisation protocols whereby the liquid supernatant waste, resulting from the fusion assisted process, can be minimised by means of recycling.
- Improve the feasibility of the fusion assisted process by incorporating sonochemical treatment in the process design.
- Reduce pre-hydrothermal treatment (aging) time of the 2-step process by incorporation of sonochemical treatment.
- Perform a HAZOP study on the principal bench scale reactor design and make design changes based on its outcome.

During this investigation the following questions were attempted to be answered:

- What are the weights of the respective products and wastes produced during the synthesis of zeolites in both principal processes?
- What is the fate of elements originating from fly ash during the synthesis of zeolites in both the 2-step and fusion assisted process?
- Can the liquid supernatant waste be recycled in the two principal synthesis approaches while still synthesizing high quality zeolitic products?
- What are the implications of using sonochemical treatment on the high temperature fusion step and the time consuming aging step?
- What is the optimum bench scale reactor design, after all safety and operability hazards have been taken into account?

1.4 Significance of investigation

By utilizing fly ash in the synthesis of zeolite products, the environmental burdens that fly ash places on South Africa will be relieved. The synthesis of this high value product from a waste product also has the potential of generating economical growth by firstly reducing the cost of fly ash disposal, and secondly creating the potential to sell a zeolite product. Studies have shown that the cost of zeolite synthesis from fly ash is one fifth of the commercial zeolite production cost (Ojha *et al.*, 2004). Since Eskom has a direct influence on the South African economy it will ultimately benefit the country as a whole. By utilizing more fly ash it will also prevent the use and contamination of vacant land, which can be used for more constructive purposes. By applying the principal process design operations on a micro scale it will be possible to avoid great financial loss and ensure consistent reliable process operations on a larger scale. Also, by performing material balance studies the required data will be available to continue with the detailed design phases of the initiative. Lastly, this study will greatly improve the feasibility of these synthesis processes.

1.5 Delineations

Since the first attempts to convert fly ash into zeolites in 1985 (Höller and Wirsching, 1985), various different synthesis techniques have been developed. However, this study will be limited to the two principal approaches applied specifically to South African Coal fly ash i.e. 2-step and fusion assisted method.

An energy balance is required in order to quantify the energy demands of the synthesis system. However, due to the small scale of the experiments performed during this investigation and the lack of specialized equipment it may be inaccurate. It is recommended that an energy balance be performed on the bench scale reactor system. This reactor design will be equipped with specialized measuring and sensor instruments, as recommended in chapter 8.

During the synthesis processes two liquid wastes are produced. The most problematic waste is the supernatant which is the most concentrated in various elements. The second liquid waste is the water recovered after washing the zeolites. This study will focus only on the supernatant waste. It is recommended that future studies should consider a whole new approach towards cleaning the zeolite product. Therefore, minimizing the washing water waste at this stage would be a waste of research time and expenditure.

1.6 Outline and structure of thesis

This thesis was prepared in article based format. However, in order to reduce repetition of results and methodologies in chapters 4-7, references are made to chapter 3 in these chapters instead of repeating data. Chapter one is the introduction to the thesis, introducing the reader to the background of the investigation. Chapter two is a review of the literature required to clarify and support the background and all results obtained throughout the study. Chapter three to seven consists of 5 separate articles either published, submitted for publication or ready for submission. These chapters each contains an introduction, methodology, results, discussion and chapter summary. Chapter eight illustrates the HAZOP study performed on the principal bench scale reactor design. This study is the only investigation not prepared in article format as it won't be published. In chapter 9 overall conclusions are drawn from the thesis and recommendations for future work are discussed.

Chapter three, titled "Distributional fate of elements during the synthesis of zeolites from South African coal fly ash", covers the overall and elemental balances performed on both principal zeolite synthesis routes. In this section the distributional fate of elements originating from coal fly ash during zeolite synthesis is determined. This article is ready for submission.

Chapter four covers the waste minimisation study that was performed on the 2-step synthesis approach. This article has been published in the journal MDPI Materials on 29 April 2013. In this study, protocols were developed whereby 100% of the liquid supernatant could be recycled. In chapter five the supernatant waste resulting from the fusion assisted process is minimised. This article is ready for submission. This chapter also takes into account the lessons learnt from the previous waste minimisation study in order to develop a general approach towards waste minimisation.

In chapters six and seven, both articles ready for submission, sonochemical treatment is introduced in both the 2-step and fusion assisted process in order to improve their feasibility. In chapter six, attempts are made to replace high temperature fusion with a short sonochemical treatment step. In chapter seven the aging step, used in the 2-step method, is replaced with sonochemical treatment to drastically reduce the overall synthesis time.

Lastly, Appendix A, B and C illustrates supporting data and information which was not included in the articles illustrated in chapter three to seven.

CHAPTER 2

2 Literature review

2.1 Coal fly ash

2.1.1 Introduction

Generally fly ash is characterized either as natural or manmade. Natural fly ash originates from volcanoes and ocean activity; while fly ash resulting from human activity includes the generation of electricity, mining activities and fuel production. Increasing energy demands globally has yielded a dramatic increase in the use of coal in the generation of electricity. In developing country such as South Africa increasing energy demands are amplified. The generation of electricity in coal fired power stations is a relatively simple process. Coal is crushed and combusted to liberate heat which in turn is used to generate steam. The steam is used to drive a turbine which generates a potential difference. The use of coal fired power stations dates back to the 1880's over 100 years ago.

Other than volatile matter and fixed carbon, both of which are combustible, coal also contains enormous amounts of incombustible material which is referred to as the ash (Vassilev *et al.*, 1996; Vassilev *et al.*, 1997; Vassilev *et al.*, 2005; Wagner and Hlatshwayo, 2005; Yossifova, 2007; Zheng *et al.*, 2008).Different ranks of coal have varying amounts of incombustible products (Vassilev et al., 1996). During the combustion of coal in power stations these ash contents forms part of coal combustion by-products (CCP's) and are collected at several points in the combustion process. The ash products collected from these points are bottom ash, boiler slag, economizer ash and fly ash (Scheetz and Earle, 1998). Amongst these CCP's fly ash is produced on the largest scale.

Fly ash is the finer particulates that are entrained in the exhaust gases (Scheetz and Earle, 1998) and usually collected by means of electrostatic precipitators or in some cases bag house dust collectors (Hower et al., 1996). The formation of fly ash is governed by a series of complex mechanisms influenced by various physical and chemical factors making it a difficult process to control and predict (Gutiérrez *et al.*, 1993; Helble, 1994; Hurley and Schobert, 1992; Liu *et al.*, 2004). Due to its complex formation mechanism the properties of fly ash varies vastly based on various factors such as coal properties, boiler design and combustion parameters (Goodarzi, 2006; Koukouzas *et al.*, 2007; Smith *et al.*, 1998). The quantities of fly ash generated are

depicted by the ash content and feed rate of the coal used by the power station. In South Africa low grade coal is used for the generation of electricity as higher grades are exported for economic benefits. In 2010 South Africa produced 36 Mt of coal fly ash and of this only 5% could be sold (Eskom, 2011a). The surplus of this 36 Mt had to be disposed of in ash dams and dumps causing environmental and economic strain for South Africa and the national power supplier.

Although fly ash is regarded as an environmental and economical problem it has found uses such as in the building industry as a additive in cement, however these uses are low end uses (Lyer and Scott, 2001). Increasing research attention is being spent on finding alternative uses for this waste material.

2.1.2 Chemical and physical nature of coal fly ash

In general coal fly ash can be described as being spherically shaped fine glassy particles. The chemical and physical properties of coal fly ash varies immensely as a function of the class of coal burnt, type of coal, boiler operating parameters, coal preparation techniques and sampling methods (Gutiérrez *et al.*, 1993; Helble, 1994; Hurley and Schobert, 1992; Kruger, 1997; Kutchko and Kim, 2006; Liu *et al.*, 2004; Scheetz and Earle, 1998; Vassilev and Vassileva, 2007).

The morphology of fly ash has been studied in various investigations (Fisher *et al.*, 1976; Fisher *et al.*, 1983; Fisher *et al.*, 1978). In total 11 different variations in the morphology of fly ash were observed (Fisher et al., 1978). The majority of fly ashes are spherically shape. The spheres can be solid, hollow or a combination called plurospheres in which microspheres are encapsulated in larger spheres (Fisher et al., 1976). The colour of fly ash varies from grey to light grey and black(Adriano *et al.*, 1980; Ahmaruzzaman, 2010; Scheetz and Earle, 1998). The colour varies based on the concentrations of Fe_2O_3 and unburnt carbon residues in the fly ash (Alexander and Klug, 1948). Lee *at al.* illustrated how the colour tone of ash varies in a power station depending on the point where it is sampled from (Lee et al., 1999). The diameter of fly ash particulates varies from 0.5 µm to 200 µm (Scheetz and Earle, 1998), with most bituminous derived fly ash having sizes smaller than 75 µm (Ahmaruzzaman, 2010). The surface area and specific gravity of coal fly ash generally varies between 170-1000 m^2/kg and 2.1-3 respectively (Ahmaruzzaman, 2010).

It is vital to understand the details of the chemical nature of coal fly ash. The constituents of the ash influence its effects on the environment, public health, legal regulatory constraints and its

possible uses. In numerous studies it has been determined that the main constituents in fly ash are Al_2O_3, Fe_2O_3, SiO_2 and CaO(Ahmaruzzaman, 2010; Hower *et al.*, 1996; Koukouzas *et al.*, 2007; Lyer and Scott, 2001; Musyoka, 2009; Musyoka *et al.*, 2012c; Scheetz and Earle, 1998). Of these components the Si and Al species makes up the highest weight % in coal fly ash. The forms in which these Si and Al species exist have been determined by X-ray diffraction spectroscopy (XRD). Authors suggests that the majority of these species exist in an amorphous phase (Goodarzi, 2006). However a considerable amount of mineral phases exist as well such as mullite ($Al_6Si_2O_{13}$), quartz (SiO_2), magnetite (Fe_3O_4) and hematite (Fe_2O_3)(Ahmaruzzaman, 2010; Goodarzi, 2006; Koukouzas *et al.*, 2007; Lyer and Scott, 2001; Musyoka, 2009; Musyoka *et al.*, 2012c; Vuthaluru and French, 2008). The composition, morphology and mineral distribution in coal ash can vary considerably with change in combustion conditions (Vuthaluru and French, 2008).For this reason the chemistry of fly ash varies from power plant to power plant as was illustrated for South African coal fly ashes (Musyoka, 2009; Musyoka *et al.*, 2012c). It was has been shown that the chemistry of the ash from the same power plant can differ dramatically from one batch of fly ash to another(Mainganye, 2012). This makes it very difficult to predict the properties of fly ash in it mass production from electricity generation in order to develop uses for this waste substance. Wagner and Hlatshwayo (2005) determined that a series of trace elements exist in South African coals used in power plants. These elements are concentrated mostly in the fly ash during the combustion process due to the physical characteristics of this finer ash (Bhanarkar *et al.*, 2008; Nathan *et al.*, 1999; Pandey *et al.*, 2011; Reto *et al.*, 2003). Figure 2-1 below illustrates the Meij's classification scheme explaining the distribution of elements in coal ash based on volatility (CCSD, 2009). According to Goodarzi (2006) the elements from groups 1 and 2, which are less volatile components, are concentrated in the amorphous layer of coal fly ash.

Group 3: Highly volatile at least partially enriched in the gas phase depleted in the condensed phases.

Group 2: Volatile which are enriched in the fly ash depleted in bottom ash.

Group 1: Low volatility being evenly distributed between fly ash and bottom ash.

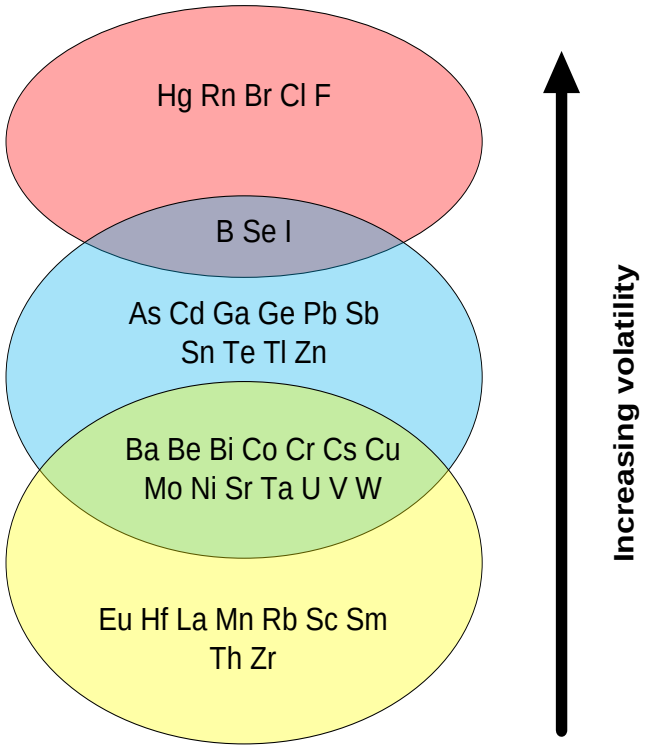

Figure 2-1: Meij's classification of elemental distribution from coal into emitted particulates.

2.1.3 Classification of fly ash

Table 2-1, derived from Scheetz and Early (1998), illustrates the ASTM standard C618 – 95 classification of fly ash into two broad groups namely class F and C. Class C fly ash exhibits cementitious characteristics (Kruger, 1997)and the sum of the weights of SiO_2, Al_2O_3 and Fe_2O_3 ranges between 50 and 70% of the total fly ash weight. This class of ash usually results when combusting sub-bituminous and lignite coals (Alonso and Wesche, 1991). Class F ash on the other hand exhibits pozzolanic characteristics (Kruger, 1997) whereby the Al and Si constituents react with CaO in the presence of water to form calcium silicate hydrate (Lyer and Scott, 2001), which is a component of Portland cement. In this class of fly ash the weights of SiO_2, Al_2O_3 and Fe_2O_3 usually exceeds 70% of the total fly ash weight. This class of ash is commonly generated from South African power stations (Mainganye, 2012; Musyoka, 2009; Musyoka *et al.*, 2012c) which is a result of burning lower grade coals including bituminous and anthracite coal (Alonso and Wesche, 1991).

Table 2-1: Fly ash classification based upon ASTM standard C618 – 95.

Properties	Fly Ash Class	
	Class F	Class C
Silicon dioxide (SiO_2) +aluminium oxide (Al_2O_3) +iron oxide (Fe_2O_3), min,(%)	70	50
Sulphur trioxide (SO_3), max, %	5	5
Moisture Content, max, %	3	3
Loss on ignition, max, %	6	6
Available Alkalis (as NaOH) max. %	1.5	1.5

2.1.4 The impacts on the environment caused by fly ash

As mentioned before, the trace elements from the coal used in combustion are concentrated on the fly ash surface in the amorphous phase when the fly ash has cooled down (Bhanarkar *et al.*, 2008; Goodarzi, 2006; Liu *et al.*, 2004). Amongst these elements are highly toxic components, as was found in South African coals (Wagner and Hlatshwayo, 2005).

The main direct concern with coal fly ash is due to its small size. Fly ash has the potential of entering the human body through inhalation to severely damage the human respiratory system (Bhanarkar et al., 2008). Silva *et al*. (2012) postulated a model whereby fly ash particles enter the respiratory system and the toxic elements then distributes through the blood system to the kidneys, liver, spleen, bone marrow, nervous system and lymph nodes. These toxins then have the potential to cause severe damage. The study on the biological effects of the toxic components in fly ash revealed that fly ash has a highly genotoxic potential due to the presence of Cr, Ni and Cu (Dwivedi et al., 2012). The concentrated heavy metals on the surface of the small ash particles has the potential to damage DNA and activate cancerous cells (Dwivedi et al., 2012). The ash therefore has to be disposed of in ash dumps and dams making large vacant land unusable (Petrik et al., 2003). The disposal of ash has become an enormous environmental and economic concern due to the extremely large quantities that need to be disposed annually.

One of the environmental concerns that have been investigated during the past decade is the question regarding leachable toxins in fly ash. The mobility of heavy metals and other toxic components has been researched by various authors (Akar *et al.*, 2012; Dosskey and Adriano, 1993; Iyer, 2002; Izquierdo and Querol, 2012; Jegadeesan *et al.*, 2008; Jones *et al.*, 2012;

Pandey *et al.*, 2011; Sočo and Kalembkiewicz, 2009; Tsiridis *et al.*, 2012). The disposal of fly ash and possible leaching of toxins from the ash could contaminate soil, ground water, aquatic ecosystems and consequently food produced (Carlson and Adriano, 1993). Although the mobility of heavy metals in most fly ashes is relatively low due to the high concentration of CaO (Akar *et al.*, 2012; Izquierdo and Querol, 2012), its long term damage may be catastrophic to ecosystems due to its continuous slow release. Due to the concentration of CaO in fly ash it also has severe effects on the pH (Izquierdo and Querol, 2012)of water aquatic systems which could have dire effects on the ecosystem. Dosskey and Adriano (1993) illustrated how heavy metals from fly ash inhibits the growth of cucumbers and found traces of the elements in the grown product.

Table 2-2: List of legislation which governs environmental management in South Africa

Legislation name	**Act number**	**Year**
The South African Constitution	108	1996
Hazardous Substances Act	5	1973
Health Act	63	1977
Environment Conservation Act	73	1989
Occupational Health and Safety Act	85	1993
National Water Act	36	1998
The National Environmental Management Act	107	1998
Municipal Structures Act	117	1998
Municipal Systems Act	32	2000
Mineral and Petroleum Resources Development Act	28	2002
Air Quality Act	39	2004
National Environmental Management: Waste Act, 2008	59	2008

The reclamation of used ash disposal sites is an extremely difficult task. The pH, toxic nature and pozzolanic nature of the ash site makes organic life impossible and yields unstable building surfaces (Haynes, 2009). With the global movements to focus on the environment and sustainability, the disposal of waste has become closely monitored and limited by legislation. In South Africa attempts are also made to minimise the effects of waste disposal on the environment. Table 2-2 (SAWIC, 2012) shows a list of legislation derived in South African law which governs the environmental management in the country. The aim of these Acts is to

provide legal grounds whereby companies, individuals and other bodies can be monitored and controlled to ensure that their activities are not harmful to the environment or public health.

For these reasons it is vital to find productive uses for fly ash which can reduce the large volumes that requires disposal annually. However, due to strict legislation, it is important to assess the fate of the toxins in fly ash when using this waste material; to prevent prosecution and economical sanctions.

2.1.5 Uses of coal fly ash

As mentioned previously, in South Africa only 5% of the total weight of fly ash produced annually is sold and finds use. This 5% is mainly used as an additive in cement and is dependent on the economic growth of the country and building industry. The addition of fly ash to Portland cement increases the strength of this vital building medium as well as increases its resistance to corrosion. Increasing research is being done on finding alternative uses for this waste product (Kruger, 1997). The following is an outline of the current and possible future uses of fly ash to supplement its current use in cement.

2.1.5.1 Treatment of acid mine drainage and other mine spoils

Acid mine drainage (AMD) refers to the production of sulphuric acid from pyritic piles left behind from coal mining activities. Pyritic material in the spoil piles react with oxygen and water to produce sulphuric acid (Vadapalli et al., 2008). This acid then pollutes the environment and leaches into the water table in rainy conditions. Due to the alkalinity of coal fly ash, which is a result of the high concentrations of CaO, it was deemed a promising material that can be used to neutralize AMD. It was proven in 2005 by Petrik *et al*. that coal fly ash can indeed be successfully applied to treat AMD. However, residual solids results from this process which requires further disposal (Gitari *et al.*, 2008; Vadapalli *et al.*, 2008). A solution to this problem was developed when it was illustrated how the solid residues resulting from AMD treatment can be used in the synthesis of zeolitic material (Petrik et al., 2003). Fly ash has been proven to be used in the remediation of other wastes produced from mining activities as well. It has been shown how sulphates can be removed from cirumneutral mine waters with the application of fly ash (Madzivire *et al.*, 2011; Madzivire *et al.*, 2010). Studies also illustrated that fly ash can be used in remediation of contaminated mine soils (Ram and Masto, 2010). Another result of mining is underground voids and tunnels supported by pillars. Older mine tunnels have caved in due to degradation of the support structures. Although modern building advances has minimised such risks, it is not advisable to leave mine voids which might cause future accidents. Due to the

large quantities of ash produced annually and its pozzolanic nature it was found to be an appropriate backfilling material for mine voids (Scheetz and Earle, 1998; Yao and Sun, 2012). The voids are filled by injecting a mixture of fly ash and soil in the tunnels which greatly reduce the risk of cave-ins.

2.1.5.2 Production of glass

An interesting new application of fly ash in the glass industry has been examined. Due to the high quantities of SiO_2 and Al_2O_3 it has been thought a viable raw material for the production of glass and glass-ceramics. It has been shown by multiple studies that it is in fact a suitable raw material to produce glass of high chemical resistivity (Erol *et al.*, 2007; Sheng *et al.*, 2003). In all studies performed it was illustrated that during vitrification and addition of NaO to the coal fly ash, the heavy metals are immobilized and solidified securely in the glass product(Erol *et al.*, 2007; Park *et al.*, 2009; Sheng *et al.*, 2003; Zhang *et al.*, 2007). With the addition of B_2O_3 and Na_2O to fly ash, borosilicate glass was successfully synthesized with properties similar to commonly used borosilicate glasses (Park et al., 2009). With variations in the amounts of NaO added to the fly ash and vitrification at lower temperatures it was also possible to synthesize chemical resistant ceramic glass (Zhang et al., 2007). However, the economic aspects of these processes still require verification.

2.1.5.3 Toxicity reduction in waste and soils

Due to the high alkalinity of fly ash it has the ability to inhibit leaching of heavy metals. It has also been studied as a possible material for the reduction of these toxic elements in waste waters and soil. A study was undertaken in 1994 in which heavy metal loaded soil was treated with varying amounts of coal fly ash (Shende et al., 1994). The authors measured the toxicity of the soil and also determined its suitability for growing crops. It was found that 5% fly ash by weight in soil was an optimum ratio in the reduction of heavy metals and improving plant growth in the contaminated soil. However, above 5% the plant growth was impeded dramatically which is similar to results reported by Dosskey& Adriano (1993). In 1998 an investigation into the reduction of heavy metals in municipal waste water by addition if fly ash was completed (Gupta and Torres, 1998). The authors reported that by treating the waste water with fly ash for 4 hours a significant reduction in toxicity was achieved. The two major elements that could be removed from the municipal waste water were Cu and Pb.

2.1.5.4 Synthesis of zeolites

Due to the high concentrations of SiO_2 and Al_2O_3 it has been found to be a suitable feedstock in the synthesis of high value zeolitic material (Höller and Wirsching, 1985; Hollman *et al.*, 1999; Molina and Poole, 2004; Moreno *et al.*, 2001; Querol *et al.*, 2002; Querol *et al.*, 1997; Querol *et al.*, 2001; Somerset *et al.*, 2005a; Somerset *et al.*, 2005b; Somerset *et al.*, 2004; Steenbruggen and Hollman, 1998; Wang and Wu, 2006). Due to the vast properties and wide range of industrial uses of zeolites, it is a promising alternative use for the large volumes of fly ash produced annually. This topic is discussed in length in section 2.2 since it is the focus of this study.

2.2 Zeolites

2.2.1 Introduction

A surprising amount of technologies that we use in our daily lives and industry was first found or deduced from nature. The use and knowledge of various technologies dates back to surprisingly historical times. Amongst these technologies are the microcrystalline materials known as zeolites. A.F Cronstedt, a mineralologist, first came across zeolites in 1756 with the discovery of the mineral stilbite. Since its first discovery, zeolite science and technology has grown immensely. Zeolites are aluminosilicate microporous crystals consisting of TO_4 (T= Si or Al) tetrahedral building blocks forming voids and pores which contain ions and water (Auerbach *et al.*, 2003c). When the tetrahedral building blocks are purely Si based the result is a neutral crystal structure since the charge on Si is +4 and is surrounded by 4 oxygen atoms, each with a charge of -1. The result of this arrangement is pure silica crystals SiO_2, which is not characterized as a zeolitic material. When one of the Si atoms in the arrangement is replace with Al, which has a charge of -3, regions are constructed with an overall negative charge. Therefore charge neutralizing extraframework ions are incorporated into the structure. Technically for a mineral to be classified as a zeolite it needs to contain the following elements (Auerbach *et al.*, 2003c):

- A framework mode connecting Al and Si with 4 oxygen atoms.
- Charge stabilizing extraframework ions.
- Water molecules or other phases absorbed in the voids.

The equation below illustrates an empirical formulae used to define zeolite types (Auerbach *et al.*, 2003c).

$$M^{m+}_{n/m} \cdot \quad [Si_{1-n}.Al_nO_2] \cdot \quad nH_2O$$

Equation 2-1

Where M refers to the charge stabilizing extraframework ions.

To date over 40 natural zeolites have been discovered and over 300 different types of synthetic zeolites produced. Zeolites, their properties and production are a well documented subject matter. A comprehensive handbook on zeolite science and technology by Auerbach *et al*. (2003b) is available and gives the reader great insight in current technologies and well documented literature on zeolites in general. The reader is encouraged to also consult a monograph published by Breck in 1974 titled “Zeolite Molecular Sieves”. The author’s monograph is regarded as the foundation for anyone seeking knowledge on the matter of zeolites and technology. Another well documented review of zeolites science and technology is a book published by Ribeiroet al. (1984) titled “Zeolites: Science and Technology”. For reference, a full list of zeolite types and structures can be found populated under “Atlas of Zeolite Framework Types” (Baerlocher *et al.*, 2001; IZA, 2012).

2.2.2 Structural chemistry of zeolite crystals

The foundation of zeolite structures are based on the basic building unit (BBU), which is a tetrahedron which consists of an atom with a low electron negativity tetrahedrally connected to 4 oxygen atoms (TO_4: T = Al or Si). Figure 2.2 illustrates a graphical representation of these basic building units. Due to the fact that Al has a charge of +3 the overall charge of its building unit is -1. The BBU’s are connected together by sharing an oxygen atom (Figure 2.3). To compensate for the negative charge surrounding the AlO_4 building units, positively charged ions are incorporated into the structure commonly referred to as extraframework cations. Figure 2-3 illustrates this concept graphically. In the figure the sodium ion is used as an example, but can be replaced by both inorganic and organic cations (Auerbach *et al.*, 2003a). The type of extraframework cations and their distribution inside the zeolite structure has a profound effect on the properties and possible uses of zeolites (Auerbach *et al.*, 2003a). The distribution of cations amongst the different negatively charged sites in zeolites have been studied to a great extend (Breck, 1974). A compilation of extraframework sites in zeolites was constructed by Mortier (1982) and published on behalf of the Structural Commission of the International Zeolite Association.

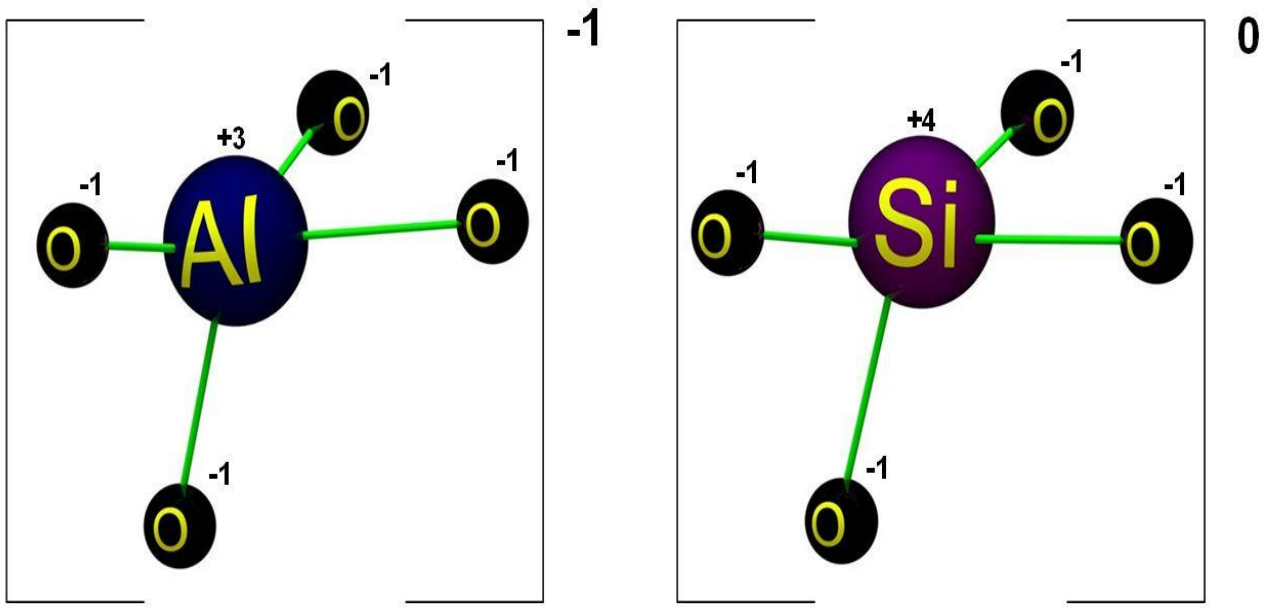

Figure 2-2: Illustration of the basic building units of zeolite structures and their respective overall charges.

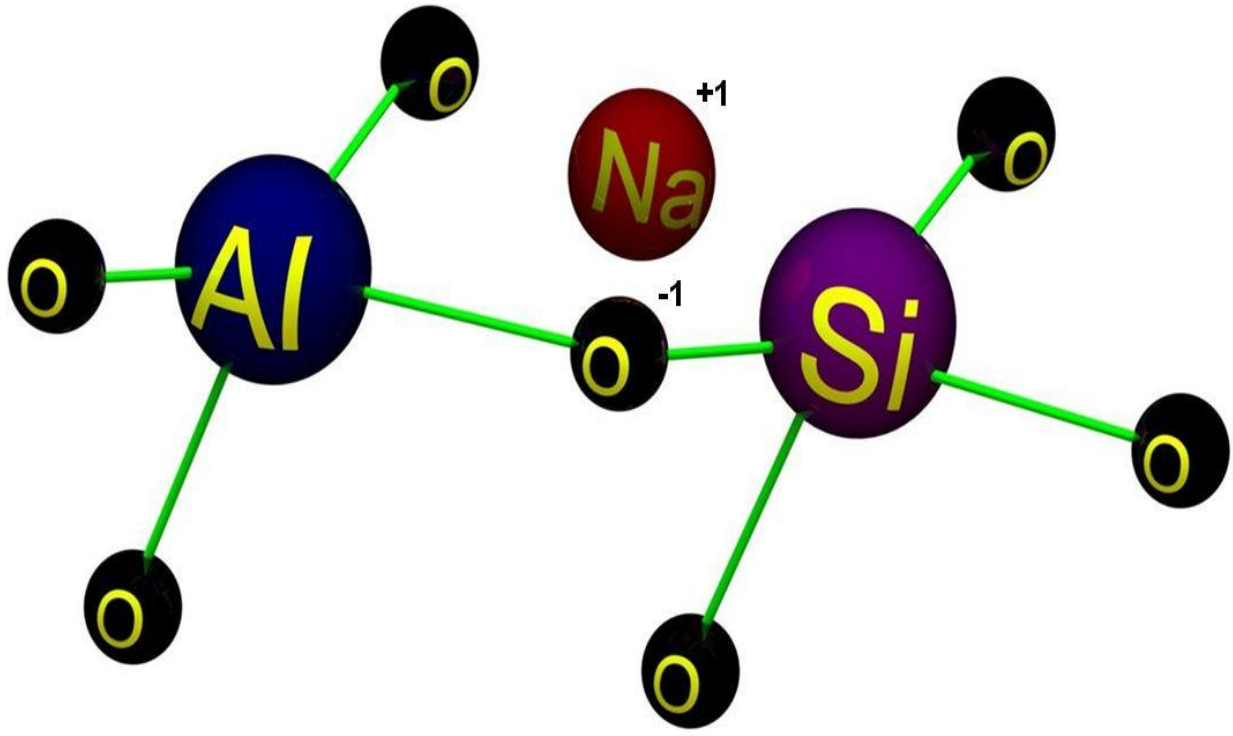

Figure 2-3: Illustration of incorporation of extraframework charge balancing ions in the zeolite structure

In a more recent publication the framework ion distribution in zeolite X and Y was reviewed by Frising and Leflaive (2008). These two zeolites are critical to industrial applications and effects of ion distribution in the structure are vital knowledge when synthesizing these structures for specific applications. In the basic building unit the O-T-O angle is almost 109°, regarded as near perfect (Auerbach *et al.*, 2003a). This angle does not change particularly and is described as a rigid body by researchers (Bartelmehs *et al.*, 1995; Dove *et al.*, 1995). It has been found that the T-O bond length differs depending on the type of tetrahedra atom (T). Researchers discovered that the bond lengths in the Si and Al tetrahedra are 1.59 – 1.64 Å (Baur, 1978) and 1.73 Å (Hill and Gibbs, 1979) respectively. The T-O-T bonds are very flexible unlike the rigidity of O-T-O bonds (Auerbach *et al.*, 2003a). These bonds are formed when the basic building units come together in a regular arrangement by sharing an oxygen atom (Byrappa and Yoshimura, 2001; Szostak, 1997; Weitkamp and Puppe, 1999). When 4 or more of these building blocks comes together a secondary building block is formed referred to as a composite building unit (CBU). Due to the flexibility of the T-O-T bond a vast number of different CBU's exist which are composed of different smaller CBU's in various arrangements. The most basic forms of CBU's are rings. Figure 2-4 illustrates the most common rings formed by joining together BBU's, as derived from Auerbach *et al*. (2003a). For simplicity oxygen atoms are omitted from the representation therefore green lines indicate the oxygen and their bonds to the T atoms. By combining rings together more complex CBU's are formed namely cages and chains, which in turn are further combined forming a vast array with pores, cavities and channels.

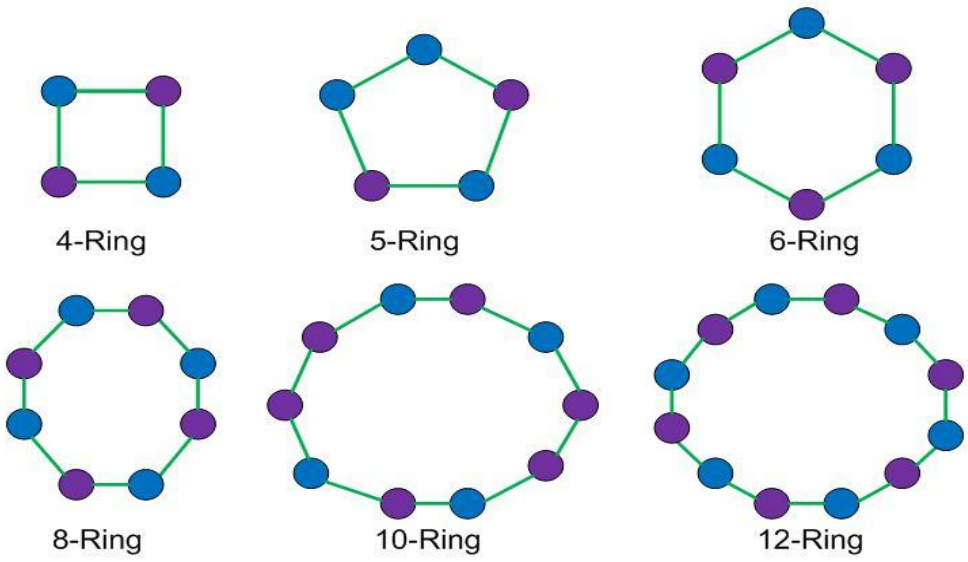

Figure 2-4: Most common composite building block rings formed by joining together basic building units.

According to Auerbach *et al*. (2003a) cages are formed with rings small enough to block access to molecules greater than the water molecules i.e. 6-Rings and smaller. A ring that defines a face of a polyhedron is referred to as a window (Auerbach *et al.*, 2003a). Figure 2-5, obtained from Newsam (1992), illustrates how BBU's are configured to form 5-Rings and 4-Rings which then combine to form the sodalite cage. The sodalite cages are then connected in different manors to form different types of zeolites containing different pore and channel sizes. Molecules bigger than water can only enter the zeolite through channels formed by cages and cannot enter the cage directly through a window.

When one of the windows of a cage is defined by a ring greater than a 6-Ring, a cavity exist which is very different from a cage (McCusker et al., 2001). A cavity has only one of its windows large enough to allow access to a molecule larger than water. Therefore access of the molecule is allowed only through the window and cannot get access to channels or pores from within the cavity.

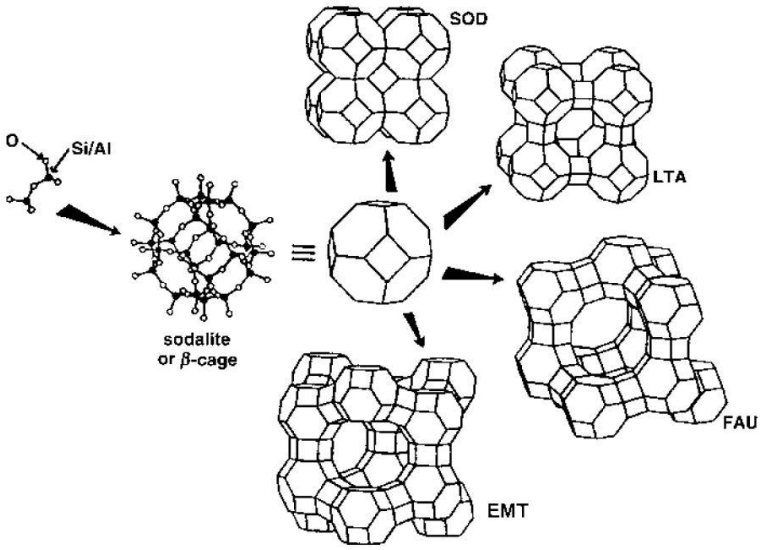

Figure 2-5: Illustration of the formation of cages from BBU's and channels by combining cages in different variations (Newsam, 1992).

The 3 letter abbreviations used in Figure 2-5 refers to a group of zeolite types based on their framework topologies. This is a system used to classify zeolite groups. Table 2-3 illustrates some examples of zeolite groups and their respective codes/abbreviations. It is important to note that these are structural groups and not zeolite names. Under each group various different zeolites may exist. A full list of zeolite structures, the group they belong to and their respective abbreviations can be found under the Atlas of Zeolite Framework Types (IZA, 2012).

Table 2-3: Examples of zeolite structural groups and their codes/abbreviations

Abbreviation	Zeolite structural group
FAU	Faujasite
GIS	Gismondine
GME	Gmelinite
BOG	Boggsite
MOR	Mordenite

2.2.3 Properties and uses of zeolites

2.2.3.1 Zeolite properties

Zeolites have various unique properties that make them useful in a vast range of industrial and environmental applications. The thermal stability of zeolites makes them useful in high temperature applications such as catalyst in the petrochemical industry. Cruciani (2006) studied the thermal stability of various zeolites and developed a stability index whereby thermal stability could be quantified. The author found that there is a direct correlation between thermal stability and the Si/Al ration of zeolites. It was determined that an Si/Al ratio of less than 1.28 is relatively unstable while a ratio of more or equal to 3.86 results in a zeolite with a very high thermal stability (Cruciani, 2006). Generally low silica zeolites have a thermal decomposition temperature of ±700 °C and high silica zeolites up to 1300 °C. In a study done by Joshi et al. (2002) it was determined that the type of extraframework cations incorporated in the zeolite pores has an effect on its thermal stability.

The physical properties of zeolites are greatly influenced by the Si/Al ratio of the structures (Breck, 1974). Table 2-4, derived from Auerbach et al. (2003e), summarizes some of the physical properties of commonly used zeolites. The pore and channel formation inside zeolite structures is another important property. Table 2-4 illustrates nominal pore opening sizes of some important zeolites. Figure 2-5 illustrates how different pore sizes can result from arranging the same CBU in different variations. From the figure it is clear that the SOD structural group is the densest group with small pore openings, while LTA and FAU groups have a considerably larger pore channel system.

Another important property of zeolites making them highly valuable is their ability to exchange their extraframework ions and be used in varies ion exchange applications (Pfenninger, 1999). This attribute arises from the fact that the cations are loosely bound at the electronegative sites in the zeolite structure. Each zeolite structure has their own distribution of sites where cations latch on to balance the charge of the structure. The cation exchange capacity greatly depends on the Si/Al ratio of the zeolite (Auerbach *et al.*, 2003c). According to Auerbach et al. (2003c) the diffusion of cations within the zeolite structure is governed by both cation concentration and electrical gradients.

Table 2-4: Physical properties of commonly used zeolites.

Zeolite	Si/Al ratio	Crystal structure symmetry	Crystal density (g/cm^{-3})	Pellet density (g/cm^{-3})	Bulk density (g/cm^{-3})	Nominal pore opening (Å)
A	0.7 - 1.2	Cubic	1.52	1.20	0.72	3,4,5
X	1.0 – 1.5	Cubic	1.47	1.05	0.65	7.5 (NaX) 10.0 (CaX)
Mordenite	4.5 - 5.0	Orthorhombic	1.83	1.39	0.88	4
Chabazite	1.6 – 3.0	Trigonal	1.67	1.16	0.73	4.9
Clinoptilolite	4.2 - 5.2	Monoclinic	1.85	-	-	3.5
Silicalite	Very high	Orthorhombic	1.79	-	-	5.3

The ion exchange capacity is governed by various factors such as zeolite structure, nature of the extraframework cations and the type of solvent from which ions are exchanged (Nagy *et al.*, 1998; Szostak, 1997; Weitkamp and Puppe, 1999). Ion exchange in both synthetic and natural zeolites has been researched extensively (Ames, 1991; Auerbach *et al.*, 2003c; Keane, 1995a; Keane, 1995b; Keane, 1996; Mondale *et al.*, 1995; Sherry, 1979). Various studies have been undertaken to even improve the cation exchange capacity of available natural occurring zeolites (Kang and Egashira, 1997; Kang *et al.*, 1998; Wang and Lin, 2009).

Other than a structured microporous system and cation exchange behaviour, zeolites also have acidic properties. This property has made zeolites a vital catalyst in the petroleum industry (Maxwell and Stork, 1991). Zeolite structures contain both Lewis and Brönsted acid sites and this coupled with their ability to allow molecules of certain sizes through their channel structures makes them optimum catalytic material (Ribeiro et al., 1995). The acidity of zeolites are preferably determined by means of infrared spectroscopy, however temperature-programmed desorption can also be used (Auerbach *et al.*, 2003c; Corma *et al.*, 1995; Robb *et al.*, 1998). The use of zeolites as catalyst is not restricted only to the petroleum industry. Many other catalytic processes involve the use of zeolites such as the synthesis of aromatics, ethers and other organic compounds (Bregolato *et al.*, 2007; García-Trenco and Martínez, 2012; Zhu *et al.*, 2006; Žilková *et al.*, 2009). The applications of zeolitic material are discussed in more depth in section 2.2.3.2.

2.2.3.2 Applications of zeolitic material

Due to the physical and chemical properties of zeolites, discussed in previous sections, a vast range of process currently makes use of these materials. Below is an overview of the three major uses of zeolites around the world.

2.2.3.2.1 Adsorption

The unique structural properties of zeolites have made them a phenomenal material to be used in adsorption processes. The uniform pore structure and spacing gives rise to channel systems able of selectively adsorbing high volumes of molecules based on their specific size. This enables the separation of specific compounds from waste streams or recovery and storage of specific wanted material from a mixed stream. With zeolites it is possible to selectively adsorb molecules with size differences of less than 1Å (Auerbach *et al.*, 2003e).

It was found that compounds such as CO_2 and SO_2 can effectively be removed from gaseous waste streams with application of zeolites (Walton *et al.*, 2006; Wu *et al.*, 2008; Wu *et al.*, 2006a).The elemental form of sulphur can also be removed from waste streams by adsorption onto zeolite A and X (Steijns and Mars, 1976). The possibility of carbon removal using zeolites would provide great economic advantages in the cleaning of waste streams and also carbon capture and storage. Walton *et al*. (2006)found that the CO_2 adsorption capacity of zeolites X and Y depends on the type of extraframework cations present in the zeolite pores. The author suggested that the adsorption capacity increases with decreasing ionic radii of the extraframework ions (Walton et al., 2006).

The adsorption and separation of various hydrocarbons by means of large pore zeolites such as zeolite X and Y has been investigated by various authors (Grande *et al.*, 2006; Miano, 1996; Papaioannou *et al.*, 1997). The authors reported that specific compounds can successfully be separated from other hydrocarbons due to the high selectivity of zeolites. In more recent work it was seen that zeolites can also be used to capture and more important store hydrogen (Langmi *et al.*, 2003; Yin *et al.*, 2007).

Other interesting current studies illustrated that the absorptive characteristics of zeolites can be used in artificial kidneys (Kubota et al., 2008) as well as selective capturing of bacterial microbes (Wernert et al., 2005).

2.2.3.2.2 Ion exchange

As mentioned previously, the loosely bound nature by which cations latch on to sites in the zeolite structure allows for their phenomenal cation exchange behaviour. This has led to numerous studies and applications into the removal of cations from solutions and waste streams. One of the most studied aspects of cation removal using zeolites is the uptake of ammonium from waste and its controlled release for fertilizers (Jha and Hayashi, 2009; Juan *et al.*, 2008; Lin *et al.*, 2013; Malekian *et al.*, 2011; Milan *et al.*, 1997; Sarioglu, 2005; Wang *et al.*, 2007). The ammonium uptake capacity of zeolites is strongly dependant on the concentration of other cations in solution due to matrix effects (Juan *et al.*, 2008; Malekian *et al.*, 2011). The slow and controlled release of ammonium from zeolites provides a useful method to dispose spent zeolites as fertilizers.

The removal of heavy metals and other toxic components from waste waters has also been the focus of zeolitic applications. It was determined that zeolites can be used to remove heavy metals in the following order of affinity: Pb>Ca>Zn>Mn>Cu>Cd>Al>Ni (Querol et al., 1995). Heavy metal removal is a costly operation and low cost zeolites can provide a cost effective alternative. Many other components have been studied as a potential to be treated with zeolites, however a detailed review would be too extensive for the purposes of this study. Table 2-5 illustrates a short overview of selected cation species studied by various authors.

Table 2-5: Overview of research on the removal of cations from solution with various zeolites.

Cations	Zeolites used	Reference
Chromium (III)	X	(Covarrubias et al., 2006)
	Y	(Covarrubias *et al.*, 2006; Mekatel *et al.*, 2012)
	Clinoptilolite	(Inglezakis and Loizidou, 2007)
Copper (II)	Clinoptilolite	(Inglezakis and Loizidou, 2007; Woinarski *et al.*, 2003)
	X	(Ursini et al., 2006)
	Y	(Ursini et al., 2006)
	A	(Biškup and Subotić, 2004)
Cadmium (II)	Clinoptilolite	(Ćurković et al., 1997)
	A	(Biškup and Subotić, 2004)
	Y	(Mekatel et al., 2012)
Iron (III)	Y	(Ostroski et al., 2009)
	Phillipsite	(Al-Anber and Al-Anber, 2008)
	Clinoptilolite	(Inglezakis and Loizidou, 2007)
Zinc (II)	Y	(Mekatel *et al.*, 2012; Ostroski *et al.*, 2009)
	Clinoptilolite	(Athanasiadis and Helmreich, 2005; Ören and Kaya, 2006)
Lithium (I)	A	(Navarrete-Casas et al., 2007)
	X	(Navarrete-Casas et al., 2007)
Manganese (II)	Clinoptilolite	(Taffarel and Rubio, 2009)
Lead (II)	Clinoptilolite	(Ćurković et al., 1997)
	Y	(Mekatel et al., 2012)
Nickel (II)	A	(Biškup and Subotić, 2004)
	Y	(Mekatel et al., 2012)

2.2.3.2.3 Catalyst

The petrochemical industry has taken great advantages of the uniform pore channels and acidic properties of zeolites. Zeolites have been used extensively in crude oil refining and have become a vital catalyst in isomerization, cracking and hydro cracking. Zeolites have been used for both organic and inorganic compound conversions. The selective admission of molecules into the zeolite pores and the presence of both Lewis and Brönsted acid sites make their use in catalytic processes highly controllable and effective (Auerbach *et al.*, 2003c). Zeolites Y (FAU) and ZSM-5 (MFI) are used in the largest volumes around the world as a solid-acid catalyst. The

pore sizes of these zeolites make it possible to convert hydrocarbon molecules. They are often used in fluid catalytic cracking units on oil refineries. New catalytic applications of zeolites are discovered every year and the consumption of zeolites ZSM-5 and zeolite Y has increased with the growth of the world economy. Extensive literature has been published on the catalytic applications of zeolites in handbooks and journal publications (Auerbach *et al.*, 2003b; Flanigen *et al.*, 1971; Maxwell and Stork, 1991; Nagy *et al.*, 1998).

2.2.4 Synthesis of zeolites

The use of synthetic zeolites over natural zeolites offers great advantages. In nature the zeolites do not crystallize under controlled conditions. For this reason various impurities can be incorporated into the structure and pore system. With relatively constant conditions the conversion of the zeolite structures cannot be stopped in nature. Most zeolites are metastable phases and when left to react will transform into more dense phases according to the Ostwald ripening rule(Boistelle and Astier, 1988). These denser phases normally have very small pore openings and low cation exchange capacities. Up till now about 40 natural zeolites have been discovered while over 300 different types of synthetic zeolites have been made. Although natural zeolites are much cheaper, synthetic zeolites can be tailor-made for specific application.

2.2.4.1 Synthesis mechanism

The mechanism of zeolite formation has been studied extensively over the past 50 years. Early ideas of the mechanism suggested a series of complex polymerization, depolymerisation and polyhedral condensation reactions (Cundy and Cox, 2005). The mechanism is said to follow the outlined overall steps (Auerbach *et al.*, 2003d; Breck, 1974; Cundy and Cox, 2005; Inada *et al.*, 2005a; Murayama *et al.*, 2002):

1. Dissolution of Si and Al species from the feedstock to form monomeric species of mostly TO_4tetrahedra.
2. Condensation of TO_4 polyhedral building blocks around hydrated cations to form simple secondary building blocks (up to double 6-ring polyhedral units).
3. Linking together of building blocks to create zeolite structural groups and large zeolites crystals with arrays of pores and channels.

The historical and current advances in the mechanisms of zeolite synthesis have been reviewed (Cundy and Cox, 2005). Their paper is highly recommended to anyone seeking a deeper understanding of the mechanisms involved. Although it is clear that different zeolites makes use of different structure-building reactions (Cao and Shah, 2007), the above steps can be used as

a guide to understand the general mechanism. The progression of zeolite formation has been studied with various analytical techniques such as infrared spectroscopy, UV Raman spectroscopy(Xiong et al., 2001), X-ray diffraction (XRD) (Breck, 1974), nuclear magnetic resonance (NMR) (Epping and Chmelka, 2006; Kosanović *et al.*, 2011), electrical conductivity analysis (Cao and Shah, 2007) and atomic force microscopy (Kosanović et al., 2011).

The first stage of the mechanism is characterized by the formation of a precursor gel. Its formation is firstly governed by the depolymerisation of the feedstock precursors to make Si polymers (Xiong et al., 2001). At this stage the solution contains monomeric species of TO_4 tetrahedra. The next step is a complex series of processes differing from zeolite to zeolite (Cao and Shah, 2007; Cundy and Cox, 2005). A series of polymerization and depolymerisation process joins the monomeric species together in a semi-regular arrangement. The monomers are joined together around hydrated cat-ionic species (balancing the charge deficiency of the structure) (Cundy and Cox, 2005). At this stage simple SBU's are formed in the precursor gel. For zeolite A, studies have revealed that mostly amorphous aluminosilicates and partially crystalline material exist in the gel before the viable nuclei are formed (Fan *et al.*, 2008; Kosanović *et al.*, 2011; Xiong *et al.*, 2001). These materials contains 4-membered and 6-membered rings, however Fan et al.(2008) also found that branched rings can exist. By means of electrical conductivity studies Cao & Shih (2007) revealed new information on the mechanisms involved in the formation of both zeolites A and ZSM-5. Making their research so novel is the proposed differences in the SBU-building reactions taking place in the precursor gel. They found that, while polymerization reactions dominate in the formation of zeolite A, oligomerisation is most likely to occur in the synthesis of ZSM-5.

In the precursor gel semi structured material start to form by the joining together of 4-membered and 6-membered rings. Once the zeolite structural unit/nuclei has been formed successfully crystal growth occurs very rapidly (Cundy and Cox, 2005). Figure 2.6 is a graphical representation of the summarized general mechanism published by Cundy and Cox in 2005. The figure was obtained from their published work and not altered in any way as their representation and summarized ideas on the general zeolite formation mechanism is very comprehensive and logical. After the building blocks and basic zeolite structural groups have been formed the crystal growth occurs in the solid phase (Bosnar *et al.*, 2004; Bosnar and Subotic, 1999; Cundy and Cox, 2005). In other words once these structures are formed, nutrients and building blocks are transferred to the solid surfaces where they interact to grow the zeolite crystals instead of forming new nuclei sites in the liquid phase. In the late 1950's

Barrer did the first pioneering work on zeolite synthesis and developed a model for the formation mechanism of zeolites (Barrer, 1982; Cundy and Cox, 2005). Barrer suggested that once the crystallization period starts, the final stage of zeolite formation, only SBU's and larger units are incorporated and rearranged in the zeolite structure. He postulated that, by taking into account the rates of crystallization and channel systems of zeolites, it won't be possible to form these large crystalline metastable phases if the basic TO_4 building were incorporated directly onto the crystal surface. This theory was further confirmed by Ren et al. (2011). The authors observed that, during crystallization, 4-membered rings and sodalite cages were rearranged to form zeolite A structural groups and the crystal further built by incorporation of more SBUs.

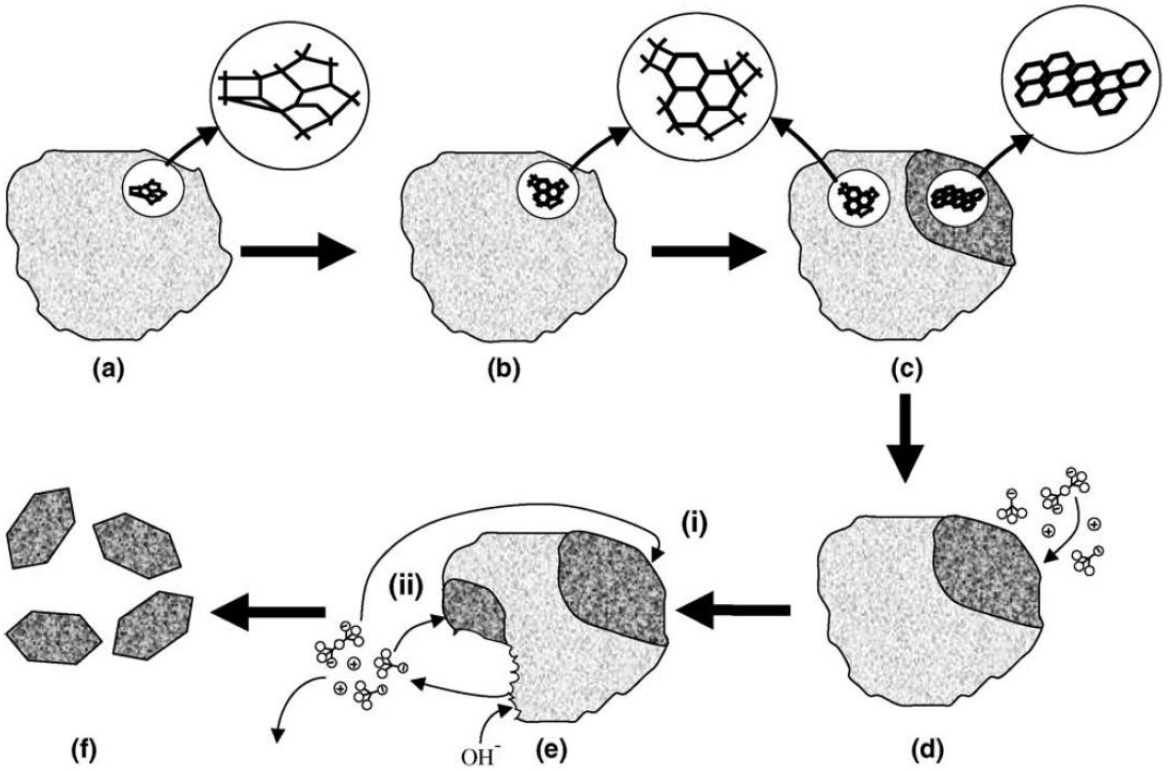

Figure 2-6: Illustration of nucleation and crystal growth mechanism from intermediate gel to final crystal forms. From the initial gel (a), to the secondary semi-ordered gel containing sites of underdeveloped nuclei (b), transforming into sites with "viable" nuclei (c), which grows by addition of building blocks transported via the solution (d). To provide building blocks the gel is dissolved (e) until all amorphous materials are dissolved and transformed to crystals (f).

(Obtained from Cundy& Cox, 2005)

This section introduced the generalized mechanism that has been built over decades of arduous research. Although the specific mechanism and reaction pathways will differ from zeolite to zeolite these generalized mechanistic concepts are sufficient for the purposes of this study.

2.2.5 Zeolite synthesis from coal fly ash

2.2.5.1 Background and reference work

Due to the high Si and Al content of coal fly ash it is regarded as an adequate feedstock for the synthesis of zeolites. This was first discovered when it was realized that coal fly ash has similarities to volcanic material found where natural zeolites were discovered. The first attempts to convert coal fly ash into zeolitic material was over 25 years ago by Höller and Wirsching (1985). Given the abundant fly ash production in South Africa, converting waste coal fly ash into zeolitic materials would present economic and environmental benefits to the country.

Since the original work on fly ash conversion to zeolites was performed by Höller and Wirsching in 1985, many studies were undertaken on this subject matter. Numerous studies have proposed different hydrothermal activation methods to synthesize different zeolites from fly ash (Chang and Shih, 1998; Hollman *et al.*, 1999; Molina and Poole, 2004; Moreno *et al.*, 2001; Musyoka, 2009; Querol *et al.*, 1995; Querol *et al.*, 2007; Querol *et al.*, 2002; Querol *et al.*, 1997; Querol *et al.*, 2001; Rayalu *et al.*, 2000; Somerset *et al.*, 2005a; Somerset *et al.*, 2005b; Somerset *et al.*, 2004; Woolard *et al.*, 2000; Yang and Yang, 1998). Other than the classical alkaline conversion of fly ash, various other techniques have been developed (Chang and Shih, 1998; Inada *et al.*, 2005b; Querol *et al.*, 2007). From these studies various valuable zeolites such as zeolite P, A, X, Y and ZSM-5 has successfully been synthesized from fly ash. A detailed account of the different zeolites synthesized from coal fly ash up till 2002 can be found in a paper published by Querol et al. (2002).

The mechanism of converting fly ash into zeolites is similar to the general mechanism described in section 2.2.4.1. Because fly ash consists of both stable crystalline material (Quartz, Mullite, Hematite and Magnetite) and amorphous materials, the dissolution phase is somewhat more complex. The dissolution of fly ash consists of complex depolymerisation reactions to release the Si and Al species as monomers into solution (Davis and Lobo, 1992). The rate of dissolution in fly ash particles is affected by the temperature, alkaline concentration and agitation conditions (Molina and Poole, 2004). After the dissolution of the ash the precursor gel is formed by the formation of dimers and trimers from monomeric TO_4 tetrahedra (Elliot and Zhang, 2005). As mentioned previously, after the formation of the precursor gel zeolite are formed by rearranging composite building units instead of forming new nucleation sites or incorporating basic building units (Bosnar *et al.*, 2004; Bosnar and Subotic, 1999). This aspect holds true when using coal fly ash as a feedstock. Studies has proven that the precursor gel derived from fly ash contains

CBU's and other short range ordered structures (Palomo et al., 2008). Earlier this aspect was contemplated for years with confusion as to why new nuclei sites do not form. In 1981, in an article published by Hawkins (1981), this concept was clearly defined. The author explained that, in any amorphous or semi-amorphous medium (precursor gel), zeolite crystallization occur at the dissolving species. This is the reason for the crystallization of zeolites around the dissolving coal fly ash particles.

Most studies to date were performed on microscale and very little literature is available on pilot scale synthesis. In 2001 Querol *et al.* synthesized a high cation exchange capacity zeolite Na-P1 at pilot scale from Spanish fly ash. The author studied the synthesis of zeolite Na-P1 first at micro scale (4 g fly ash) followed by lab scale (24 kg fly ash) and ultimately at pilot scale (1100 kg fly ash). The first activity in the scale-up of the zeolite synthesis process is the optimization of the process at micro and lab scale. Querol *et al.* (2001) reported high reproducibility at pilot scale utilizing the optimized lab scale conditions. Querol *et al.* (2001) also suggested that the zeolite synthesis process needs to be optimized for each of the different power station fly ashes since their compositions differ. Other than process optimization, knowledge regarding the economics, mixing power requirements, efficiency, safety, energy requirements and environmental effects are required to successfully scale-up the synthesis process. By performing fundamental process engineering studies such as material balances, energy balances, HAZOP studies and waste minimisation studies these critical questions can be answered.

The first steps in the overall goal of utilizing South African coal fly ash in zeolite synthesis has begun very recently. Various authors have studied the synthesis of varies zeolites from different South African coal fly ashes (Hendricks, 2005; Musyoka *et al.*, 2012c; Somerset *et al.*, 2005a). Studies was undertaken that saw the successful synthesis of zeolites P1, A, X and sodalite (Musyoka *et al.*, 2012a; Musyoka, 2009; Musyoka *et al.*, 2012b; Musyoka *et al.*, 2011a; Musyoka *et al.*, 2012c). The authors optimized conditions on micro scale and utilized two synthesis approaches. The first involves classical alkaline conversion of fly ash. In this approach the fly ash is activated by aging with an alkaline solution to form the precursor gel followed by high temperature hydrothermal treatment. The approach step involved replacing the aging step with high temperature fusion. These methods are explained in more detail in section 2.2.5. In a more recent study an attempt was made to complete some of the activities required for scale-up of the synthesis process. The effect of agitation and the type of impeller have been shown to be critical to the synthesis of zeolites (Mainganye *et al.*, 2013). Studies done by Musyoka were

performed under static conditions, while the scale-up process would have to occur in an agitated vessel (Bebon *et al.*, 2002; Casci, 2005; Marrot *et al.*, 2001). Mainganye effectively optimized the agitation conditions and filled this gap in literature. However, large gaps in literature still exist which disables the scale-up of the process. Material balances are required in order to better understand the distribution of elements from the fly ash to the different products generated in the process. The processes also generate significant amounts of waste and consume large amounts of energy. Due to South African environmental law and increasing energy prices this renders the process industrially unfeasible. A study is required to develop protocols and new approaches to minimise the waste generated and energy consumed. Lastly, before a pilot scale synthesis process can be attempted, well documented hazard and operability studies are required on the principal reactor design.

2.2.5.2 Methods of synthesis

In 2001 the IZA synthesis commission published a second review on the known synthesis routes of various zeolites (Robson and Lillerud, 2001). This handbook provided details on reactor setups, feedstock and synthesis conditions and is available online at http://www.iza-online.org/synthesis/default.htm (IZA, 2013). Various improvements have been made to the conventional synthesis method from fly ash since the first attempts by Höller and Wirsching in 1985. The early conventional method to convert fly ash into zeolites involved only one step. In this step fly ash was contacted with an alkaline solution dissolving the fly ash to release Si and Al species. Simultaneously crystallization of the zeolites occurred during this step. By altering the synthesis parameters (pressure, temperature and activation time) various different types of zeolites can be synthesized (Moreno et al., 2001). Although the one step method was a simple and robust process it suffered in efficiency with low yields. It was found that zeolite yields from coal fly ash could not be improved above ±50% (Berkgaut and Singer, 1996). Various improvements have been made on this conventional method as described in the sections 2.2.5.2.1 –2.2.5.2.3 below.

2.2.5.2.1 Two step method of aging followed by hydrothermal treatment

In 1999, Hollman *et al.* made great advances in improving this basic synthesis route. The authors developed a two step method whereby yields were drastically improved to above 99%. The first step involves alkaline aging. During the aging step fly ash is dissolved and the Si/Al species released from the amorphous and crystalline phases. This concurs with the early phases of the generalized zeolite formation mechanism. Al and Si are released into solution as TO_4 tetrahedra after which the CBU's are formed to generate the precursor gel. The second

step developed by Hollman *et al.* is the hydrothermal treatment phase. During this phase more of the crystalline material is dissolved while the zeolite crystals are formed. The crystallization then occurs at the solid dissolving species' surfaces, as mentioned previously. The difference between the two steps is that large amounts of water are added to the precursor gel, obtained after aging, and the temperatures are elevated.

This 2 step method was applied to South African coal fly ashes as mentioned before (Musyoka *et al.*, 2012a; Musyoka, 2009; Musyoka *et al.*, 2012c). The author found optimum conditions for both the aging and hydrothermal conditions in order to synthesize high cation exchange capacity zeolites. During the period of 2010 - 2012, with a view of scaling up this process, further optimized this process by introducing mechanical agitation during the aging step (Mainganye, 2012; Mainganye *et al.*, 2013). The synthesis approach utilized in this study is a combination of the optimized results obtained from both Musyoka and Mainganye as summarized below.

Aging step:

- Feedstock – 5 M NaOH solutions (prepared with ultrapure water and analytical grade NaOH pellets) combined with South African coal fly ash in a volume: mass ratio of 5 ml: 1 g (NaOH: fly ash).
- Pressure – Atmospheric
- Temperature – 47 ^{o}C
- Agitation state – 200 rpm with a 4-blade paddle impeller

Hydrothermal treatment step:

- Feedstock – Precursor gel obtained after aging mixed with ultrapure water in a volume: volume ratio of 2.5: 1 (ultrapure water: gel).
- Pressure – Autogenious
- Temperature – 140 ^{o}C
- Agitation state – Static

The fundamental problem with this process, as well as the fusion assisted process, is the large amounts of liquid waste generated by the process. This issue is one of the problems aimed to be remedied by this study.

2.2.5.2.2 Fusion assisted synthesis

In the early to mid 1990's attempts were made to introduce a high temperature (500-600 ^{o}C) fusion step before hydrothermal treatment (Shigemoto *et al.*, 1993; Singer and Berkgaut, 1995). The authors found that zeolites such as A and X could be synthesized by means of this method. In previous sections it was seen that these two zeolites are highly valuable and their synthesis from coal fly ash yield great economic opportunities. Various other researchers have also studied this fusion assisted route and reported successful synthesis of highly these valuable zeolitic products (Chang and Shih, 1998; Molina and Poole, 2004; Ojha *et al.*, 2004; Rayalu *et al.*, 2000; Ríos *et al.*, 2009; Somerset *et al.*, 2005a; Wang *et al.*, 2008). Due to the variations in fly ash properties from different power stations, the fusion assisted process was found to be the most robust process under these varying conditions (Chang and Shih, 1998; Molina and Poole, 2004). During the fusion process the crystalline and amorphous Al/Si bearing phases are converted into sodium silicates and aluminosilicates which easily dissolves into solution (Molina and Poole, 2004). Once in solution, the Si/Al ratio can be altered depending on the required zeolite, making this process easily controllable even with the variations in coal fly ash composition.

Locally, this process was adapted to South African coal ashes (Musyoka et al., 2012b). Musyoka *et al.* successfully synthesized zeolites A and X using this fusion assisted process. However, other than the waste produced in this process it consumes high amounts of energy. This is another issue that was attempted to be addressed by this study to close this gap in literature and increase the process' upscale feasibility. The synthesis procedure used in this study was adopted from Musyoka et al. (2012b). The author fused the ash by mixing raw fly ash with powdered dry NaOH in a mass ratio of 1.2:1 (NaOH: ash). The mixture was subjected to fusion at 550 ^{o}C for 90 minutes in an electric furnace. Details of this process are discussed in chapters 3, 5 and 6.

2.2.5.2.3 Microwave assisted synthesis

Microwaves are electromagnetic waves operating in a wave band range between infrared and radio waves. Microwaves are used widely in heating applications both domestically and industrially. The heating of substances by application of these waves is based on the dielectric heating effect. Due to the rapid bulk substance heating caused by this effect the use of microwaves in zeolite synthesis was studied by various authors (Andrés *et al.*, 1999; Hu *et al.*, 2009; Inada and Hojo, 2007; Inada *et al.*, 2005b; Li *et al.*, 2006; Li and Yang, 2008; Querol *et al.*, 2002; Querol *et al.*, 1997; Sathupunya *et al.*, 2004; Sistani *et al.*, 2010; Tatlier *et al.*, 2007).

From all these studies two major conclusions was drawn. The application of microwaves during the synthesis of zeolites, from both fly ash and pure chemicals, results in increase crystallization rates and drastically reduced crystal sizes. Very little literature has been published on the mechanism of zeolite formation from microwave assistance (Li and Yang, 2008). Li and Yang (2008) published a well researched review of microwave assistance and current advances in its mechanism. It is speculated that microwaves causes rapid simultaneous nucleation in the precursor gel(Li and Yang, 2008). With a substantially larger amount of nucleation sites the crystal sizes consequently reduces.

2.2.5.3 Influence of chemical and physical parameters

Due to the fact that most zeolites are metastable phases and the complexity of its formation mechanisms, changing a single chemical or physical parameter has drastic effects on the type and quality of zeolites formed (Barrer, 1982; Bebon *et al.*, 2002; Cundy and Cox, 2005; Pfenninger, 1999; Szostak, 1997). The next subsections discuss the effects of some of the major parameters on the zeolite synthesis system.

2.2.5.3.1 SiO_2/Al_2O_3 ratio in the feedstock

The main impact factor of the raw feedstock in zeolite synthesis is the Si/Al ratio. As discussed previously the zeolite building blocks and structural groups are formed by joining together of the AlO_4 and SiO_4 building units by sharing an oxygen atom. It is however vital to point out that not only Al-O-Si bonds exist. In the zeolite structure Al-O-Al as well as Si-O-Si links are formed. By increasing the Si/Al ratio in the feedstock more Si-O-Si bonds are formed and therefore altering the structure, Si/Al ratio and the available cation exchange sites in the zeolite crystal (Cao and Shah, 2007). Since the cation exchange capabilities of zeolites are due to the negatively charges sites caused by AlO_4tetrahedra, increasing the Si/Al ratio decreases its cation exchange capacity (Szostak, 1997). It was also found that increasing the Si/Al ratio will: increase thermal stability, increase acid attack resistance but decrease absorbance of polar molecules (Szostak, 1997). The concluding fact is that each zeolite structure has a specific Si/Al ratio which is governed by a Si/Al range in the starting material(Auerbach *et al.*, 2003d). Within this range/window, that will generate a specific zeolite type, changing the Si/Al ratio can still have other effects on a specific zeolite. It was found in a study by Basaldella et al. (1997) that a SiO_2/Al_2O_3ratio window of 1.48 – 2.69 generated zeolite A, but dramatically altered the morphology and size of the crystals.

Using coal fly ash as a raw material brings about more complications with respect to the Si/Al ratios. The different Si and Al bearing phases in fly ash; i.e. amorphous material, quartz and mullite; dissolve with different degrees of ease (Fernandez-Jimenez and Palomo, 2005). Therefore the Si/Al ratio changes as the reactions proceed. This is one of the reasons that fusion assisted synthesis was developed to provide a more robust method. It was reported that a SiO_2/Al_2O_3 ratio of more than 1.5 in fly ash is required for zeolites synthesis (Querol et al., 1997). However, it was also seen that ratios as low as 1.2 can be used in the synthesis of high cation exchange capacity zeolites such as zeolite Na-P1 (Molina and Poole, 2004).

2.2.5.3.2 Alkalinity

Various studies investigated the effects of alkalinity in the zeolite synthesis (Molina and Poole, 2004; Querol *et al.*, 1997; Rayalu *et al.*, 2000; Ríos *et al.*, 2009; Somerset *et al.*, 2004). All these studies came to the same general conclusion which is that an increase in alkalinity results in an increased crystallization rate (Auerbach *et al.*, 2003a). However this is a consequent effect of the increasing dissolution rate of the raw material (Bosnar and Subotic, 1999; Držaj, 1985). The increase in dissolution rate increases the super saturation of Al and Si species in the precursor gel. This leads to an increase in nucleation growth and consequently an increase in the rate of crystallization. This holds true when using fly ash as a raw material source (Molina and Poole, 2004). The increase in dissolution of fly ash favours the existence of metastable phases (Molina and Poole, 2004) and leads to a higher overall purity in the synthesized zeolites (Casci, 2005). Evidently variations in the dissolution and growth rates can yield different types of zeolites from fly ash. Woolard et al. (2000) illustrated this by altering the starting NaOH concentration from 1 M to above 3 M and in doing so synthesized zeolite hydroxysodalite instead of Na-P1. Murayama et al. (2002) speculated that during the dissolution phase alkalinity is the major rate controlling factor.

2.2.5.3.3 Extraframework cations

The type of extraframework cations present during the synthesis of zeolites is very important in determining the rate of crystallization (Murayama *et al.*, 2002). Studies have revealed that varying the type of cations present during synthesis dramatically influences the nucleation and growth rate. It has been seen that using Na^+ instead of K^+ ions is highly advantageous (Querol *et al.*, 1995; Querol *et al.*, 1997; Ríos *et al.*, 2009). Studies revealed that K^+ ions greatly suppress the rate of nucleation and crystallization (Warzywoda and Thompson, 1991) while Na^+ ions greatly enhances it (Querol *et al.*, 1995; Querol *et al.*, 1997). As discussed before the CBU's are formed by joining the BBU's around a hydrated cation. Therefore the size and type of

cation directly affects the mechanism and consequently the type of structure formed. Warzywoda and Thompson (1991) illustrated that by varying the ratio of NaOH to KOH in the synthesis system different types of zeolites result. The results of his work showed that by increasing the amount of K^+ ions in the synthesis system zeolite K-F was favoured over zeolite A. Other than zeolite type and crystallization rates, the extraframework cations also influences the morphology of the zeolite crystals (Auerbach *et al.*, 2003d). In fly ash various cationic species leach out into solution such as Na^+, K^+, Mg^{2+} and Ca^{2+}. This complicates the synthesis of zeolites even further since these cationic species compete in the structure forming process.

2.2.5.3.4 Water content

As it was mentioned previously zeolite building blocks are formed around hydrated cationic species. Therefore water is a vital part in the synthesis of zeolites. The water molecules act as templates by filling the voids of the zeolite structure during synthesis (Feijen et al., 1994). Water also acts as a solvent during the process and transports nutrients to the crystal structure during nucleation and crystallization. Theoretically, according to general crystallization theories, an increase in water content should depress crystal growth (Iwasaki et al., 1996). This is due to the fact that increasing water content decreases species' concentration in solution and consequently supersaturation. Iwasaki et al. (1996) illustrated that this holds true in zeolite synthesis. However, most zeolite systems contradict the author's results, and the general crystallization principals, by illustrating an increase in crystal growth rate (Auerbach *et al.*, 2003d; Criado *et al.*, 2010; Cundy and Cox, 2005). The reason for this was found to be the presence of colloidal silica (Iwasaki et al., 1997). An increase in water content increases the dissolution rate of colloidal silica and therefore increasing the bulk crystal growth rate. When using fly ash as a feedstock an increase in water content increases the yield and purity by increasing the dissolution rate of crystalline and amorphous phases in the ash (Querol *et al.*, 1995; Querol *et al.*, 2001).

In the previous section it was discussed how different cationic species can alter the mechanism, growth rate and type of zeolites. For this reason ultrapure water is used when synthesizing zeolites to avoid complications. However, it has been seen from various studies that zeolites can be synthesized from different water sources such as sea water, acid mine drainage, municipal water, distilled water and brine (Belviso *et al.*, 2010; Mainganye, 2012; Musyoka, 2009; Musyoka *et al.*, 2011a).

2.2.5.3.5 Synthesis time

In zeolite synthesis the duration of the reaction is a vital factor (Nagy et al., 1998). The reason being that zeolites are metastable phases and can transform into different zeolites when left to react (Auerbach *et al.*, 2003d). According to the phenomenon of Ostwald ripening, zeolites will continue to transform into more dense phases if the reaction is not halted (Boistelle and Astier, 1988). Figure 2.5 illustrates how the sodalite cages can be rearranged to form different structural groups. According to Ostwald ripening these groups are rearranged continuously in order to form the most stable form, which is usually the densest structure. Therefore it is vital to determine the time of crystallization that would generate the wanted metastable phases and then terminate the reaction at that time.

2.2.5.3.6 Temperature

According to Auerbach et al. (2003d) temperature is the most studied physical parameter in zeolites synthesis systems. This is due to the dramatic effects that a change in temperature brings about in the process kinetics and product formed. In all studies performed it was found that an increase in crystallization temperature brings about an increase in the growth rate of zeolites (Breck, 1974; Elliot and Zhang, 2005; Hould *et al.*, 2011; Hsu *et al.*, 2008; Molina and Poole, 2004; Murayama *et al.*, 2002; Rayalu *et al.*, 2000). In all reactions, according to the laws of reaction kinetics, temperature and time are interconnected(Fogler, 2006; Levenspiel, 1999). Increasing the crystallization temperature has the same effect as increasing the crystallization time due to the higher rates of nucleation and crystal growth. This consequently accelerates the effects of Ostwald ripening. With coal fly ash as a feedstock source an increase in temperature during the aging step of synthesis increases the dissolution rate of both amorphous and crystalline phases (Querol et al., 1997). However, it was found that increasing the temperature favours the release of Si in solution more than Al (Catalfamo *et al.*, 1993; Elliot and Zhang, 2005). This occurrence can be attributed to the variation in dissolution characteristics of the different phases present in coal fly ash (Fernandez-Jimenez and Palomo, 2005).

2.2.5.3.7 Agitation

Mixing, as a unit operation, can be described as the process of increasing homogeneity, in process parameters, of a process medium to attain a certain level of uniformity (Paul *et al.*, 2004a). Casci (2005) reported that the scaled up version of the zeolite synthesis process will have to be performed in an agitated vessel. An unmixed system will result in non-uniformity in elemental concentrations throughout the reactor system resulting in the formation of different types of zeolites in the system. This results in an impure product and once this is formed it is

almost impossible to separate the different zeolite phases formed in the product (Marrot et al., 2001). Mixing is also needed during crystallization to transport nutrients to the surface of the growing crystals (Casci, 2005). However, mechanical agitation affects the nature of the precursor gel, crystal sizes, particle size distribution and mechanisms of crystallization (Ding et al., 2006). It was found that mixing in the early stages of synthesis reduces the overall reaction time compared to static aging (Molina and Poole, 2004). In a recent study it was found that during the aging step high shearing impellers like the 4-blade paddle are optimum (Mainganye, 2012; Mainganye *et al.*, 2013). On the other hand, high uneven shearing during the crystallization step causes a retarding and structure breaking effect (Bebon *et al.*, 2002; Marrot *et al.*, 2001).

2.2.6 Characterization of zeolites

Various techniques have been developed in order to characterize zeolites chemically, mineralologically and morphologically. In a book published by Auerbach et al. (2003) a full review of the various different characterization techniques can be found. However, in this section focus will be placed only on the techniques used in this study.

2.2.6.1 Mineralology by X-ray powder diffraction (XRD)

To determine the type of zeolite structure and its purity XRD is the most widely used technique by most researchers (Auerbach *et al.*, 2003c; Kokotailo *et al.*, 1995). The principals of X-ray diffraction were studied by von Laue over a century ago in 1912. The simplest way to explain the base principal of XRD is as follow. When a beam of electromagnetic waves impinges on a structure containing periodically arranged obstacles (atoms), and the distances between these obstacles are of similar magnitude as the wavelengths in that specific electromagnetic spectrum, then the waves become scattered (Cullity, 1956). Some of these scattered waves come together to form a new beam which is diffracted from the original beam as illustrated in Figure 2.7. According to Bragg's law the diffracted angle (2θ) is always twice the incident angle (θ in Figure 2.7). Due to the variation in distances between atoms in a crystal structure like zeolites, each crystal will diffract a beam of waves at various different angles. Therefore each crystal structure will have its own unique pattern/range of diffraction angles which becomes like a fingerprint of that material. As an example, Figure 2.8 illustrates the diffraction pattern of zeolite a plotted against the intensity (obtained from Chang & Shih, 1998). The intensity is a function of the concentration and crystallinity of the crystal in the material being analyzed. A full record of the diffraction patterns of known inorganic and organic materials is populated in the JCPDS database. It is therefore easy to determine a material's mineral identity and purity by

comparing it with the standard patterns in the JCPDS. Materials not documented in the JCPDS, which is rare, can be analyzed by determining the inter-planar spacing pattern of the crystal. Using Bragg's formula (Equation 2.2) the inter-planar spacing can be determined from the incident angle and wavelength of the incident x-rays(Cullity, 1956).

$$n\gamma = 2d \sin\theta$$

Equation 2-2

Where:

- γ = Wavelength of the incident x-ray wave beam.
- n = an integer.
- d = Inter-planar spacing.
- θ = Incident angle of the incoming x-rays

From XRD results a semi quantitative estimation of the phases in the sample can be made. Throughout this thesis this quantification is known as relative crystallinity. In order to determine relative crystallinity, standard XRD patterns for zeolitic material are required. The standard is the XRD patterns obtained from a pure phase zeolite product which is assumed to be 100% crystalline. By taking the sums of the XRD peak heights, the relative crystallinity of the zeolite in the mixed sample can be calculated with equation 2.3 below.

$$\%\, Relative\ crystalinity\ = \frac{XRD\ peak\ height\ sum\ (zeolite\ in\ mix\ phase)}{XRD\ peak\ height\ sum\ (zeolite\ standard)} \times 100$$

Equation 2-3

(Adapted from Szostak, 1997)

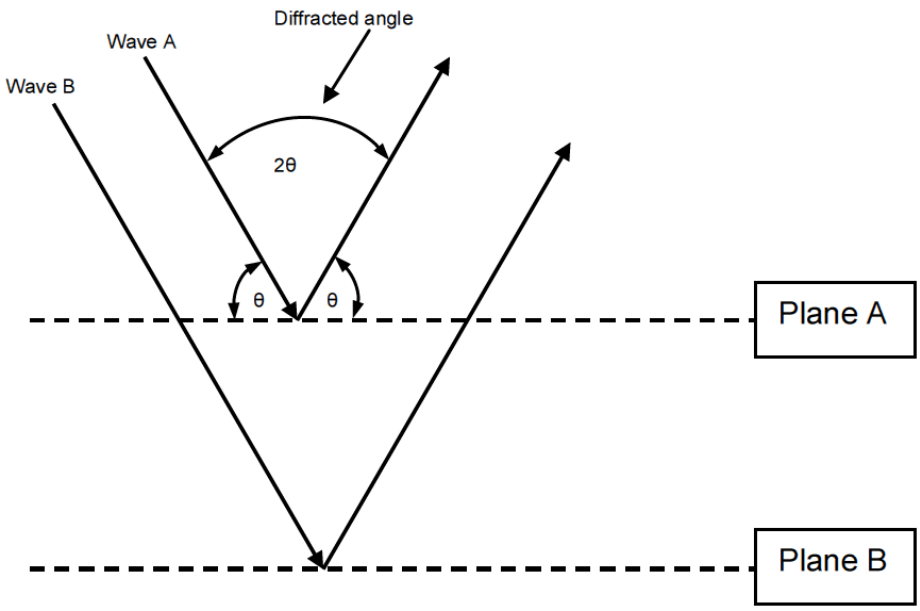

Figure 2-7: Graphical illustration of the concept whereby a beam of electromagnetic waves are scattered and then reformed to generate a diffracted beam of waves.

(Adapted from Cullity, 1956)

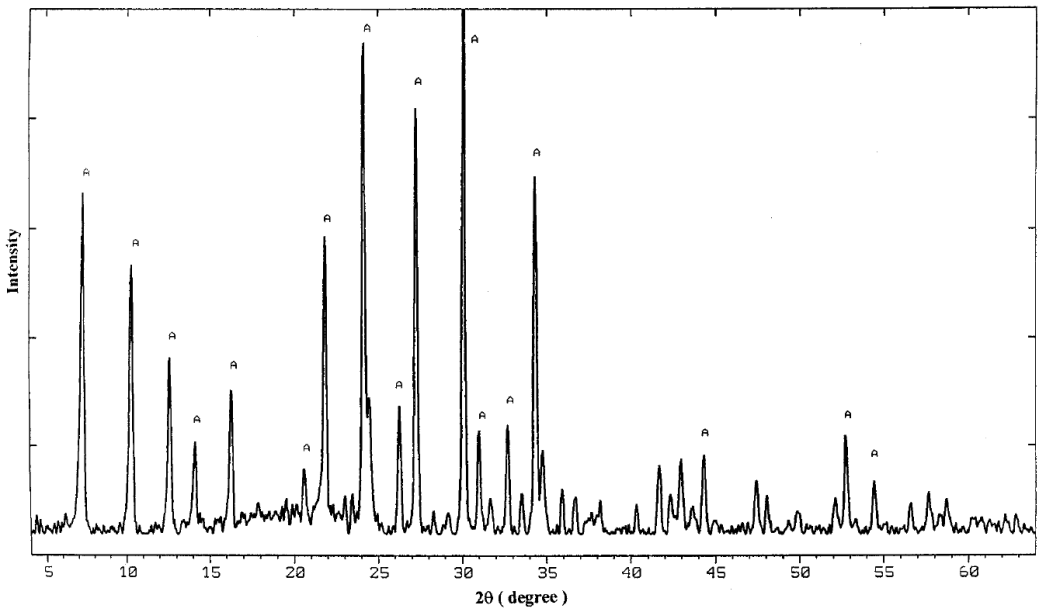

Figure 2-8: XRD pattern of zeolite A

(Obtained from Chang & Shih, 1998)

2.2.6.2 Structural analysis by infrared spectroscopy

The concept of infrared spectroscopy is based on the vibratory nature of atoms. The atoms of molecules have the ability to absorb infrared radiation at specific wavelengths leading to higher vibrational states (Stuart, 2005). Molecules can be seen as bodies wherein atoms are joined together (bonds) by spring-like forces. These bonds can change in length and move to a different plane and these actions are referred to as vibrations (stretching and bending vibrational modes). The one main rule to infrared absorption is that the vibrations should bring about a change in the dipole moment of the molecules (Stuart, 2005). When infrared radiation is passed through a sample, at varying wavelengths, and the radiation is absorbed at a specific wavelength the intensity of the signal at that wavelength is weakened. This weakened signal is recorded in the spectrum and displayed as a transmission or absorbance peak. Modern instruments plot results as either relative % absorbance or transmission (y-axis) against wavelength (x-axis usually in cm^{-1}). An improvement to the basic analysis with the incorporation of Fourier transforms (Fourier transform infrared spectroscopy, FT-IR) has greatly improved its accuracy (Stuart, 2005). Some samples are sensitive to the preparation techniques used in normal FT-IR and can be analyzed by means of reflectance methods. The attenuated total reflectance Fourier transform infrared spectroscopy (ATR-FTIR) method is widely used for difficult samples.

A comprehensive database of absorption spectrum bands for various zeolites was set up by Flanigen et al. (1971), making it very simple to determine the structural characteristics of zeolite samples. The three bands most common to zeolites can be found in the regions of 1250-950 cm^{-1}, 790-650 cm^{-1} and 500-420 cm^{-1}. These absorption bands are characteristic of the internal TO_4 (T = Si/Al) vibrations indicating the O-T-O asymmetrical stretching modes, O-T-O symmetrical stretching modes and T-O bending modes respectively.

2.2.6.3 Morphology by scanning electron transmission (SEM)

Scanning electron microscopy (SEM) is used to generate micrographs of nano-sized particles. It is the most widely used technique to analyze the morphology and size of zeolite crystals (Auerbach *et al.*, 2003c). The principal of scanning electron microscopy has been compared to scanning a wall in a dark room with a thin directional flashlight (FEI, 2010). One would scan the wall from side to side with the thin light source slowly moving up or down forming a mental image of the wall in one's memory. SEM works on the same principal except that instead of light a beam of electrons are used. A variation of signals are generated when the surfaces are bombarded with energized electrons which can be detected and an image generated from these

signals (Kutchko and Kim, 2006). The image can then be retrieve from the microscopes internal memory with computer software provided with the instrument. The resolution power of modern electron microscopes can be better than 1 nm (FEI, 2010).

2.2.6.4 Chemical analysis of solids by X-ray fluorescence spectrometry (XRF)

The principals of X-ray fluorescence spectrometry (XRF) is based on the effects X-ray bombardment has on atoms. When high intensity X-rays are passed through samples, the atoms are bombarded with enough energy for them to displace electrons (excited state). When these electrons return from their excited state to their original orbital, radiation is emitted within a certain spectrum(Mantler and Schreiner, 2000). Each atom emits radiation of a specific wavelength and by measuring this emitted radiation it is possible to determine the elemental composition of any solid sample (Cullity, 1956). This phenomenon is present in normal XRD analysis as well and for long it was seen as a nuisance until its use in compositional analysis was developed. The various elements present in a sample can also be quantified with XRF analysis. By comparing the intensity of the emitted radiation to that of a pure sample for that specific atom its weight % in the sample can be calculated (Cullity, 1956). One drawbacks of XRF analysis is that the sample being analyzed undergoes destructive preparation and cannot be recovered after analysis. Also, a fairly large sample is required for XRF analysis (±20 g).

2.2.6.5 Chemical analysis of liquids by atomic emission spectrometry (AES)

Inductively coupled plasma atomic emission spectrometry (ICP-AES) is an analytical technique used to identify and quantify elements in samples. The difference between this analytical technique and XRF is that ICP-AES is used on liquid samples and not powders. However, the principal of AES is based on the exact same principals as XRF. During analysis atoms are bombarded with enough energy to excite the electrons in the valance orbital of an atom and expel them. When they return to the original orbital they emit radiation which is captured and analyzed for each atom, i.e. the same concept as XRF.

In the first phase of ICP-AES the liquid sample is transformed into an aerosol, a process known as nebulisation. Next the aerosol is atomized in order to prevent the interference of the different radiation spectra of individual atoms. Plasma is used in this step to obtain the atomized state. The final steps are similar to XRF. The atoms' electrons are converted to the excited state and the radiation measured when they return to the relaxed state. The radiation emitted is then used to identify and quantify the elements present in the liquid sample. (Manning and Grow, 1997)

2.3 Ultrasonics

Ultrasound has been studied extensively over the past century. Applications of ultrasound are extremely diverse being applied in engineering, medical fields and process control. The following section is intended to introduce the basic fundamentals of ultrasound and to discuss some of its important applications.

2.3.1 Basic fundamentals

As the name suggests ultrasound is a study of sound waves and therefore forms part of physical acoustics. Due to this fact, it is not possible to prove exactly when first ultrasound was studied since the study of sound can date back centuries ago. Ultrasound, like all sound waves, requires a physical medium to exist and propagate through. Therefore ultrasound cannot move through a vacuum. In its simplest form these waves are vibrations of particles and its induction can be described by the sine function in mathematics (Ensminger and Bond, 2011a). Figure 2.9 illustrates graphically this mathematical function governing waves. The frequency of waves is the amount of wave periods/cycles passing a point in a medium per second. Ultrasound operates in a frequency above the hearing limit of the human ear which is most commonly above 16 kHz (Ensminger and Bond, 2011a). Another important factor of waves is its amplitude (Figure 2.9). The amplitude of waves has a great effect on the amount of energy transferred to the medium when the wave travels through it (Ensminger and Bond, 2011b).

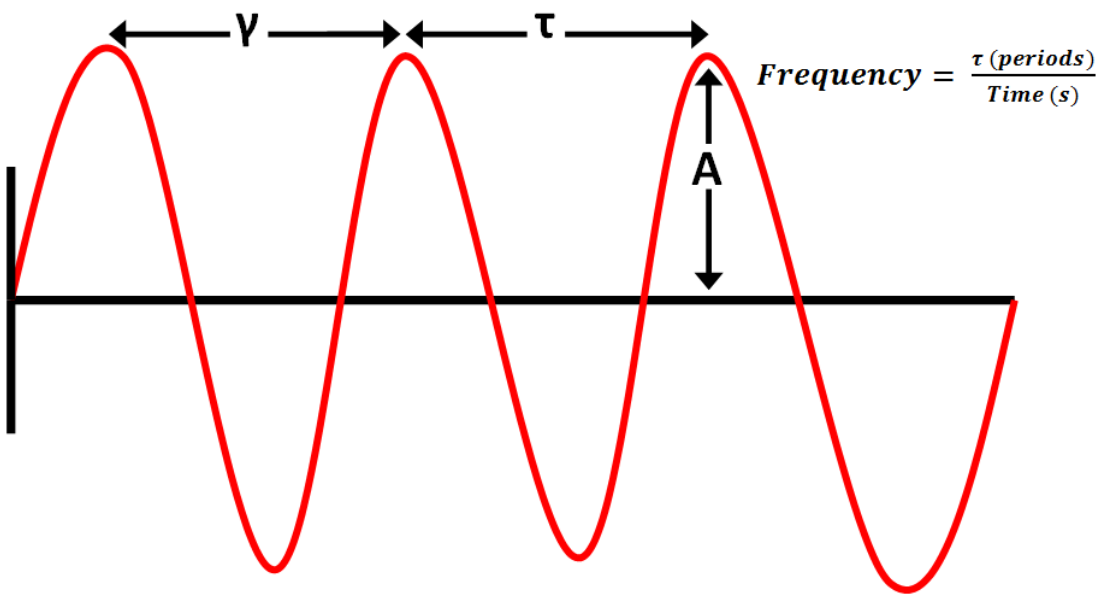

Figure 2-9: Representation of the sine function governing all acoustical and electromagnetic waves (γ) Wavelength (τ) Period Amplitude

Ultrasound shares several of the same properties of light, since light partly acts as a wave. When ultrasound passes through mediums of varying density its velocity changes (Skubas, 2003). This property of ultrasound has made it extremely useful in studying the physical properties of solid and liquid materials. Ultrasound can also be reflected, diffracted and scattered around the edges of objects (Ensminger and Bond, 2011a). This has made it a vital tool in industry and medicine as a sensor and imaging tool respectively.

2.3.2 Applications of ultrasound in zeolite synthesis

The use of ultrasound in the synthesis and application of zeolites is relatively new. A couple of studies utilizing lower intensity ultrasound has been published (Andaç *et al.*, 2006; Andaç *et al.*, 2005; Belviso *et al.*, 2011; Erten-Kaya and Cakicioglu-Ozkan, 2012; Wu *et al.*, 2006b). It was found that in all cases where ultrasound was applied during the crystallization step, the rate of crystallization increased dramatically (Andaç *et al.*, 2005; Belviso *et al.*, 2011). It was speculated that this was a direct result of the increase in crystallization temperature brought about by the ultrasound waves. However, similar end results were found when applying ultrasonic treatment during aging (Wu et al., 2006b). This was found to be a result of the formation of new nucleation sites during the aging process. It was also found that the average crystal sizes decreases making it possible to coat objects with very thin layers of zeolites (Andaç et al., 2006). This may a direct result of the generation of more nucleation sites as found by Wu et al. (2006b).

Ultrasound has been used extensively as a monitoring tool and analysis technique to determine physical properties of substances. In a recent study ultrasound was used as in-situ monitoring tool to study the crystallization of zeolite A from coal fly ash (Musyoka et al., 2012d). The authors reported that the use of ultrasound unveiled a greater degree of mechanistic and formation detail when compared to other techniques used to date.

High intensity sonication has also opened up exciting new opportunities in the synthesis of zeolites from coal fly ash (Musyoka, 2012; Musyoka *et al.*, 2011b). In 2012 Musyoka found that by applying high intensity ultrasound coal fly ash can be dissolved and converted directly into cancrinite within 30 minutes. This was possible due to the violent cavitation caused when a liquid is subjected to high intensity ultrasound. Cavitation is caused due to the formation of vapour bubbles in the low pressure regions of the ultrasound waves (Ensminger and Bond, 2011b). The vapour bubbles then collapses violently against the surfaces of objects transferring a considerable amount of energy in the process. This cavitation effect is one of the fundamental characteristics utilized in this study in order to minimise the energy consumption when synthesizing zeolite A from South African coal fly ash.

The use of ultrasound though is not only limited to the synthesis of zeolites. Very interesting results from a recent study illustrated how ultrasound can greatly enhance the application and recovery of zeolites. Erten-Kaya and Cakicioglu-Ozkan found in 2012 that the application of ultrasound during ion-exchange in zeolites increased the efficiency of ion uptake by up to 76%.

2.4 Material balances

Material balances form a vital part of any chemical engineer's role and responsibilities in both research and industry. The easiest way to explain material balances is to compare it with accounting. With material balances, engineers try to achieve with material what accountants try to achieve with financial data. In any chemical or physical process all the material in the system has to be accounted for. It is merely an application of the law of conservation of mass as discovered in 1789 by Antoine Lavoisier(Himmelblau and Riggs, 2004). The law of conservation of mass states that material cannot be created or destroyed. This holds true in all processes except for nuclear reactions where mass is converted to energy according to Albert Einstein's famous mass/energy relationship he proposed in 1905.The first step in performing material balances is to define the systems boundary. The system boundary defines the system limits around which to perform the balance. Figure 2.10 illustrates a simplified block flow diagram of the 2 step process of converting fly ash into zeolites. The red dashed line represents the system

boundary around the entire process, while the green dashed line defines only a single unit operation in the process. The arrows crossing the boundary lines illustrate the flow (input and outputs) of material in and out of the system.

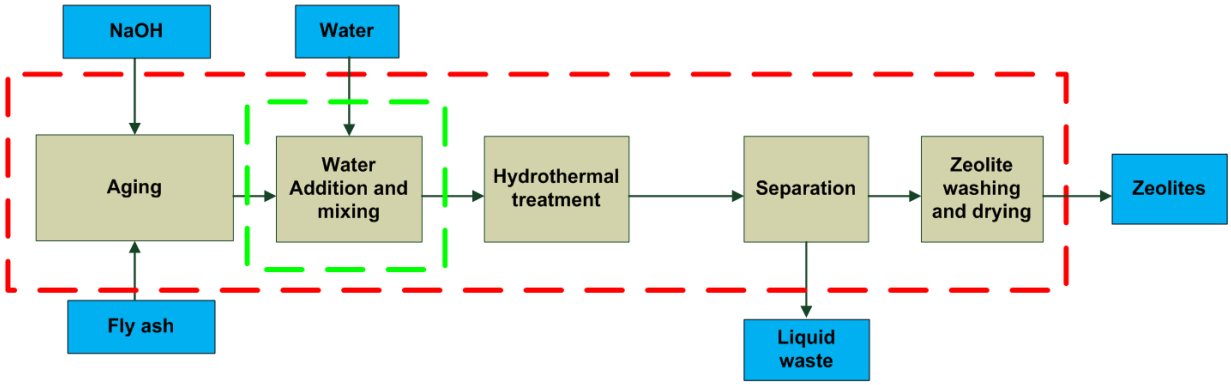

Figure 2-10: Block flow diagram depicting the 2 step method of converting fly ash into zeolites.

Generally three types of material balances exist namely overall, component and elemental balances (Himmelblau and Riggs, 2004). As an example, Figure 2.11 illustrates a single unit operation (defined by a system boundary) on which the three different material balances were performed. The green arrows represent material entering the system while red arrows indicate material exiting across the system boundary. The figure illustrates a simple operation where 10 g concentrated (conc.) NaOH is diluted with the addition of 100 g water. The purpose of the overall material balance is to determine the total flow of material across the system boundary. In the component balance the masses of the individual components, in this case compounds are determined. In the case depicted by Figure 2.11 (B) these different components are the various compounds present. The components can then be broken down further to determine the amounts of individual elements that exist in the material stream (Item C in Figure 2.11). The amounts in Figure 2.11 are expressed in terms of weight. However, they can be expressed in volume, mole, volume fraction, weight fraction and mole fractions as well. By using the density and molecular weights these weights can be converted into volume or mole respectively.

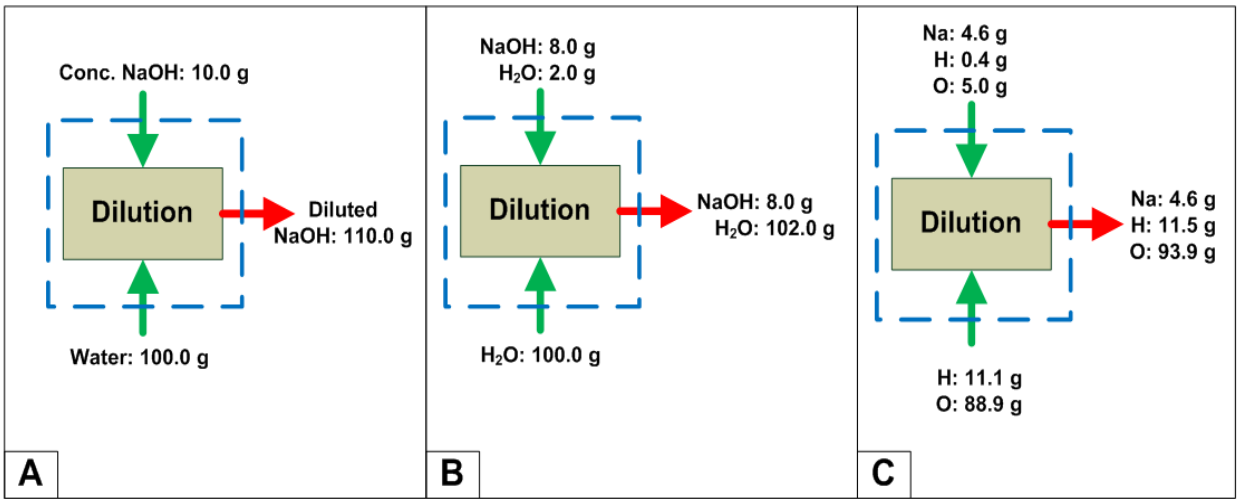

Figure 2-11: Block flow diagrams illustrating the various types of material balances A) Overall material balance B) Component balance C) Elemental balance.

The next step, and most important step of all, is deciding on a basis for the material balance (Himmelblau & Riggs, 2004). The material balance needs to be based on a fixed or known material stream or amount. In the example depicted in Figure 2.11, by taking a basis of 10 g concentrated NaOH, the other streams could be calculated based on this amount.

In the synthesis of zeolites from coal fly ash it is vital to know the fate of the toxic elements for legal and environmental considerations. Very little literature is available on this subject matter and therefore this study attempted to fill this literary gap. An extremely large variety of elements exist in coal fly ash making material balances a very arduous task. The first aspect of it involves analysis of the different product and raw material streams crossing the system boundary. The composition of solid materials can be determined with great accuracy by XRF analysis while liquid samples can be analyzed with ICP-AES. Since the synthesis of zeolites from fly ash is done on microscale, variations in the weights of products obtained greatly influences the accuracy of material balances. The one mass that researchers has control over is the amount of raw fly ash fed to the synthesis system. For this reason it is most accurate to make the raw fly ash feed weight and composition the basis of all calculations.

2.5 Hazard and operability studies

Identifying risks in an operations environment is a crucial activity to ensure safe and reliable production. Operations staff should consistently be aware of the possible risks affecting their safety, the safety of the environment and the reliability of production. However, identifying risks in the design phases of a process is equally if not more important. The technique utilized to

identify risks and operation hazards is the well known HAZOP, short for hazard and operability study. A book written by Trevor Kletz in 1999 titled “HAZOP and HAZAN” explains in detail the importance and procedures of HAZOPS. The book is highly recommended for process engineers wishing to acquire a better understanding of the procedures involved in performing a HAZOP. The HAZOP is a systematic hazard identification process and its development dates back to 1963 (Kletz, 1999). By performing a HAZOP study it aids the engineer not only in identifying and preventing operation problems, but also identifying required control configurations and shortcomings in operating procedures. Figure 2.12 illustrates the different steps of the HAZOP process. The process was simplified to be applied to the zeolite synthesis system which is a batch operation. The first step is to generate a deviation which is done by combining a guide word with a variable. Guide words can be any of the following words listed below:

- Less of
- More of
- None
- Reverse
- Other than
- As well
- Part of

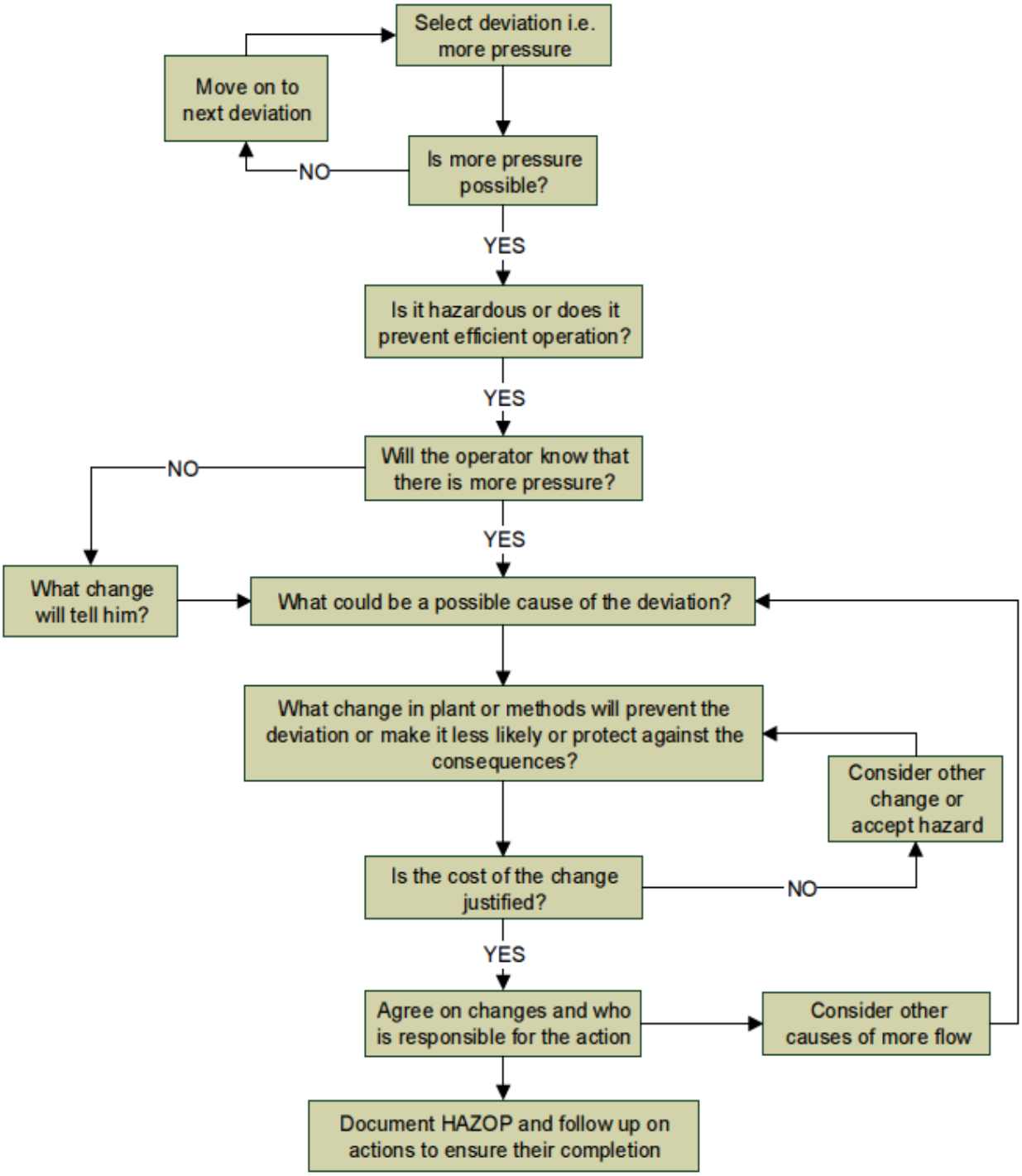

Figure 2-12: Basic HAZOP procedure

(Adapted from Kletz, 1999)

By combining one of the guide words such as “More of” with a process variable like pressure a deviation is generated, i.e. more pressure (Higher pressure). The next step is to decide whether the deviation is hazardous by looking at its consequences and causes. It is also vital to determine whether the operator of the plant or vessel will be able to see the deviation by means of a measuring instrument or alarm. If it was determined that the deviation is in fact hazardous then changes to the plant, vessel, operating procedures or training needs to be considered in order to prevent such an event or mitigate its effects. If the change is justified the task is delegated to the responsible parties and documented. The guide word is then applied to the next variable until all variables have been covered, after which another guide word is chosen and again applied to each variable. In this way all possible deviations are systematically identified and their effects mitigated. It is important to understand that not all the steps described in Figure 2.12 are documented, and some steps omitted from the Figure 2.12 may be documented. Each institution or department may have their own HAZOP form and procedures based on their own requirements and preferences.

Table 2-6 below illustrates a simple HAZOP template form used in this study. This type of simple layout is commonly used in the conceptual process and equipment design stages. Before the zeolite synthesis system can be scaled up to 0.5-1.0 kg scales the principal reactor design will have to be closely scrutinized by means of a HAZOP study. The autoclave reactor design, discussed in chapter 8, would be required to reach temperatures of >140 ^{o}C. All safety and operability hazards need to be minimised in order to prevent equipment failure costs, environmental contamination and operator injuries.

Table 2-6: HAZOP template

Process unit:					
Guide word	**Deviation**	**Cause**	**Consequence**	**Action**	**Ref No.**

After commissioning a plant or vessel, HAZOP’s are performed on a periodic basis or before a process/equipment change is made to the existing vessel. Statistical process data is documented and used in these HAZOP’s to determine the probability and risk level of each deviation.

2.6 Chapter summary

In this chapter the most relevant and important literature regarding coal fly ash, zeolites, zeolite synthesis, analytical techniques and engineering concepts was highlighted. The properties of fly ash was discussed in an attempt to shed light on its impact on the environment and also its potential use as a feedstock in zeolite synthesis. Zeolites are used in various industries as catalysts, molecular sieves and cation exchange beds. This is due to their diverse structures and unique physical and chemical properties. Various mechanisms and synthesis routes were discussed whereby fly ash can be used to prepare zeolites on a bench scale. The gaps in literature required for the upscale synthesis of zeolites from fly ash was highlighted in this chapter.

The upscale synthesis of zeolites require principal process engineering activities to be performed on the bench scale process. This chapter discussed the core engineering techniques applied to the process in an attempt to gather critical information for upscale purposes. The chapter also discusses the shortcomings of the synthesis process from an process engineering viewpoint.

CHAPTER 3

3 Distributional fate of elements during the synthesis of zeolites from South African coal fly ash.

3.1 Introduction

The use of coal fired power stations dates back to the 1880's over 100 years ago (Termuehlen and Emsperger, 2003). During the generation of electricity, the combustion of coal leads the formation of incombustible solid residues. Of these residues, fly ash is the finest of the particulates and is produced the greatest volume (Scheetz and Earle, 1998). In a developing country such as South Africa, where coal supplies are abundant, the use of coal as source of energy forms a core part of economic growth. However, the cost of managing the effects caused on the environment has become a nationwide concern.

In South Africa a total of 36 Mt coal fly ash is produced annually from electricity generation alone (ESKOM, 2010). On average 95% of the fly ash generated is disposed in ash dams and dumps (ESKOM, 2010). The construction and maintenance of these dams requires large vacant land and has become a economic concern for South Africa's national power supplier. Once the land has been utilized for the disposal of fly ash it is close to impossible to rehabilitate the soil in order to make it suitable for crops or any form of organic life (Haynes, 2009). The reason for this irreversible damage is due to the slow release of toxic elements from coal ash, as well as the changes in soil pH from the release of CaO (Dosskey and Adriano, 1993; Jegadeesan *et al.*, 2008; Pandey *et al.*, 2011; Tsiridis *et al.*, 2012). Thus far the only major use of fly ash has been as an additive in Portland cement (Kruger, 1997). The production of fly ash greatly outweighs the volumes required by the building industry thus limiting its use. With plans to increase South Africa's coal fired electricity generation capacity (Rafey and Sovacool, 2011), it is crucial to explore other alternative uses for coal fly ash with a view to minimise its environmental impact.

In numerous studies it has been determined that the main constituents in fly ash are Al_2O_3, Fe_2O_3, SiO_2 and CaO (Hower *et al.*, 1996; Koukouzas *et al.*, 2007; Lyer and Scott, 2001; Scheetz and Earle, 1998). Due to the high concentrations of SiO_2 and Al_2O_3 it is a suitable feedstock in the synthesis of zeolites as was first discovered by Höller and Wirsching in 1985 (Höller and Wirsching, 1985). Since the first work done on the subject matter various authors investigated the synthesis of a range of different zeolites from coal fly ash (Chang and Shih,

1998; Hollman *et al.*, 1999; Molina and Poole, 2004; Rayalu *et al.*, 2000; Steenbruggen and Hollman, 1998). However, very little work has been done in an effort to use South African coal fly ash.

In recent endeavours studies have been performed with a view of synthesizing high quality zeolites from South African coal fly ashes (Mainganye *et al.*, 2013). In the studies performed to date it has been possible to synthesize a range of zeolites using different South African coal fly ashes and different synthesis techniques. These zeolites include zeolite Na-P1, X, A, sodalite, cancrinite and analcime(Mainganye *et al.*, 2013; Musyoka *et al.*, 2012b; Musyoka *et al.*, 2011a). The use of fly ash as a feedstock in the synthesis of zeolites is a promising alternative to the current environmental predicament caused by its disposal. However, South African coals have been shown to contain various toxic elements such as As, Pb, Sb, Ba, V etc. (Wagner and Hlatshwayo, 2005). These elements are concentrated mostly in the fly ash during the combustion process due to the physical characteristics of this finer ash (Bhanarkar *et al.*, 2008; Nathan *et al.*, 1999). This aspect greatly complicates its use as a feedstock in zeolite synthesis. Details regarding the fate of these toxins during the synthesis process are not known. Environmental conservation is governed by strict legislation in South Africa such as the National Environmental Management: Waste Act 59 of 2008.

Two principal processes have been used to synthesize zeolites with South African coal fly ashes. The first process consists of two steps namely alkaline aging of the ash followed by hydrothermal treatment (Musyoka *et al.*, 2012a; Musyoka, 2009; Musyoka *et al.*, 2012c; Somerset *et al.*, 2005a; Somerset *et al.*, 2005b). The second synthesis route makes use of a pre-fusion step (Musyoka et al., 2012b). The fly ash is fused at high temperatures in order to dissolve the various components in the ash and generate soluble sodium silicates and aluminosilicates(Molina and Poole, 2004). Thereafter the Si and Al components are extracted from the fused ash and hydrothermal treatment applied whereby zeolites are formed. However, the fate of the elements originating from the fly ash is unknown in either of these two processes. To date no studies have been performed in which accurate material balances were conducted over these synthesis systems. It is vital to determine the distribution of the toxic elements origination from coal fly ash between the zeolitic products and the associated waste, i.e. whether the elements report to the liquid/solid wastes or the zeolite itself. This will enable environmental management plans to be set out for each process. Also, tracking the elements in these systems will allow for accurate determination of yields and yield efficiencies.

The aim of this study was to determine the distributional fate of elements during the two principal zeolite synthesis approaches. The first objective was to determine the elemental composition and mineralogy of the raw feedstock, products and wastes. The second objective was to perform overall material balances in order to accurately quantify the weights of the various products and wastes resulting from the two processes. Lastly, to perform an elemental balance with the data obtained from the overall material balance and the elemental composition data.

3.2 Experimental Section

3.2.1 Experimental approach

In order to determine the fate of elements originating from coal fly ash during the synthesis of zeolites, a generalized approach was formulated. The first step was to identify the compositional characteristics of the raw fly ash feed used. After determining the composition if the feed a basis needed to be determined for the material balance. Before commencing with the overall material balance, zeolites were synthesised and the results obtained by Musyoka *et al.* 2012b confirmed. After performing the overall material balances, the elemental compositions of all material streams crossing the system boundaries were determined in order to perform detailed elemental balances and determine the distributional fate of elements in the system.

3.2.2 Zeolite synthesis

3.2.2.1 2-step alkaline activation method

The zeolite synthesis procedure was adopted from Musyoka (Musyoka et al., 2012c) which consists of two steps i.e. aging followed by hydrothermal treatment. The aging step was performed in a 100 ml double walled glass reactor (Figure 3-1). The reactor was connected to a variable temperature water bath which maintained the aging medium at 47 ^{o}C (Figure 3-2). First 50 ml 5 M NaOH solution was prepared and preheated inside the 100 ml glass reactor. Once the NaOH solution reached the required temperature the aging step was initiated with the addition of 10 g of coal fly ash to the heated solution. The aging medium was stirred utilizing a 4-blade paddle impeller at 200 rpm as recommended by Mainganye *et al*. (2013). The aging step then proceeded for 48 hours. The aging step is characterised by the formation of the pre-cursor gel. The process follows the general mechanism outlined in section 2.2.4.1. Depolymerisation of the feedstock occurs to form Si monomers. The monomeric species are joined together to form larger building units and regions with semi-regular arrangements, which is characteristic of the intermediate gel formation.

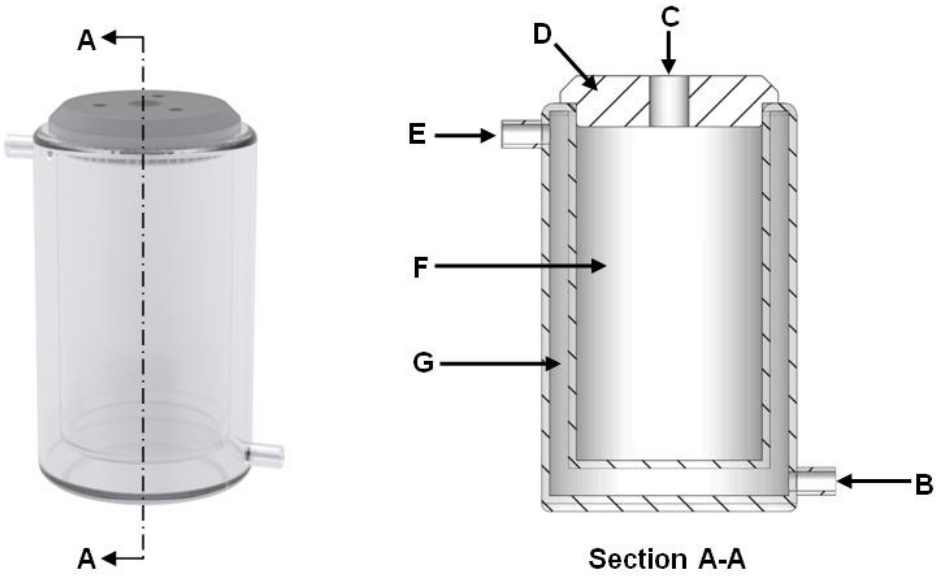

Figure 3-1: Double walled glass reactor used during the aging step (A-A) Section cut-out view (B) Hot water inlet (C) Cut-out in reactor lid allowing the impeller shaft to pass through (D) Reactor lid (E) Hot water outlet (F) Reaction volume (G) Heating/cooling water space surrounding the inner reactor wall

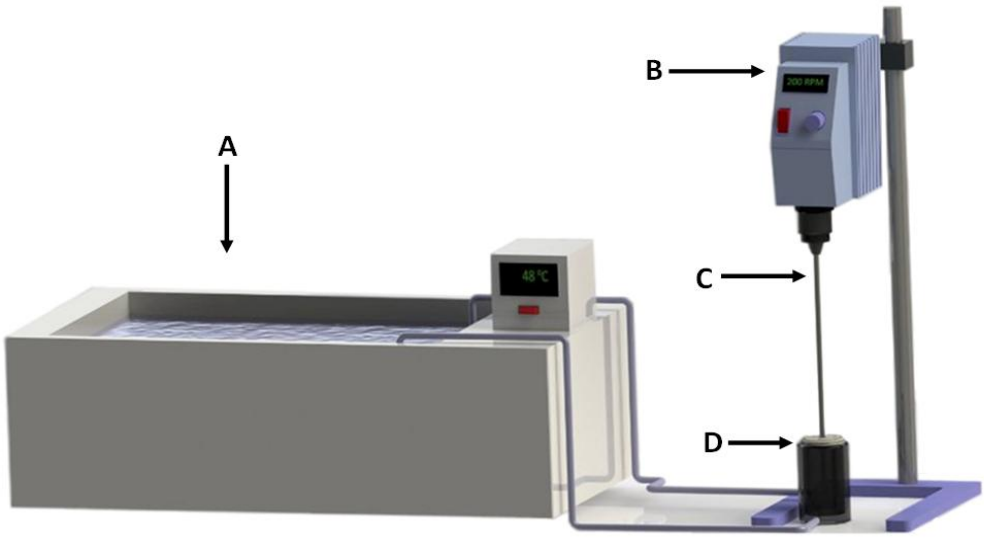

Figure 3-2: Experimental setup for aging step (A) Water bath (B) Variable speed mixer (C) 4-blade paddle impeller (D) Double walled glass reactor

After the aging step, 75 ml ultrapure water was added to the aged medium under agitation, after which the mixture was transferred into Teflon lined autoclave reactors (Figure 3-3). The autoclave reactor used was the 23 ml general purpose digestion vessel from the Parr Instrument Company (Model number: 4745). The autoclave reactors were placed in a hot air oven at 140 ^{o}C in order for the hydrothermal treatment stage to commence. The hydrothermal stage proceeded statically for 48 hours after which the solid zeolite product was separated from the liquid waste supernatant through filtration. The zeolite product was then washed with 2500 ml ultrapure water and dried in a hot air oven at 80 ^{o}C. During the hydrothermal treatment step, crystallisation occurs by means of the general nucleation and crystallisation mechanism as illustrated in Figure 2-6. The two step method does not make use of any Si or Al additives to alter the Si/Al ratio. Throughout the synthesis process the only source of Si and Al originates from the raw fly ash feedstock.

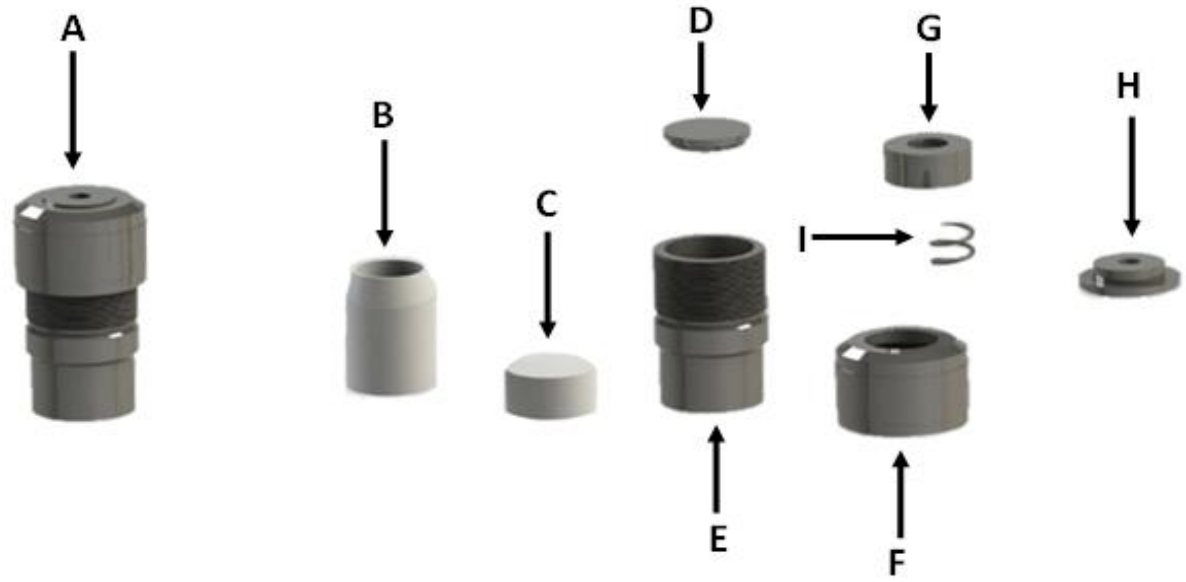

Figure 3-3: Parr bomb reactor assembly (A) Assembled reactor (B) Teflon lining (C) Teflon lid (D) Bottom metal plate (E) Metal casing (F) Metal lid (G) Metal weight keeping teflon lid in place (H) Top metal plate (I) Spring separating metal weight and top plate

3.2.2.2 Fusion assisted synthesis

The method used to produce zeolite A from South African ash was adopted from work done by Musyoka et al. (2012b). The process starts off by mixing coal fly ash with crushed analytical grade sodium hydroxide in a mass ratio of 1:1.2 (ash: NaOH). The mixture of NaOH and fly ash

was then fused at 550 °C for 90 min in an electrical furnace (Figure 3-4). The fused ash was allowed to cool to ambient temperature and then ground into a fine powder using a mortar and pestle. 50 g of the ground ash and 250 ml ultrapure water was added to a rectangular plastic mixing vessel (Figure 3-4). The mixture was closed and agitated with an overhead stirrer equipped with a 4-blade paddle impeller mixing at a speed of 1400 rpm for 120 minutes to allow extraction of Si and Al into solution. This step was performed at ambient temperature. The mixing vessel was not equipped with baffles due to the fact that the corners of the vessel broke the tangential flow (Paul *et al.*, 2004b) inducing a baffling effect which improved mixing. The mixed slurry was then filtered and the clear solution's Si/Al adjusted by the addition of 0.59 M sodium aluminate solution in a volume ratio of 5:2 (clear solution: sodium aluminate solution). The mixture was agitated, at ambient temperature, using a magnetic stirrer for approximately 10 min or until a milky suspension started to form. The aluminate solution was made up by dissolving analytical grades sodium aluminate and sodium hydroxide in separate batches of ultrapure water. The NaOH and $NaAlO_2$ were dissolved in ultrapure water in mass ratios of 50:4.8 (ultrapure water: NaOH) and 50:2.4 (ultrapure water: $NaAlO_2$) respectively. The two solutions were then added together and mixed using a magnetic stirrer for 30 min.

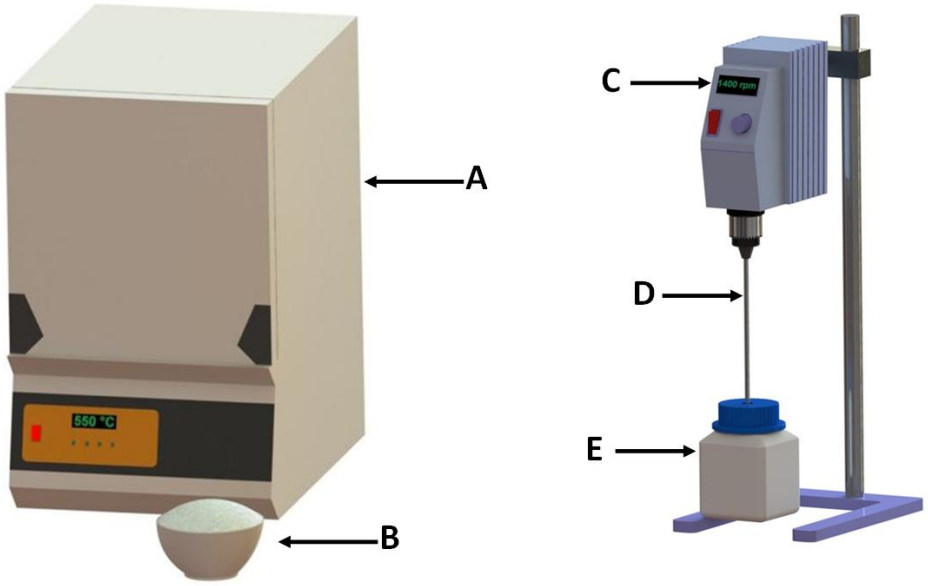

Figure 3-4: Experimental setup illustrating the fusion of ash and extraction of Si and Al from fused ash (A) Electrical furnace(B) Mixture of fly ash and NaOH powder in a crucible(C) Overhead stirrer set at 1400 rpm(D) 4-blade paddle impeller(E) Rectangular mixing vessel

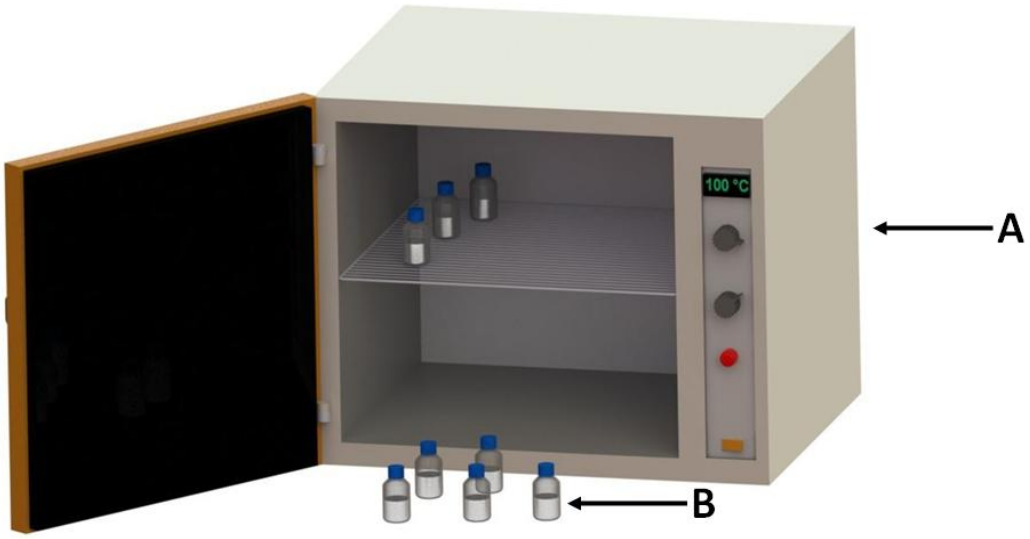

Figure 3-5: Experimental setup illustrating the hydrothermal treatment step whereby zeolite A crystals are formed (A) Hot air oven(B) 250 ml glass bottles containing adjusted clear solution ready for hydrothermal treatment

The milky solution was then transferred into 250 ml glass bottles in aliquots of 100 ml per bottle. The solutions were then subjected to static hydrothermal treatment by placing the glass bottles in a hot air oven for 120 min at 100 °C (Figure 3-5). The products were then separated by filtration and washed with ultrapure water. The supernatant wastes and washing water wastes obtained from filtration were retained for further analysis. The washed zeolite product was dried at 80 °C in a hot air oven after which it was crushed and stored in airtight containers.

The fusion assisted synthesis approach does not follow the general mechanism as set out in section 2.2.4.1. Instead of forming a pre-cursor gel, the fusion step dissolves the feedstock to form dissolvable sodium silicates and aluminosilicates (Molina and Poole, 2004). Therefore, unlike the 2-step process, this process makes use of only the filtrate obtained after extracting the Si and Al species from the fused ash. The solid residue, after filtration, is discarded. Another core difference between these two synthesis approaches is the addition of the sodium aluminate solution.

3.2.3 Materials and characterization techniques

The coal fly ash used in this study was collected from a power station situated in Mpumalanga, South Africa. Analytical grade sodium hydroxide pellets were used for the preparation of 5 M NaOH solutions and sodium aluminate solutions. Ultrapure water was use in all water applications during the process which includes the preparation of all solutions, water addition

step during the 2-step method and washing of zeolite products. The elemental composition of all solid material; including raw fly ash, zeolite products and solid waste; was determined by performing X-ray fluorescence (XRF) spectrometry. The instrument used for this analysis was the ARL 9400XP+ wavelength dispersive XRF spectrometer. Elemental concentrations in liquid products and wastes were determined with inductively coupled plasma atomic emission spectrometry (ICP-AES). The instrument used to perform ICP analysis was the Agilent 7500ce. All liquid samples were diluted 100 times with 2% analytical grade nitric acid solution before analysis. The mineralogy of zeolite products was revealed by means of X-ray powder diffraction using Cu-Kα radiation in a range of $4<2\theta<60$. All quantitative XRD analysis was done on a Philips PW 1390 XRD diffractometer.

3.3 Results and Discussion

3.3.1 Raw material characterisation

The mechanism for zeolite formation dictates that primary TO_4 tetrahedral (T = Al or Si) building blocks are first joined together by sharing an oxygen atom to form secondary building blocks (Barrer, 1982). The secondary building blocks are then rearranged to form zeolite structural groups. For this reason the mineralogy of the feedstock is of great importance. Figure 3-6 illustrates the mineralogy of the coal fly ash used in this study, as observed through powder X-ray diffraction. The XRD pattern indicates that the mineral phases in the fly ash consist of mainly quartz and mullite. The broad hump in the diffraction range of 20-30$2\theta$ illustrates the presence of an amorphous aluminosilicate phase. From quantitative X-ray diffraction techniques the % weight contribution of each of these phases was determined and is illustrated by the pie chart in Figure 3-6. The amorphous phase contribute to nearly 50% of the ash while large amounts of quartz and mullite exist. These phases need to be dissolved during the synthesis process in order to free the Si and Al and make them available for the crystallization process. However, the existence of these different mineral phases complicates the mechanism of zeolite formation due to the fact that they dissolve at different rates (Fernandez-Jimenez and Palomo, 2005).

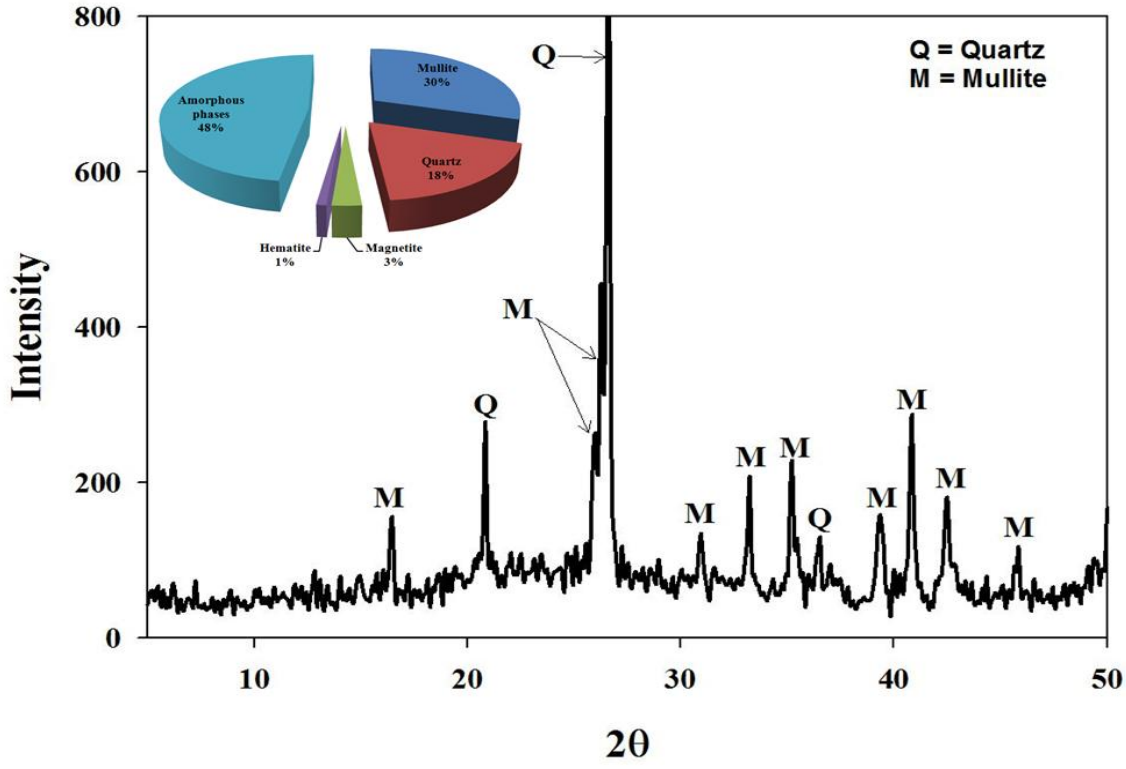

Figure 3-6: Powder X-ray diffraction patterns of coal fly ash from the Arnot power station

Table 3-1 illustrates the major oxides and trace elements in Arnot fly ash as presented by X-Ray Fluorescence spectroscopy analysis (XRF). The fly ash used in this study was classified as class F ash, whereby the + Al_2O_3 + Fe_2O_3 mass exceeds 70% of the total fly ash mass. The major elements found in the ash were Si and Al, which are the two main elements which zeolites are composed of. The ratio of SiO_2/Al_2O_3, a factor greatly influencing the mechanism of zeolite formation (Cao and Shah, 2007), was found to be 1.76 (Cao and Shah, 2007). The ratio of available Si and Al in solution determines which zeolite structural groups are formed and ultimately which zeolite crystal (Molina and Poole, 2004; Querol *et al.*, 1997). The ratio of Si to Al also determines what crystallization mechanism takes place during the formation of the zeolite crystals (Cao and Shah, 2007). Amongst the trace elements, the most concentrated elements were found to be Sr, Ce and Ba. It is clear that the toxic elements found in South African coals (Wagner and Hlatshwayo, 2005) are concentrated in the fly ash during the combustion process.

By performing material both overall and elemental material balances the distribution of these elements throughout the zeolite synthesis process were tracked. The final destination of toxic

elements will greatly affect the disposal costs and pre-treatment requirements as set forth in South African legislation (South African Government, 2008).

Table 3-1: X-ray fluorescence results of Arnot coal fly ash illustrating the quantities (wt%) of the major oxides and trace elements (ppm) that it's composed of

Major oxides (mean wt%)		Trace elemental concentrations (ppm)	
Al_2O_3	31.51	Ba	486
CaO	3.76	Ce	254
Fe_2O_3	4.94	Co	30
K_2O	0.47	Cu	110
MgO	1.18	Nb	37
MnO	0.03	Ni	125
Na_2O	0.04	Pb	90
P_2O_5	0.30	Rb	56
SiO_2	55.44	Sr	989
SO_3	0.06	V	79
TiO_2	1.11	Y	94
Loss On Ignition	1.22	Zn	135
SiO_2/Al_2O_3	1.76		

3.3.2 Synthesis and material balance using the 2-step synthesis method

Figure 3-7 illustrates the XRD results obtained after synthesizing zeolites from fly ash using the 2-step approach. Two main zeolite products were obtained namely analcime and Na-P1. These results are comparable to those obtained by Mainganye(2012) when applying the same operating conditions. With the author's results successfully reproduced the next steps of the material balance approach were initiated. The basis of the material balances performed over this synthesis process was taken as 10 g of fly ash feed. Figure 3-8 illustrates a simple block flow diagram of the synthesis process with the respective weights of material crossing the system boundary. From this overall material balance it was seen that from 10 g of fly ash, on average, 9.7 g of zeolite product was obtained.

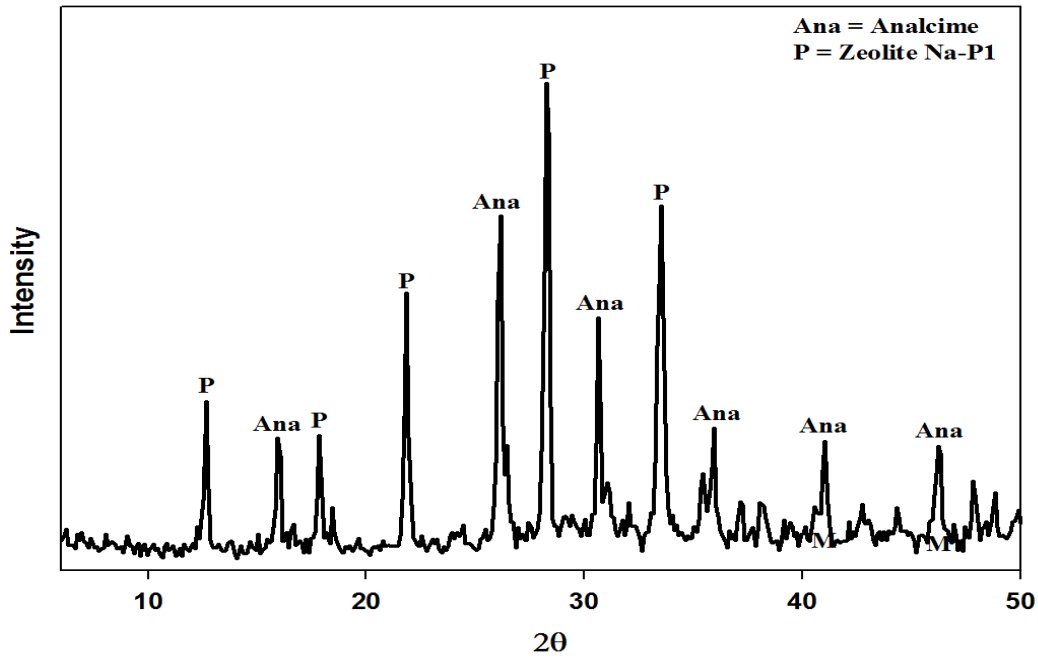

Figure 3-7: X-Ray powder diffraction patterns illustrating the two zeolite crystal products produced by applying the 2-step method as synthesis approach

The water used to wash the zeolite products could be recovered effectively through filtration. From the 2500 ml ultrapure water passed through the zeolite product, 2490 ml liquid could be recovered. On average 110 g of liquid supernatant waste resulted from the synthesis process. The overall balance also revealed that 25.3 g of losses resulted from the process in the form of water vapour. It was assumed that the vapour contained no trace elements. These losses were due to evaporation at two main stages in the process. The aging step was performed in an open reactor which allowed vapour to escape. It is recommended that an improved (sealed) reactor design should be considered for this stage. The second step where water loss occurs is during drying of the zeolite product in a hot air oven.

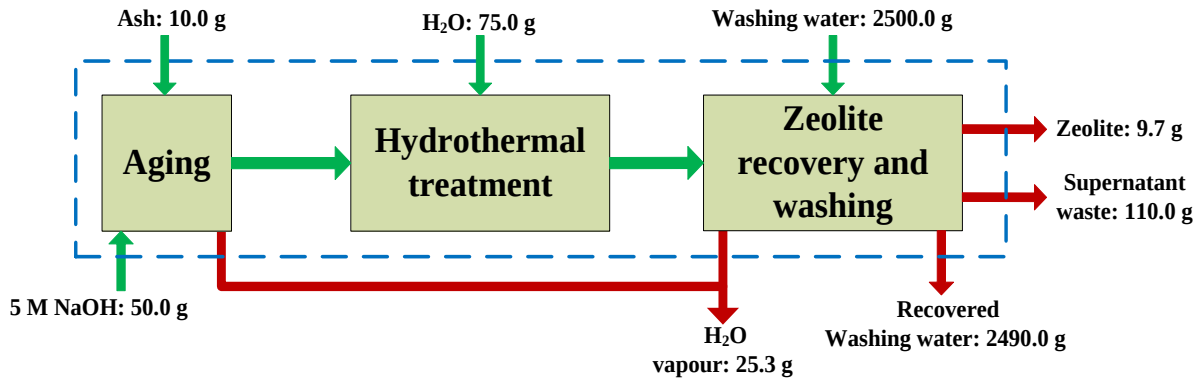

Figure 3-8: Block flow diagram illustrating the overall mass balance of the 2-step method

Table 3-2 illustrates the weight% distribution of elements from fly ash amongst the various products and wastes generated during the synthesis process.

Table 3-2: Elemental balance illustrating the distribution of the elements (wt%) originating from fly ash amongst the wastes and zeolite product resulting from the 2-step synthesis method

Fractional mass distribution of elements originating from coal fly ash			
Element	Zeolite product	Supernatant waste	Washing water
Al	81.5%	15.8%	2.7%
Ba	100.0%	0.0%	0.0%
Ca	100.0%	0.0%	0.0%
Ce	100.0%	0.0%	0.0%
Co	100.0%	0.0%	0.0%
Cu	100.0%	0.0%	0.0%
Fe	86.5%	11.4%	2.1%
K	49.4%	50.6%	0.0%
Mg	100.0%	0.0%	0.0%
Mn	100.0%	0.0%	0.0%
Na	12.4%	45.2%	42.3%
Nb	80.7%	3.2%	16.2%
Ni	64.5%	35.5%	0.0%
P	3.2%	78.9%	17.9%
Pb	63.2%	21.4%	15.5%
Rb	78.2%	17.9%	3.9%
S	100.0%	0.0%	0.0%
Si	72.2%	23.7%	4.1%
Sr	100.0%	0.0%	0.0%
Ti	100.0%	0.0%	0.0%
V	50.8%	49.2%	0.0%
Y	100.0%	0.0%	0.0%
Zn	100.0%	0.0%	0.0%

For supporting data, used to perform the material balances, refer to Appendix A. As can be seen from table 3-2, most of the Si and Al from fly ash, 72.2% and 81.5% respectively, reports to the zeolite product. Nearly 50% of the K from the fly ash reported to the zeolite product which could possibly have as a competing charge stabilizing ion (Querol et al., 1995). However, at this point in the investigation it was not clear whether the K was incorporated in the zeolite pores as charge stabilising ions. The values for Na in table 2 takes into account the total Na input into the system i.e. from fly ash and the 5 M NaOH solution. A mere 12.4% of Na incorporated into the zeolite product points to a great wastage of NaOH in the system. The possibility of recycling waste streams containing this product needs to be investigated. With 23.7% of the Si and 15.8% Al still left in the supernatant waste there is some room for improvement in conversion efficiency. It was found that most elements in the fly ash remain in the solid zeolite product. From the list of elements 100% of Mn, Mg, Ca, Ti, S, Ba, Ce, Co, Cu, Sr, Y and Zn were found in the synthesized product. Although it is not known what affect this has on the application of the zeolite products, it does make disposal of the spent material less complicated. It has been shown that the elements originating from fly ash show relatively low mobility when included in the solid products (Akar et al., 2012). It was found that when CaO is included in the fly ash these elements tend to stay in solid form and not leach into solution (Akar *et al.*, 2012; Izquierdo and Querol, 2012).From XRF results (Table 3-1) it was seen that the fly ash used in this study had a significant amount of CaO (3.76%). For this reason it was speculated that these elements did not leach into solution to form part of the zeolite structure. The only elements found in significant quantities in the supernatant waste were Si, Al, Fe, Na, K, P, Ni, Pb, Rb and V. The presence of these elements complicates the disposal of the liquid waste. Toxic elements such as Pb, Nb and Al are of especially great concern due to their toxic nature. Treatment, especially the neutralisation of the NaOH in solution, and disposal of this liquid waste would be an expensive process operation. This questions the feasibility of the initiative to synthesize zeolites from coal fly ash. The possibility to recycle the liquid waste needs to be given serious consideration in order to promote scale-up of this process. It is expected that these elements should accumulate in the liquid waste if it is recycled. Traces of two other highly toxic elements, namely As and Hg, were found in the supernatant waste. These two elements were not included in the material balance since they could not be detected through XRF analysis. The average concentration of As and Hg in the supernatant waste were found to be 0.5 ppm and 0.2 ppm respectively. The water recovered from washing the zeolite products has also illustrated levels of contamination. The three main concerns are the toxic elements Pb, Nb and Al. Although a large weight fraction of these two elements report to the liquid waste, their concentrations are

very low due to the volumes of washing water produced. The concentrations of Pb, Nb and Al were found to be 0.056 ppm, 0.075 ppm and 0.020 respectively.

The average concentration of Hg was 0.4 ppm. Although all these metals exist in low concentrations it will still complicate its disposal. Alternative zeolite washing methods need to be investigated to avoid generating waste containing these three highly toxic elements.

3.3.3 Synthesis and material balance using the fusion assisted synthesis method

Figure 3-9 illustrates the XRD pattern obtained of the zeolite product synthesized by applying the fusion assisted method. The results indicate that a highly crystalline pure phase zeolite A was produced. These results are similar to those obtained by Musyoka (Musyoka et al., 2012b) proving the reproducibility of the authors' results.

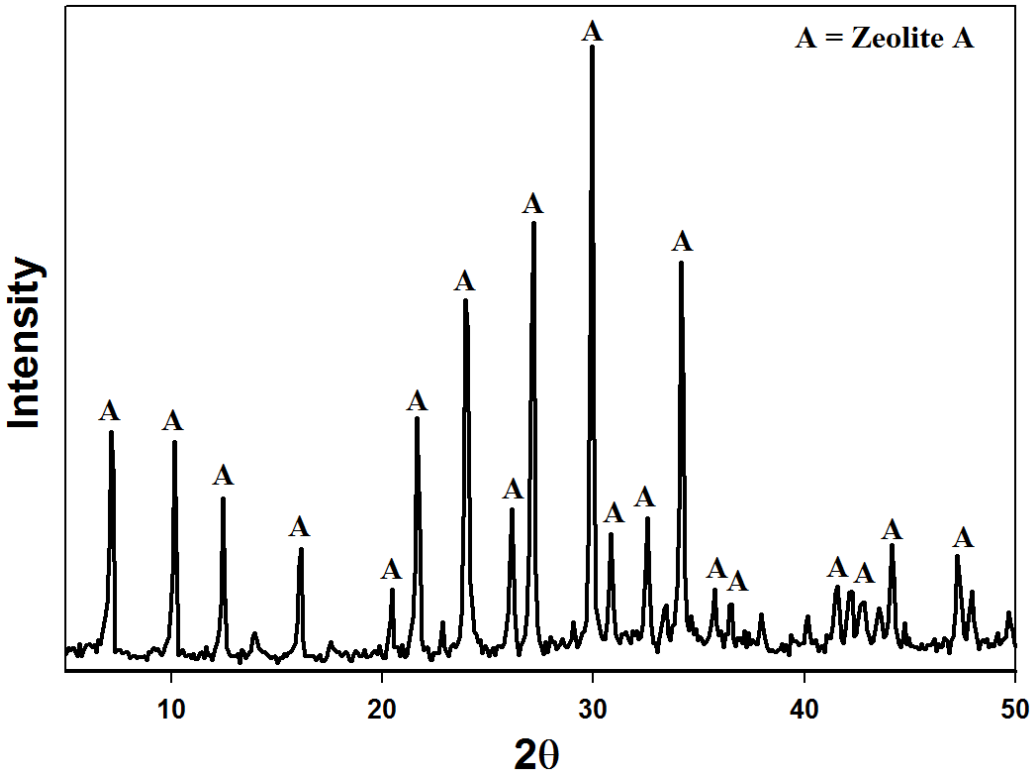

Figure 3-9: XRD powder diffraction pattern illustrating zeolite A product obtained by means of the fusion assisted process

Figure 3-10 illustrates the overall material balance performed over this synthesis approach. The basis of the material balance was taken as 50 g of fused fly ash feed. The fused ash consequently consisted of 22.3 g raw fly ash and 27.7 g analytical grade NaOH powder. As discussed in section 3.2.2.2, the fused ash was mixed with 250 g of ultrapure water and agitated

for 120 min to allow the dissolution of Al and Si species from the fused ash. The slurry was then filtered and only the clear filtrate used to synthesise the zeolite A. The solid residues resulting from the filtration was dried, weighed and analysed. These solid residues represent the material that did not dissolve during the extraction step and was regarded as a solid waste. On average 38.5 g of solid waste resulted from a fused ash feed of 50 g. This shows that the extraction step was inadequate to recover the Si and Al precursor feedstock from the fused ash. The Si/Al ratio of the clear filtrate was adjusted with the addition, on average, of 76.0 g sodium aluminate solution. This adjusted solutions was then subjected to hydrothermal treatment as discussed in section 3.2.2.2. The final zeolite product was washed with 1250 g ultrapure water and of this water an average of 1540 g could be recovered. The supernatant waste liquor separated from the zeolite product totalled 257 g. However, an average of 7.0 g of pure phase zeolite A was synthesized per run. This overall product yield is markedly poor relative to the 2-step process which produced 9.7 g of zeolite product from 10 g of fly ash feed. On the other hand the 2-step process is time consuming and less robust. Also, the fusion assisted process produces a pure phase zeolite product which has a higher market value (Auerbach *et al.*, 2003b). It is clear that both synthesis approaches have certain drawbacks and advantages over each other.

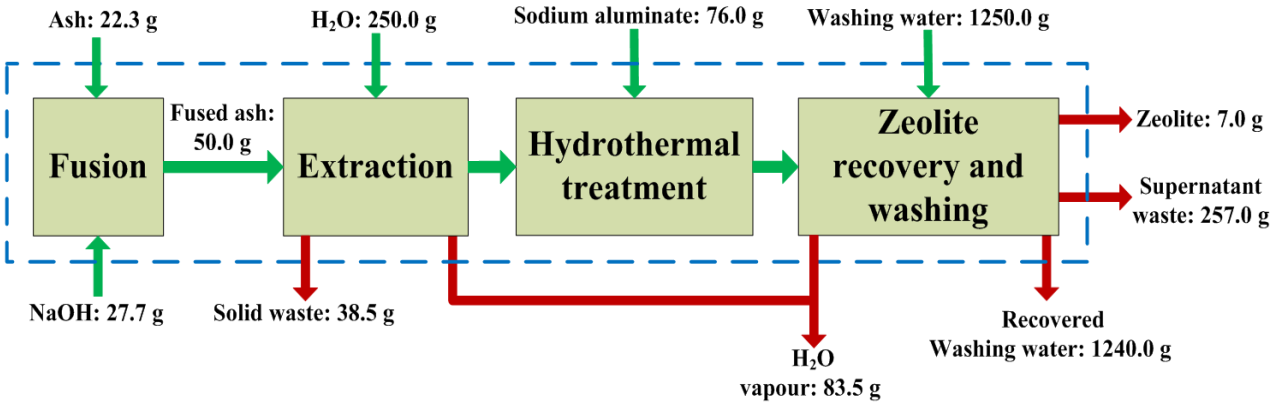

Figure 3-10: Block flow diagram illustrating the overall mass balance of the fusion assisted method

The weight% distribution of elements amongst the different liquid and solid products is tabulated in Table 3-3 below.

Table 3-3: Elemental balance illustrating the distribution of the elements (wt%) originating from fly ash amongst the zeolite product and wastes resulting from the fusion assisted synthesis method

Fractional mass distribution of elements originating from coal fly ash				
Elemental	Solid waste	Zeolite A product	Supernatant waste	Washing water
Al	68.7%	21.6%	7.9%	1.8%
Ba	89.4%	2.4%	3.2%	5.0%
Ca	97.2%	0.0%	0.7%	2.2%
Ce	100.0%	0.0%	0.0%	0.0%
Co	100.0%	0.0%	0.0%	0.0%
Cu	100.0%	0.0%	0.0%	0.0%
Fe	98.8%	0.3%	0.2%	0.7%
K	23.5%	21.2%	40.5%	14.7%
Mg	97.2%	0.0%	0.6%	2.2%
Mn	87.9%	0.0%	9.3%	2.7%
Na	26.3%	4.8%	33.9%	35.0%
Nb	54.3%	0.0%	3.9%	41.8%
Ni	78.5%	0.0%	21.5%	0.0%
P	24.5%	0.0%	63.8%	11.6%
Pb	51.1%	0.0%	6.8%	42.1%
Rb	89.3%	0.0%	10.7%	0.0%
S	26.0%	74.0%	0.0%	0.0%
Si	66.2%	19.6%	9.5%	4.7%
Sr	99.6%	0.0%	0.0%	0.4%
Ti	99.6%	0.2%	0.1%	0.2%
V	45.2%	0.0%	39.6%	15.3%
Y	100.0%	0.0%	0.0%	0.0%
Zn	53.8%	3.6%	11.9%	30.8%

From Table 3-3 it can be seen that a mere 19.1% of the Si originating from the fly ash reported to the zeolite product as opposed to the 72.2% of the 2-step process. This was due to the fact that most Si was lost in the solid waste after extraction of clear solution from the fused ash. This is the main reason why a mere 7.0 g zeolite yield was obtained. To improve the yield a new approach needs to be investigated towards extracting optimum amounts of Si and Al from the fused ash to reduce wastage. The weight% of Al takes into account the Al input from both fly ash and the sodium aluminate solution. Once again, most Al reported to the solid waste. Other than these two critical elements, it was found that almost all elements originating from the fly ash reported to the solid residual waste. In section 3.3.2 it was speculated that these elements did not form part of the zeolite structure, during the 2-step synthesis approach, but was incorporated in the product due to the low mobility in the presence of CaO (Akar *et al.*, 2012). In the fusion assisted process only the clear filtrate is used to synthesise zeolite A. Therefore, if this speculation mad in section 3.3.2 holds true, in the fusion assisted process these elements will not report to the zeolite product but to the solid waste. The results obtained for the fusion assisted process did indeed conform with this speculation, thereby strengthening its validity. Out of the list of elements 100% of Ce, Co, Cu and Y were found in these solids. Also nearing 100% concentration in the solids were Fe,Mn, Mg, Ca, Ti, Ba, Rb and Sr. It is clear that the fate of these elements is not dependable on the zeolite synthesis mechanism involved. Therefore, whenever all the solids in the system is used to produce the zeolite product (2-step method), these elements will form part of the overall zeolite product. When only the clear solution, rich in Si and Al, is used (fusion assisted process) then these elements will report to the solid waste. The zeolite product, similar to the 2-step process, contained a significant amount of the K originating from fly ash. Therefore, because this process makes use of only the clear filtrate, it can be assumed that the K^+ ions are incorporated in the zeolite pores as charge stabilizing ions in both these synthesis approaches. It was also seen that in the fusion assisted process 74.0% of the sulphur reports to the zeolite product. This was believed to occur due to adsorption of sulphur onto zeolite A. This capability of zeolite A to adsorb sulphur in various forms was illustrated by Steijns and Mars (Steijns and Mars, 1976). In the supernatant waste a fairly significant of the Si, Al and Na were found resulting in a loss of these elements. The elements P and V were concentrated in the supernatant waste, which was also seen in the 2-step process. The toxic element Ba was also included in the supernatant waste contrary to the 2-step process. Other toxic elements such as As, Hg, Pb, Rb and Al were also found in the supernatant and washing water waste. Particularly concerning is the large fraction of lead (42.1%) reporting to the washing water waste. 41.8% of the niobium was found in the washing

water waste, as opposed to the 16.2% of the 2-step process. This element form part of the list of rare earth elements (REE) and its extraction from the liquid could yield promising benefits.

3.4 Chapter summary

Material balances were performed on the two process routes used in the synthesis of zeolites from South African coal fly ash. The various elements originating from coal fly ash were tracked throughout the processes to determine their distributional fate. In the 2-step process, the majority of the elements report to the solid zeolite product, while in the fusion assisted process nearly all elements concentrated in the solid waste. Hence, the majority of the elements do not leach out into solution. It was speculated that this occurs due to the low mobility of these elements in the presence of CaO found in the coal fly ash. Both processes generated liquid wastes with highly toxic elements. Amongst these elements were found As, Pb, Hg, Al and Nb. Disposal of these toxic wastes will create severe environmental and economical problems. It is recommended that the possibility to recycle the liquid supernatant waste be investigated. Also, alternative zeolite washing approaches needs to be considered to avoid the production of large volumes of washing water waste. It was found in both synthesis approaches that vanadium (±50%) and phosphorous (75.5-97%) mostly reports to the supernatant and washing water waste. The yield efficiency of the fusion assisted synthesis approach was found to be very poor. A mere 19.6% of Si and 21.6% Al from the fly ash were incorporated into the zeolite product (Refer to Appendix A for supporting data and calculations). However, the zeolite product obtained (zeolite A) was of high purity and has a high industrial value. On the other hand, the 2-step process generated 9.7 g of zeolite product from 10 g of fly ash. Although it has a high yield efficiency, a mixture of different zeolite crystals were found in the product. Therefore there is a trade-off between these two processes with respect to yield efficiency and product purity. In the fusion assisted process, it is recommended that the extraction of Si and Al from fused ash be optimized in order to optimize its yield efficiency. Also, in this synthesis route it was discovered that niobium (Nb) is concentrated in the liquid waste. Being a rare earth element, recovery of this element might be an advantageous avenue to pursue.

CHAPTER 4

4 Waste minimisation protocols for the process of synthesizing zeolites from South African coal fly ash

4.1 Introduction

It has been shown that a pure phase zeolite Na-P1 can be synthesized from South African coal fly ash using a two-step method, namely aging followed by hydrothermal treatment (Musyoka, 2009; Musyoka *et al.*, 2012c). The authors reported the optimum conditions for the Aging and Hydrothermal steps to be 47°C for 48 h and 140°C for 48h, respectively. The first activity in the scale-up of a zeolite synthesis system is to optimize the process at micro scale. Since the composition of fly ash will differ from country to country and different power stations, it is also necessary to optimize the process for each fly ash (Querol *et al.*, 2001). Our recent study has shown the possibility to scale-up zeolite Na-P1 synthesis (Mainganye *et al.*, 2013). The authors synthesized a pure phase zeolite Na-P1 using the optimum condition reported previously (Musyoka *et al.*, 2012c), but at an ageing agitation rate of 200 rpm (Mainganye *et al.*, 2013), using a four-blade impeller compared to 800 rpm reported by Musyoka et al using a magnetic stirrer (Musyoka *et al.*, 2012c).

However, for the successful scale-up of the synthesis of high value zeolites from South African coal fly ash to be made possible, a clear understanding is required of the engineering design aspects of the synthesis system. One such critical aspect is the environmental concerns resulting from the waste generated through the process. It is important to characterize and quantify the waste generated from the process with a view to minimizing the waste by critical analysis of the processes involved in the synthesis of the target zeolitic product. One of the wastes generated during the synthesis of zeolite Na-P1 is the post synthesis liquid supernatant. Resulting from a material balance performed on this synthesis system, it has become known that this supernatant waste contains high levels of Sodium (refer to section 3.3.2). Since sodium hydroxide is a raw material utilized in the synthesis process, the opportunity exists to recycle the supernatant back into the synthesis process and effectively reduce the volumes of waste generated. It has been shown that zeolite Na-P1 can be synthesized from Chinese fly ash by reusing the waste supernatant generated (Wu *et al.*, 2006a), however the authors used a single step alkaline activation method with addition of sodium halide to promote the crystallization of

the zeolitic product. The chemical composition of South African fly is vastly different; the Si/Al ratios are much less than that of the Chinese fly ash, thus making the single step method unsuitable for this fly ash. The differences in Si/Al ratios in different ashes results in a waste product rich in either Si or Al and thus changes the effects that recycling the waste solution has on the formed zeolitic product.

The aim of this study was to use the knowledge gleaned from previous studies (Chapter 3) to investigate waste minimisation options for the synthesis of high value zeolites from South African coal fly ash. This study explored the opportunity to recycle the post synthesis supernatant waste back into the synthesis system with a view to minimizing waste generation in a scale-up process which is currently being investigated.

4.2 Experimental Section

4.2.1 Experimental approach

Table 4-1 outlines the experimental approach followed during this investigation. After initial runs were completed using fresh NaOH (Run 1, 5 and 8), the post supernatant was recycled. First the supernatant was used without adjustment to establish a starting base for the research (Runs 2-3). After these set of experiments were completed the supernatant was titrated to determine the OH^- ion concentration. With this data in hand the concentration of NaOH in the waste was adjusted to match that of the fresh 5 M solution, by addition of NaOH pellets, before being recycled (Runs 6-7). In each set of experiments the supernatant was recycled twice. With this protocol a total of 40% liquid waste could be recycled. In order to recycle 100% of the waste the starting liquid volume should be similar to the waste volume. This was achieved in the following set of experiments (Runs 8-10) whereby the 75 ml post aging water was added at the start of the aging process, thus changing the NaOH concentration from 5 M to 2 M. In doing so 100% could be recycled without the need to adjust the alkalinity.

Table 4-1: Experimental structure

Run	Description
1	Synthesis of zeolites using 50 ml of a fresh 5 M NaOH batch as alkali source
2	Utilizing the supernatant waste generated from run 1 as alkali source without pH adjustments
3	Utilizing the supernatant waste generated from run 2 as alkali source without pH adjustments
4	Repetition of reference run (Run 1) to generate supernatant for titration purposes
5	Synthesis of zeolites using 50 ml of a fresh 5 M NaOH batch as alkali source
6	Utilizing the supernatant waste generated from run 5 as alkali source with prior pH adjustment
7	Utilizing the supernatant waste generated from run 6 as alkali source with prior pH adjustment
8	Synthesis of zeolites using 125 ml of a fresh 2 M NaOH batch as alkali source
9	Utilizing the supernatant waste generated from run 8 as alkali source without any adjustments
10	Utilizing the supernatant waste generated from run 9 as alkali source without any adjustments

4.2.2 Synthesis of zeolites from coal fly ash

The zeolite synthesis procedure for this study was adopted from Musyoka (2012c) and is discussed in section 3.2.2.1. Figure 4-1 below illustrates a summarised overview of the main processes in this synthesis approach. A minor alteration to this process was made during runs 8-10, as discussed in section 4.2.1, whereby the water addition step was moved to the aging step. All synthesis conditions and equipment used in this study was consistent with the procedure discussed in section 3.2.2.1.

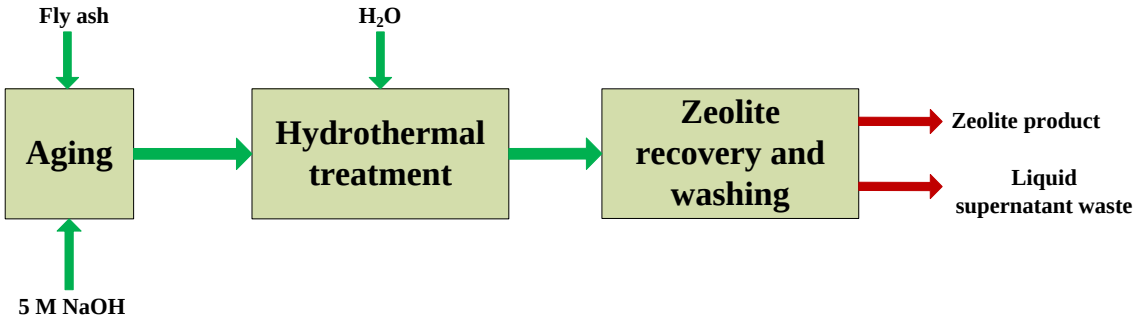

Figure 4-1: Process overview of the 2-step zeolite synthesis approach

4.2.3 Materials and characterization techniques

To ensure accurate results, the same batch of coal fly ash was used throughout each study in chapters 3-7. This was important for accuracy since it has been shown that the mineralogy of fly ash from the same power station can differ greatly between batches (Mainganye, 2012). For the preparation of fresh NaOH solution and the washing of zeolite products, ultra pure water was used and analytical grade sodium hydroxide pellets. The elemental composition of the supernatant waste generated during the process was determined by means of ICP-AES as described in section 3.2.3. The mineralology of zeolite products was observed through XRD (refer to section 3.2.3). Changes in zeolite structure were observed by means of attenuated total reflectance Fourier transform infrared spectroscopy (ATR-FTIR). FTIR was performed using a Perkin Elmer spectrum 100 FT-IR spectrometer in wavelength range of 1800 - 300 cm^{-1}. The morphology of zeolitic products was observed by means of scanning electron microscopy (SEM) with a Nova Nano SEM electron microscope.

4.3 Results and Discussion

4.3.1 Waste recycle without a prior pH adjustment

Figure 4-2 shows the XRD results of the products obtained for the experimental runs 1-3. After the initial baseline experiment (Run 1), the supernatant waste was reused without adjusting its pH. XRD results indicated that during Run 1 all of the quartz from the ash feedstock was dissolved. With small amounts of mullite the main crystal phases were found to be zeolite Na-P1 and analcime. After the first re-utilization of the supernatant (Run 2); it was observed that no analcime was formed, Na-P1 was reduced and less quartz and mullite dissolved. Also, after the second time of reusing the supernatant, only trace amounts of Na-P1 was found and almost none of the quartz and mullite dissolved. The quality of zeolites formed and the dissolution of crystalline phases decreased after each successive run reusing the supernatant. The crystalline

quantity of zeolite Na-P1 decreased from 55% in run 1, to a mere 17% in run 3. The reason being that after each successive run the pH of the supernatant decreased, resulting in poor mineralization of fly ash during reuse.

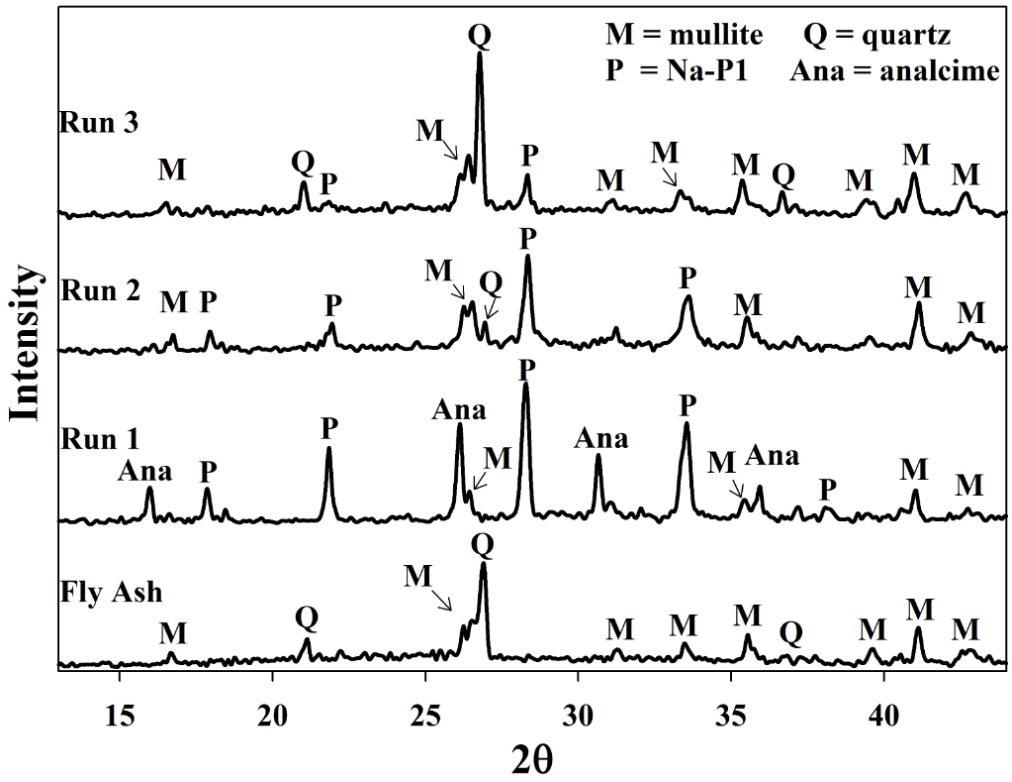

Figure 4-2: Powder X-ray diffraction patterns of products obtained after recycling waste supernatant back into the system as a NaOH source without a prior pH adjustment of the waste.

Figure 4-3 illustrates a micrograph taken of the resulting product after recycling the waste supernatant for a second consecutive time (Run 3). Results clearly indicate the spherically shaped, poorly dissolved fly ash particles as well as small traces of zeolite Na-P1. The structural information of the products obtained, as seen by ATR-FTIR, is shown in Figure 4-4. From the figure it is clear that the main absorption band in the 1000 cm^{-1} wavelength region shifted to the right from run 1 to run 3. This band represents the asymmetric stretching mode of the T-O (T= Si, Al) bonds that are found in the fly ash and zeolites (Breck, 1974; Rios R *et al.*, 2009). This shift in the main band, from left to right, indicates a higher Si-O concentration in the crystal product (Fernandez-Jimenez and Palomo, 2005). This illustrates how less of the crystalline products in the original fly ash were dissolved and less zeolite products formed. Also, the bands appearing at around 700 and 800 cm^{-1} have been reported to be associated with the T-O (T=Al, Si) symmetric stretching vibrations that correspond to quartz present in the original fly ash starting material (Criado *et al.*, 2010; Rios R *et al.*, 2009). From these results it was clear that

the pH of the waste supernatant would have to be adjusted prior to being recycled back into the synthesis system.

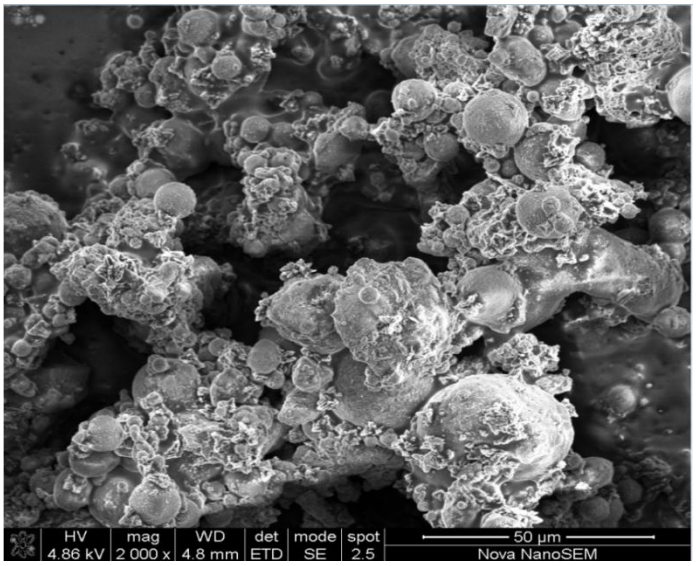

Figure 4-3: Micrographs taken of the products obtained after Run 3, at a magnification of 2000 times

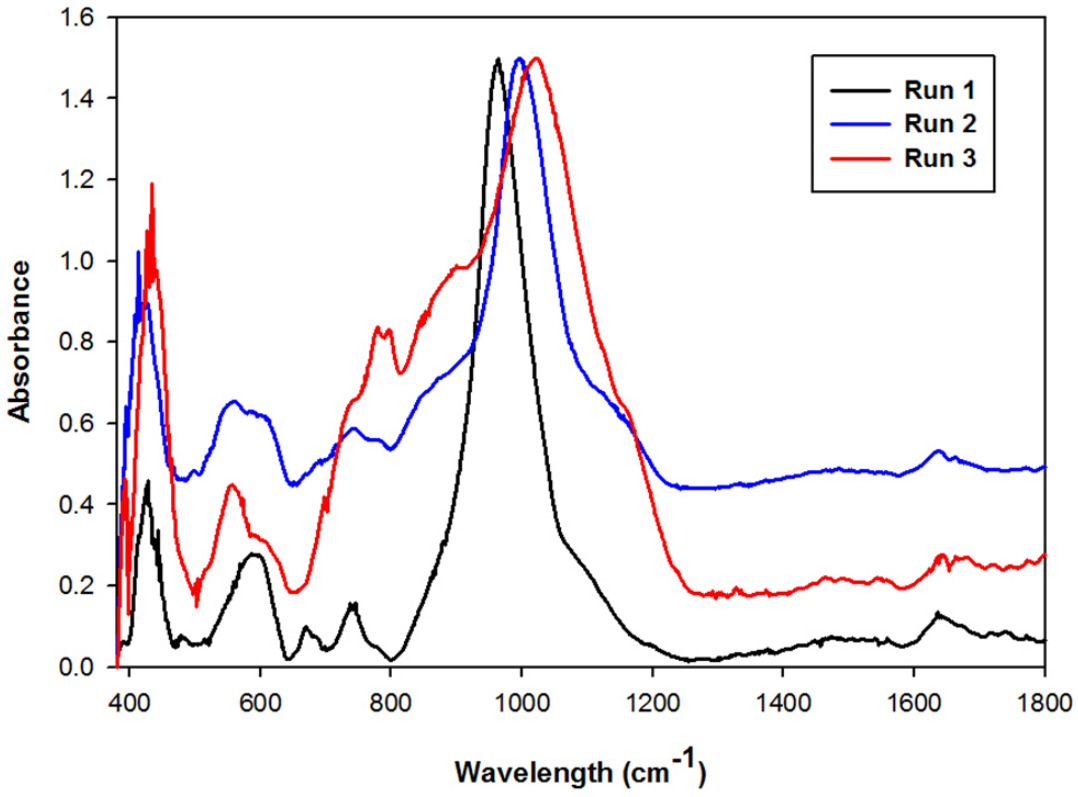

Figure 4-4: Infrared spectra of products obtained of products after recycling the supernatant waste as a source of NaOH.

4.3.2 Waste recycles with prior pH adjustment

In the second set of experiments once again the baseline experiment (Run 5 and Run 1) indicated the formation of both zeolites Na-P1 and analcime (Figure 4-5). However, by adjusting the pH of the supernatant before reusing it (Run 6), all the quartz and most of the mullite were dissolved. Also, after reusing the supernatant from run 6–7 zeolite analcime became more prominent and became the only crystalline phase present. The crystalline quantity of analcime increased from 36% in run 5 to 73% after run 7. One of the distinct differences between analcime and Na-P1 is the Si/Al ratio. While Na-P1 is a high Si/Al zeolite, analcime is a low Si/Al zeolite. The Al and Si content of the aging slurry are dependent on the dissolution of the amorphous phases and crystalline phases in fly ash. The dissolution process is complex due the fact that the different mineral phases in fly ash dissolve with different degrees of ease(Fernandez-Jimenez and Palomo, 2005).

Figure 4-6 illustrates a micrograph, magnified 2000 times, of the product obtained after the second consecutive recycle of the waste supernatant. The product contains mostly analcime but traces of amorphous material could also be observed. This agrees with the relative crystallinity results of 73%, and can possibly be increased by optimizing the hydrothermal treatment time.

From Figure 4-7 it can be seen that the main absorption band in the 1000 cm^{-1} wavelength region did not shift its position considerably. The minor, almost unnoticeable shift in its position was due to the fact that the Al-O and Si-O concentrations in the two zeolite structures, analcime and Na-P1, differs (Auerbach *et al.*, 2003b; Breck, 1974). The increase in the band intensities in the 650 and 750 cm^{-1} regions, as well as the hump illustrated in the 900 cm^{-1} region, illustrates analcime becoming the more dominant phase in the product (Azizi and Yousefpour, 2009).

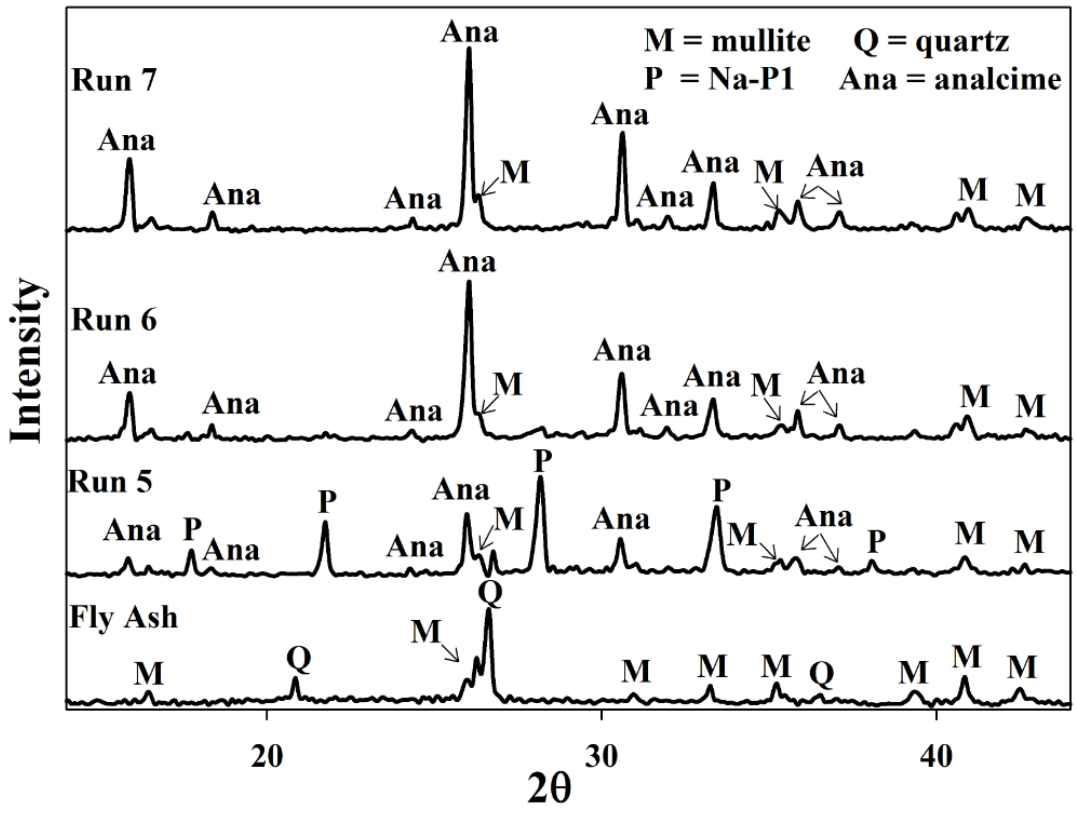

Figure 4-5: Powder X-ray diffraction patterns of products obtained after synthesis with supernatant waste as NaOH source after adjusting the pH of the waste.

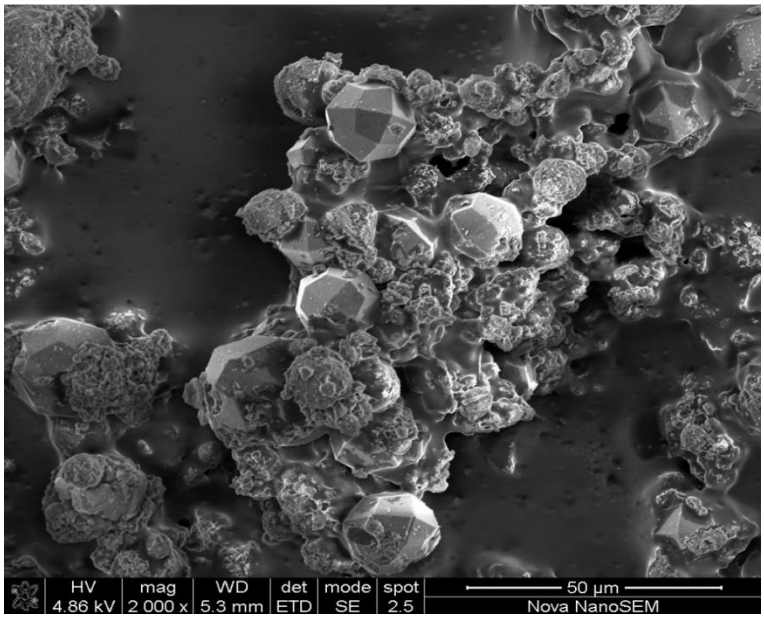

Figure 4-6: Micrographs taken of the products obtained after Run 7, at a magnification of 2000 times

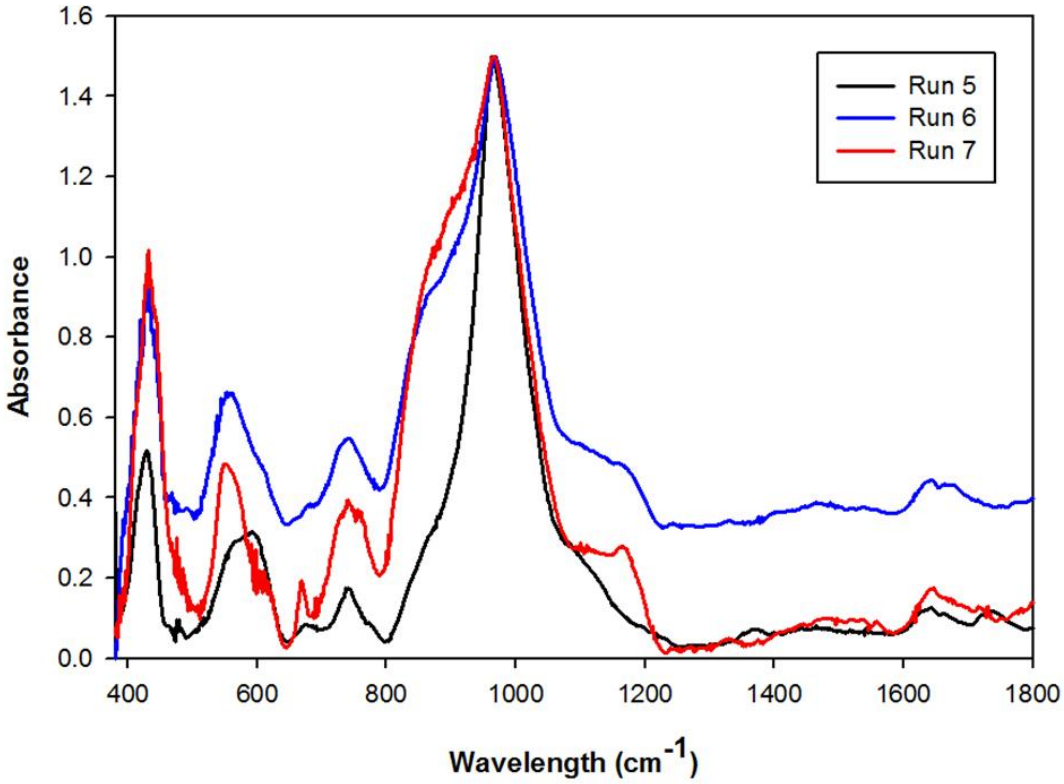

Figure 4-7: Infrared spectra of products obtained of products after recycling the supernatant waste as a source of NaOH

In order to establish a basis for environmental and legal requirements for the disposal of waste solutions, the concentrations of the major species found in the waste solutions were determined. Table 4-3 illustrates the concentrations of these species as determine by inductively coupled plasma atomic emission spectrometry (ICP-AES). From the results it was clear that all the elemental concentrations in the waste solution increased as the waste was reused indicating a continuous accumulation of these species. However, aluminium did not accumulate and was found to be the limiting element for zeolite growth. It is clear that the accumulation of Si as the waste was reused favoured the formation of analcime (Tatlier *et al.*, 2007). This indicated that in order to further increase the relative crystallinity of the final analcime product, both crystallization time and the Si/Al ratio of the reacting slurry needs to be optimized. With a pore size of about 0.25 nm, zeolite analcime can be use in the absorption of NH_3 molecules (Breck, 1974). The trace elements from the fly ash do not affect the zeolite product during the synthesis process. This was found to be a result of their low mobility due to the CaO content in fly ash (Akar *et al.*, 2012). Thus the majority of the elements do not leach out into solution during the dissolution of the Si and Al species from the ash, as seen in chapter 3.

Table 4-2: Atomic emission spectrometry results indicating elemental concentrations of major species found in the waste supernatant after each successive run

	Mean elemental concentration (ppm)		
	Run 5	**Run 6**	**Run 7**
Al	35.5	34.0	31.3
Fe	5.3	6.9	7.4
K	215.1	434.6	497.2
Na	20971.3	25348.0	26101.4
P	80.6	163.5	196.8
Si	7198.7	15124.7	16624.1
Ti	4.9	11.3	12.8
V	5.1	9.8	11.3

4.3.3 Recycling 100% waste supernatant

The waste minimisation protocol discussed in section 4.3.2 could only recycle 40% of the waste supernatant. The reason for this is that the process starts off with a 5 M NaOH solution and after the aging step and addition of ultrapure water,150% by volume of the starting 5 M NaOH solution, is added to the reacting slurry. Thus the volume of waste generated far exceeds the volume of NaOH in the feedstock. This water addition step could not be omitted completely. When using fly ash as a feedstock in zeolite synthesis, the liquid volumes need to be kept at a much higher level than in commercial synthesis. The reason for this is that an increase in water content increases the dissolution of Al and Si species from fly ash, and favours the existence of metastable species (Iwasaki *et al.*, 1997; Querol *et al.*, 1995). When the water addition step is omitted completely a poorly crystallized product was obtained with various contaminating phases. Figure 4-8 illustrates the XRD patterns of the resulting product when this attempt was made. Three different crystalline phases were found in the product namely zeolite Na-P1, sodalite and cancrinite. The two broad humps in the angle ranges of 20 <2θ< 40 and 2θ> 50 indicates undissolved amorphous phases. The relative crystallinity of zeolite Na-P1, cancrinite and sodalite was found to be 26%, 12% and 7% respectively. The majority of the sample was found to exist in an amorphous state. This poor formation of metastable phases highlighted the importance of using higher water content when using ash as a feedstock.

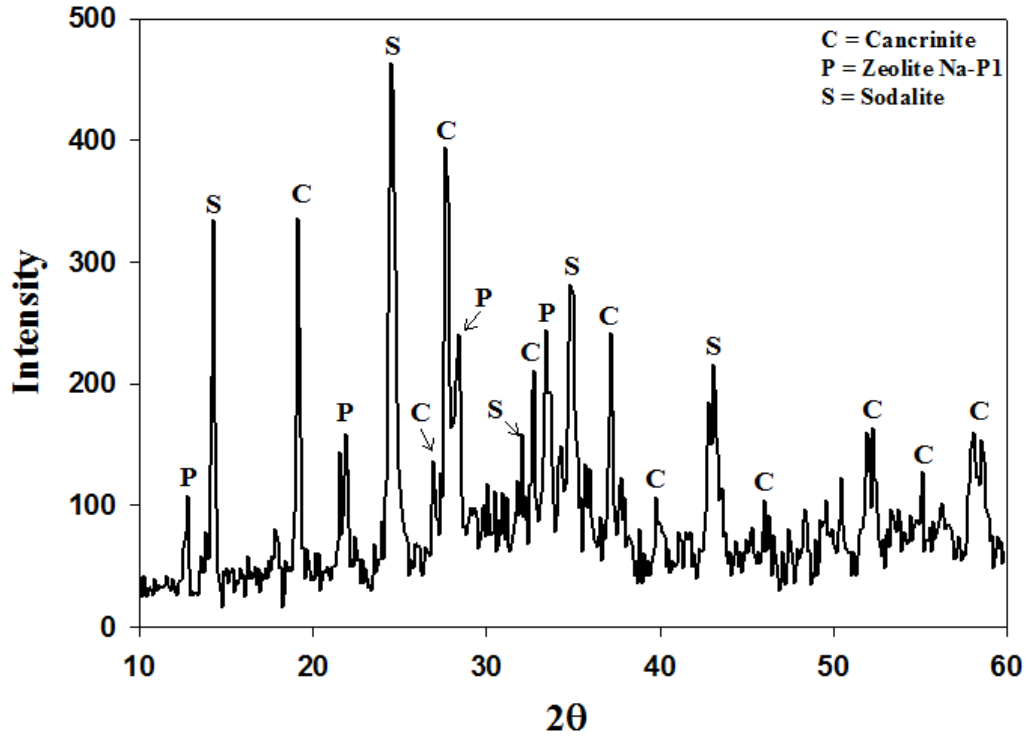

Figure 4-8: XRD patterns of the resulting product after removing the water addition step during the synthesis of zeolites from coal fly ash.

In order to remedy this bottleneck in the system an attempt was made to introduce the addition of ultrapure water at a much earlier stage before the aging stage commences. This step kept the process liquid volume constant throughout the different synthesis stages. The consequence of this was that the starting NaOH solution would have a molarity of 2 M, but 100% of the waste could be introduced into the system without a pH adjustment. In the process of aging fly ash in an alkaline solution a decrease in pH results in a decrease in the rate of quartz dissolution (Choi *et al.*, 2011) and also in the rate of hydrolysis of the glassy phases (Li *et al.*, 2011). However, Figure 4-9 depicts that the quartz and mullite did indeed dissolve with only traces of mullite visible after ultrapure water was introduced before the aging step. From the first set of Runs (Run 8) it can be seen that the two major crystalline phases formed were zeolites Na-P1 and analcime. As the supernatant waste was reused from run 8 to 10, the amount of analcime increased from 80% to a near pure phase. This trend is similar to that seen in Figure 4-5.

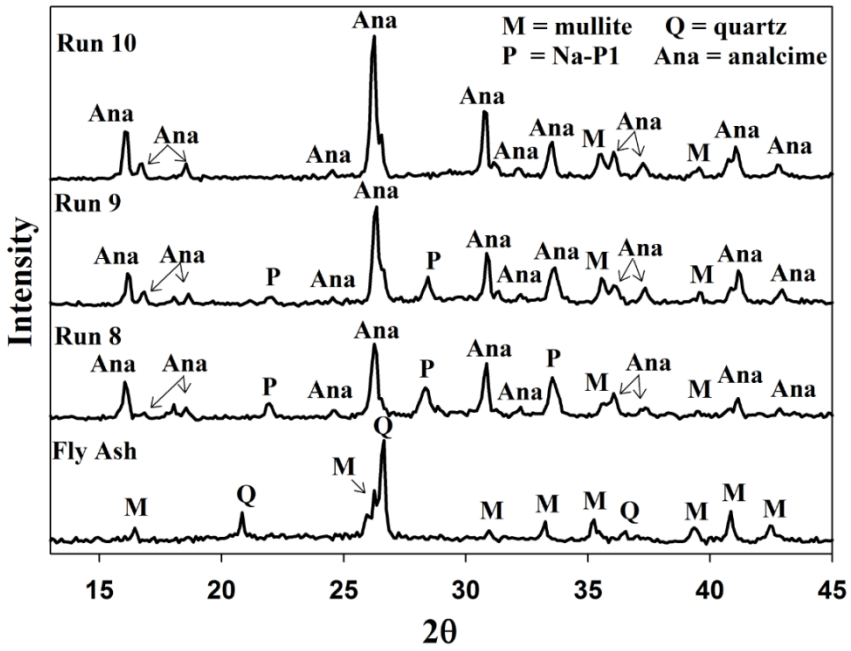

Figure 4-9: Powder X-ray diffraction patterns of products obtained after synthesis with supernatant waste as NaOH source using the amended synthesis approach.

A micrograph of the zeolite analcime crystals obtained, magnified 10,000 times, show the well defined faces and crystal structure of the analcime product (Figure 4-10). The analcime crystal can be described as a trapezohedron shape, with a total of 24 faces.

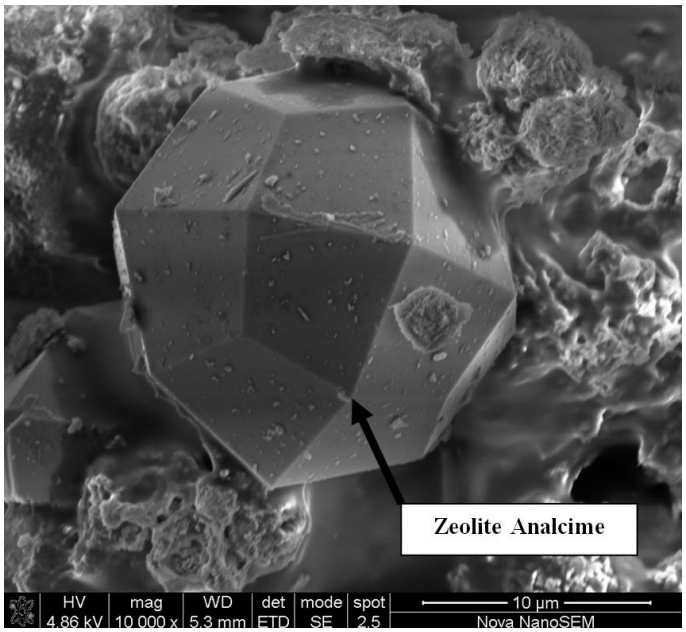

Figure 4-10: Micrographs taken of zeolite analcime obtained after Run 10, at a magnification of 10,000 times.

By means of ICP-AES analysis the concentrations of the elements in the final waste solution were obtained. The concentrations of Al, Fe, K, Na, P, Si, Ti and V were found to be 25.9, 11.6, 550.4, 25,803.5, 237.9, 19,783.2, 14.1 and 13.2 ppm respectively. The concentrations of the elements were found to be in the same range as the data for the second recycle (Run 7) in Table 2. This illustrates that the same rate of accumulation among the elements exists in the two different synthesis processes. However, a much higher Si concentration exists because this protocol recycles 100% of the Si in the waste back into the system.

This alteration in the basic synthesis process illustrated great success in significantly reducing the amount of waste produced by the process and consequently the cost of disposal. By reducing the waste produced from this process the feasibility of a scale-up operation has been reinstated and can be applied to relieve the difficulties faced with the generation of coal fly ash in South Africa. Figures 4-11 and 4-12 illustrate the reproducibility of this new synthesis approach. It was found to be highly reproducible with the relative crystallinity of analcime, in all cases, increasing from ±75% to near 100% after the second recycle of the supernatant waste. In all cases the average product yield was found to be 9.7 g from an ash feed of 10 g, while the space time yield was found to be 14.5 kg m^{-3} day^{-1}.

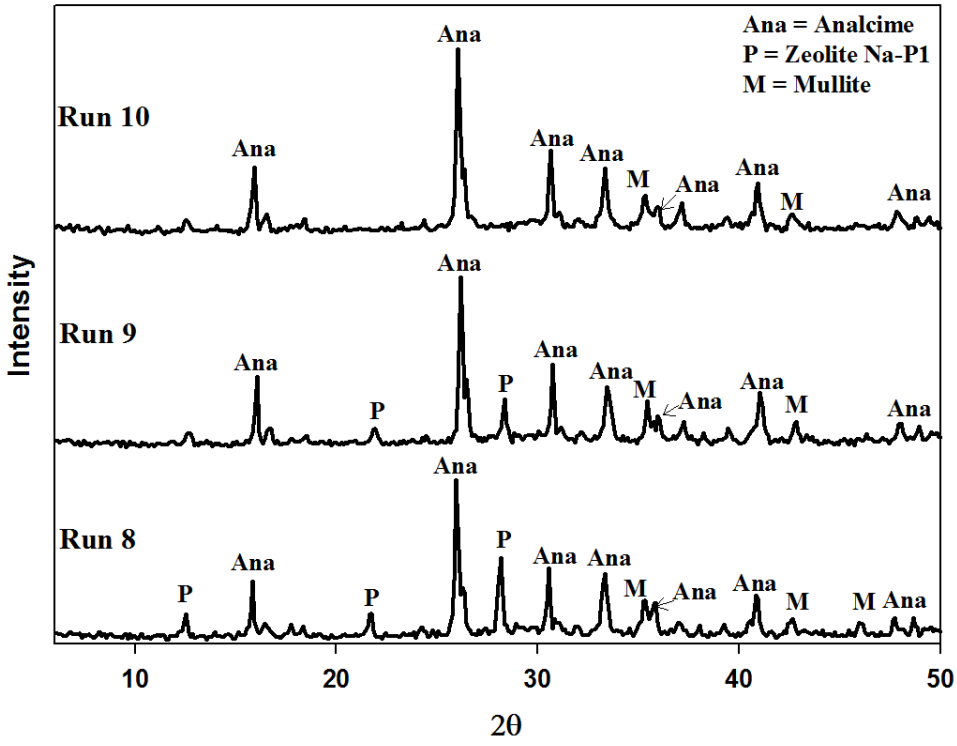

Figure 4-11: XRD patterns illustrating reproducibility of results depicted in figure 8 (Second results set).

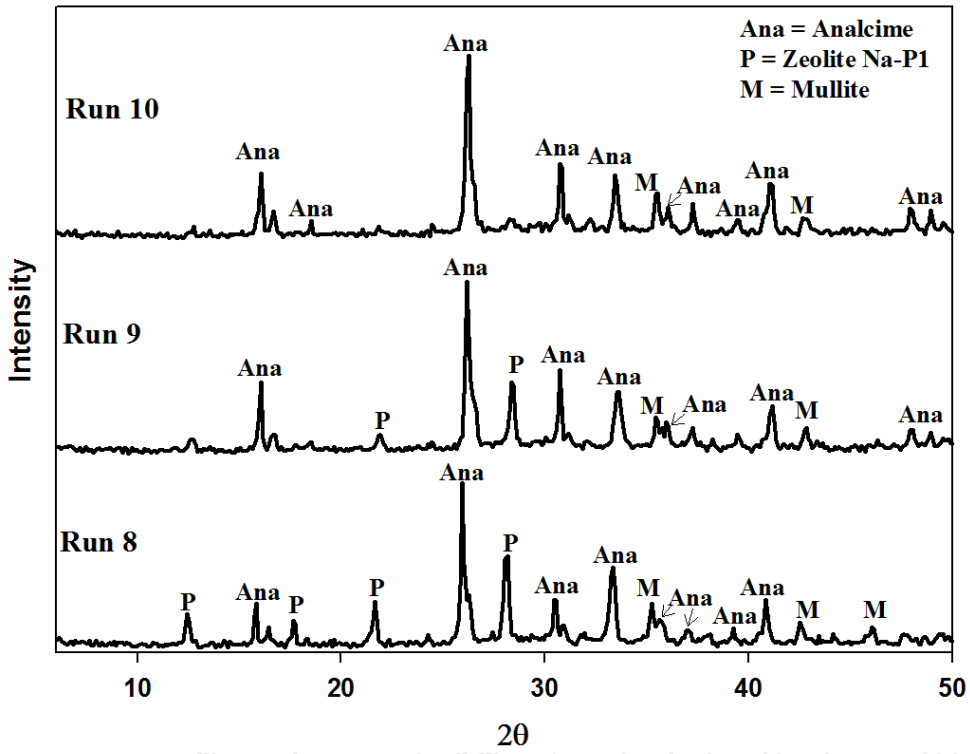

Figure 4-12: XRD patterns illustrating reproducibility of results depicted in Figure 8 (third results set).

4.4 Chapter summary

Waste minimisation options for the synthesis of zeolites from South African coal fly ash were investigated. The opportunity to recycle 40% of the waste supernatant back into the system illustrated that to successfully synthesize zeolites with the waste solution, its pH needs adjustment. By adjusting the pH of the supernatant prior to being reused, zeolites analcime and Na-P1 were successfully synthesized while dissolving unwanted crystalline minerals from fly ash. Zeolite analcime was found to be the dominant phase after reusing the supernatant waste due to a high Si/Al ratio in the waste. By altering the basic synthesis process slightly it was also possible to recycle 100% of the supernatant waste without an adjustment to its alkalinity. This study effectively developed two protocols in which waste supernatant can be reduced drastically and thereby improving the scale-up feasibility. It is recommended that future studies should investigate altering the Si/Al ratio of both the fly ash and supernatant to obtain the more desirable zeolite Na-P1 as dominant zeolite phase.

CHAPTER 5

5 Waste and water minimisation during the synthesis of zeolite A from South African coal fly ash

5.1 Introduction

Recently a study has proven that South African coal fly ash is a suitable feedstock in the synthesis of Zeolite A (Musyoka *et al.*, 2012b). Zeolite A would be of high interest, from an economical view, to be synthesized on an industrial scale due to its importance in industrial applications (Auerbach *et al.*, 2003c). Musyoka's study (Musyoka *et al.*, 2012b) in 2012 was done on a micro scale and in order to scale-up the synthesis process it needs to be optimized (Chang and Shih, 1998). Two critical problems exist in the synthesis process namely the consumption of ultrapure water and generation of significant quantities of liquid supernatant waste (see section 3.3.3). The use of ultrapure water on an industrial scale would not be financially viable and therefore it needs to be minimised or replaced. The liquid waste produced from the process contains sodium hydroxide and also levels of Si and Al. The disposal of large quantities of liquid waste would contradict the aim of the utilization of fly ash which is to relieve the environmental stress caused by its disposal. In a recent study it was proven that, in the conventional hydrothermal synthesis of zeolites from South African coal fly ash, the liquid waste can be recycled without compromising the zeolite product (Du Plessis *et al.*, 2013). This was done using the conventional synthesis approach which excludes a fusion step. It was speculated that the protocols developed in the study could be applied to the synthesis of zeolite A which contains a pre-fusion step. Although the mechanisms of the two synthesis approaches differs vastly, both the synthesis process and the waste minimisation protocols can be optimized to yield the required zeolite product from the given ash source.

The aim of this study was to investigate the opportunity to minimise the supernatant waste generated and ultrapure water consumed in the fusion assisted synthesis of zeolite A from South African coal fly ash. The first objective was to use the knowledge obtained from the previous study (Du Plessis *et al.*, 2013) to develop a structured research methodology. With a properly structured methodology, the objective was to develop protocols whereby the liquid supernatant waste could be recycled back into the system as a source of water. This serve as a solution to two critical process problems i.e. the excessive consumption of ultrapure water and the production of liquid waste.

5.2 Experimental Section

5.2.1 Experimental approach

Figure 5-1 illustrates a schematic of the process used to synthesize zeolite A from South African coal fly ash. For a detailed description of the experimental procedure of the fusion assisted synthesis approach refer to section 3.2.2.2.

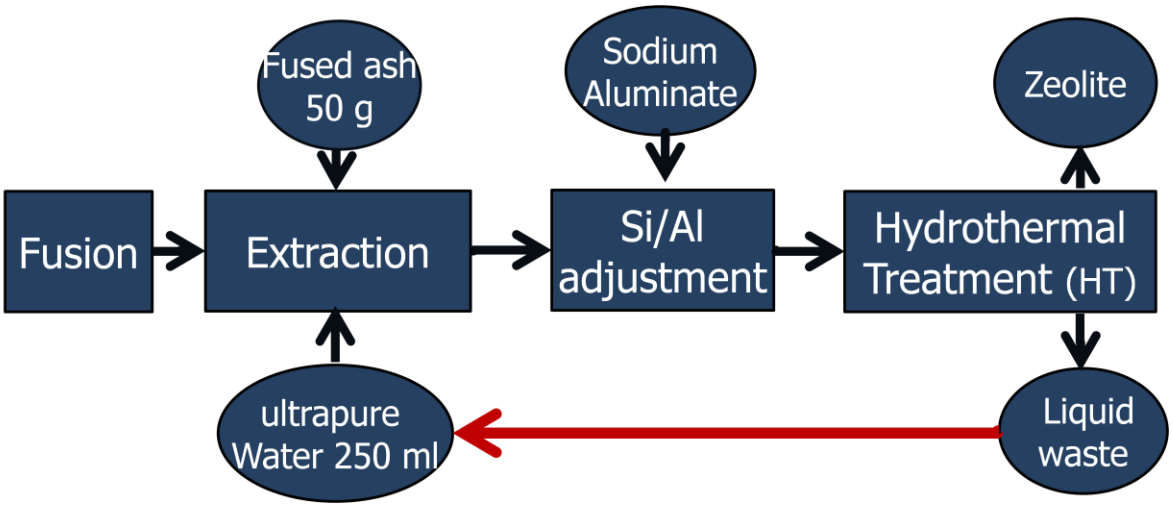

Figure 5-1: Schematic of the process used to minimise the consumption of ultrapure water and the minimisation of liquid waste produced

The aim of the study was to use the liquid waste generated by the process, also referred to as supernatant, and replace the 250 ml of ultrapure water with the waste. In Du Plessis *et al*. (2013) the importance of following a structured approach was illustrated when developing a protocol whereby liquid waste can be recycled. By following a structured approach and not altering the waste before initial recycles, it is possible to understand better how the zeolite synthesis process behaves under different conditions. Figure 5-2 illustrates a general approach that was developed by taking into account the previous work (Du Plessis *et al.*, 2013). The first and most important step in recycling waste during the synthesis of zeolites is to recycle the waste without any adjustments to its pH or Si/Al ratio, even if it is almost certain that an adjustment would be required. The next step is to reproduce the results to prove the consistency of the process. If the correct zeolite phase is successfully formed the last step is to critically analyze the waste solution to determine which elements are concentrated in the liquid waste and also if Si or Al accumulates when recycling the waste. If the incorrect zeolite phase is formed the waste needs to be analyzed and adjusted before being recycled until a pure phase of zeolite A is once again formed. During this study in all cases the waste was recycled 2 consecutive times.

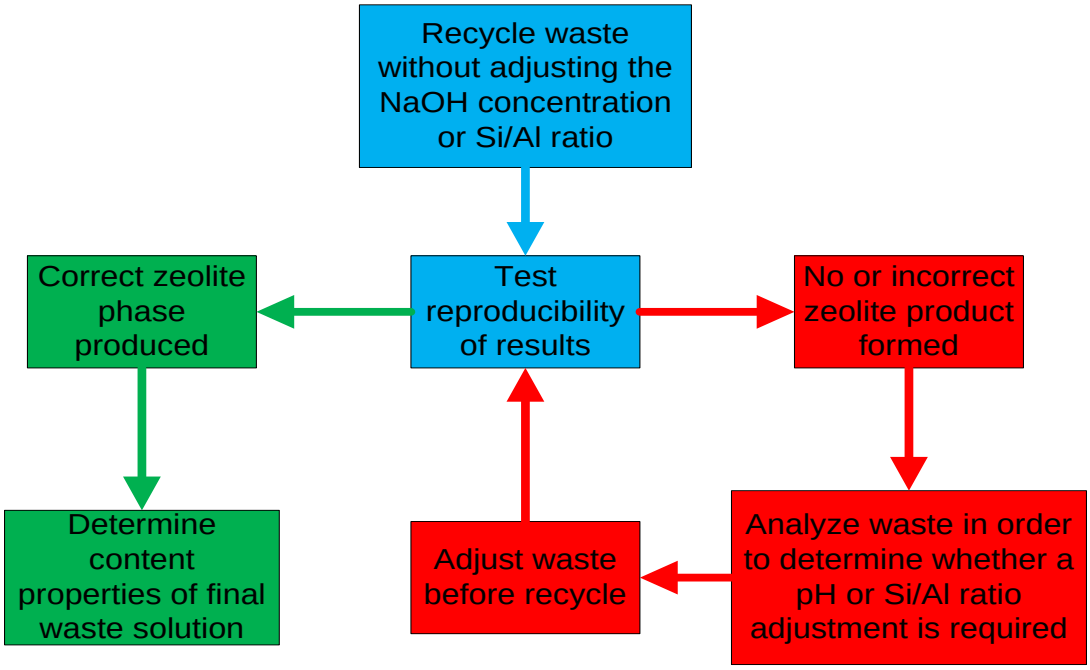

Figure 5-2: General approach to develop waste minimisation protocols for the synthesis of zeolites from coal fly ash

5.2.2 Materials and characterization techniques

The coal fly ash used in this study was collected from a South African coal fired power station situated in Mpumalanga. All water used in the synthesis procedure were ultrapure quality. For information regarding the chemicals, and their respective qualities, used in this process refer to section 3.2.3. The mineralology and the structural changes of the zeolite products were inspected by performing XRD (see section 3.2.3) and ATR-FTIR (see section 4.2.3) respectively. The concentrations of elements in the liquid waste produced from the process were determined by ICP-AES (see section 3.2.3).

5.3 Results and Discussion

5.3.1 Waste recycle without a prior pH adjustment

Figure 5-3 illustrates the XRD results of the first attempt to recycle the supernatant waste produced from the synthesis process. The first run, which was produced using fresh ultrapure water, illustrates a pure phase of zeolite A. The pattern for this first reference run agrees with the results obtained by Musyoka in 2012 (Musyoka *et al.*, 2012b). After the first run the waste was recycled, replacing the ultrapure water, and still a pure phase of zeolite A was produced. Similarly, when the waste was recycled for a second consecutive time a pure phase of this zeolite was still produced. The mean volume of waste produced was 207 ml, the surplus of the require 250 ml of water for the extraction step was supplemented with ultrapure water.

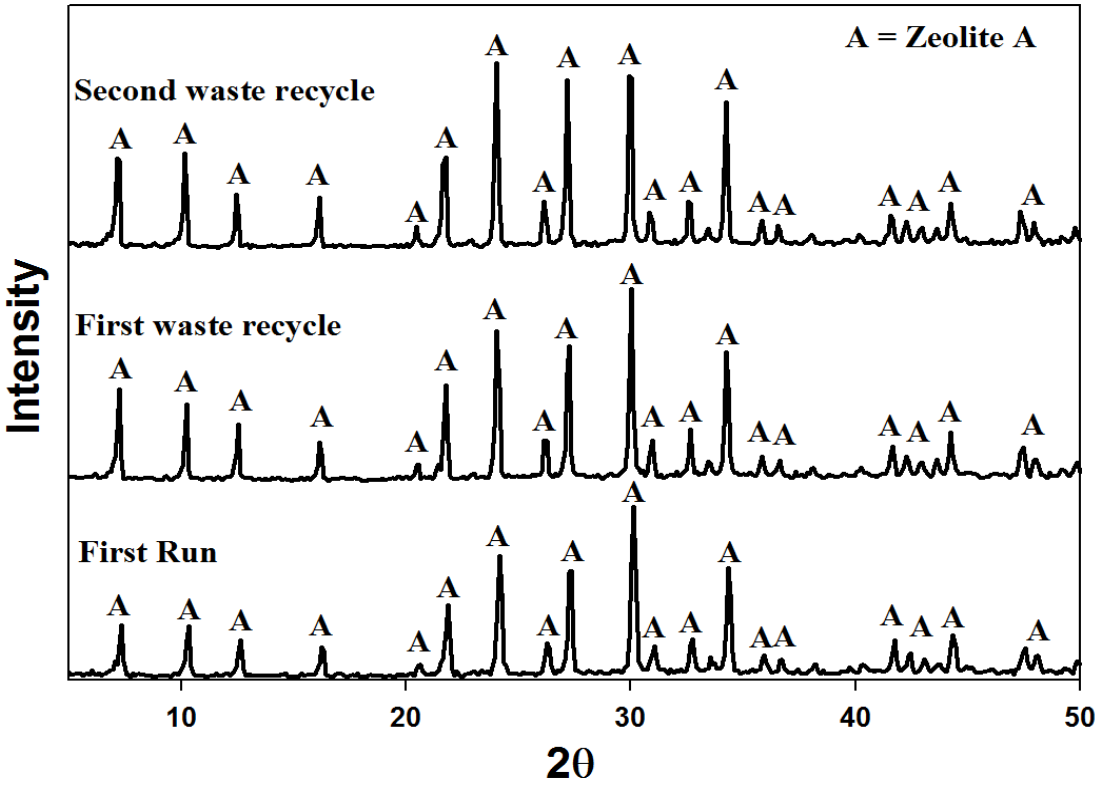

Figure 5-3: XRD patterns illustrating the results of recycling the waste supernatant back into the system and replacing ultrapure water

In order to confirm these results attenuated total reflectance Fourier transform infrared spectroscopy (ATR-FTIR) was performed on the product samples (Figure 5-4). The main spectra band around 950 cm^{-1} is due to the internal crystal structural vibrations from O-T-O (T = Si/Al) asymmetrical stretching modes (Flanigen *et al.*, 1971). Another characteristic zeolite

spectral band can be found in the region of 420 – 500 cm^{-1}(Flanigen *et al.*, 1971). Zeolite A contains 4-membered double rings and evidence of this can be seen in the region of 500 – 650 cm^{-1} which illustrates the external linkage vibrations (Flanigen *et al.*, 1971). No other bands were found that were not characteristic of zeolite A confirming results seen from XRD patterns (Figure 5-3).

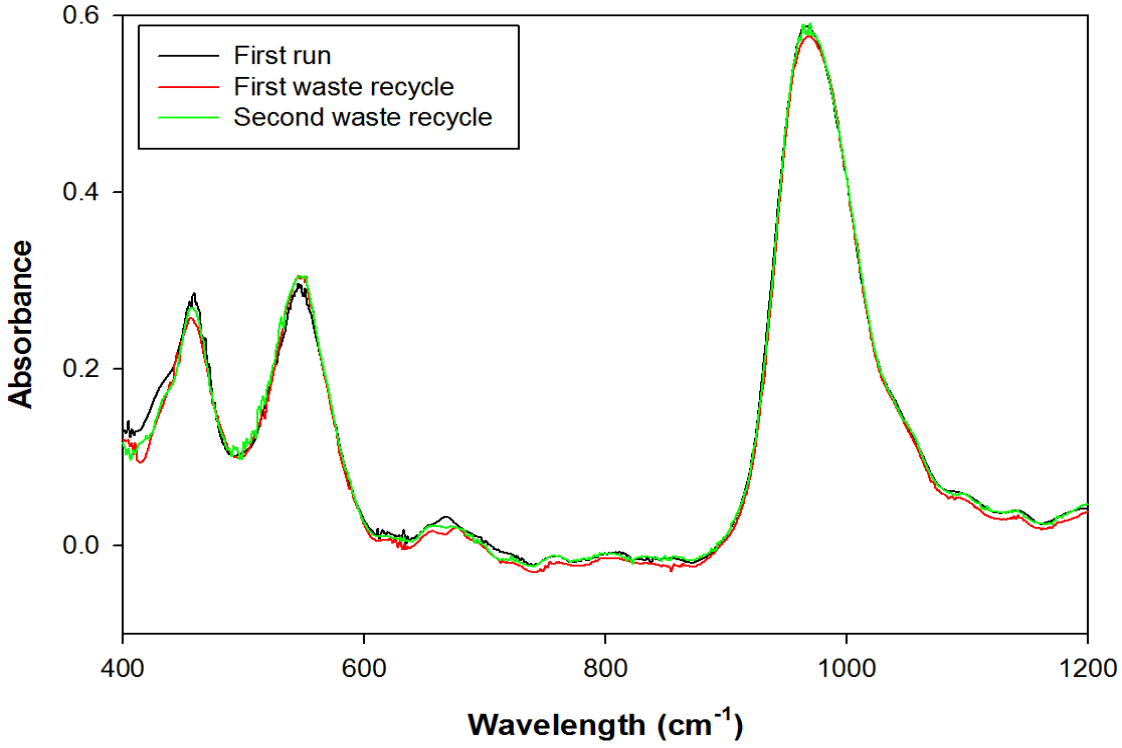

Figure 5-4: ATR-FTIR results for the first attempts at recycling the liquid waste replacing the use of ultrapure water

According to the developed general approach illustrated in Figure 5-2 the next step is to test the reproducibility of these results. Figure 5-5 and 5-6 shows the results of the reproducibility study. Figure 5-6 illustrates the XRD patterns of the resulting products after repeating the experiments as illustrated previously. From the XRD patterns it can be seen that the zeolite product was highly reproducible. Figure 5-5 presents the ATR-FTIR spectra for the products resulting from the process. If any structural changes in the products had occurred it would be noticed from ATR-FTIR results. Once again no major changes were seen in these results proving that no structural changes occurred in the zeolite product showing its reproducibility. The phase purity of zeolite A was found to be 100% in all cases due to the fact it was the only crystalline phase present.

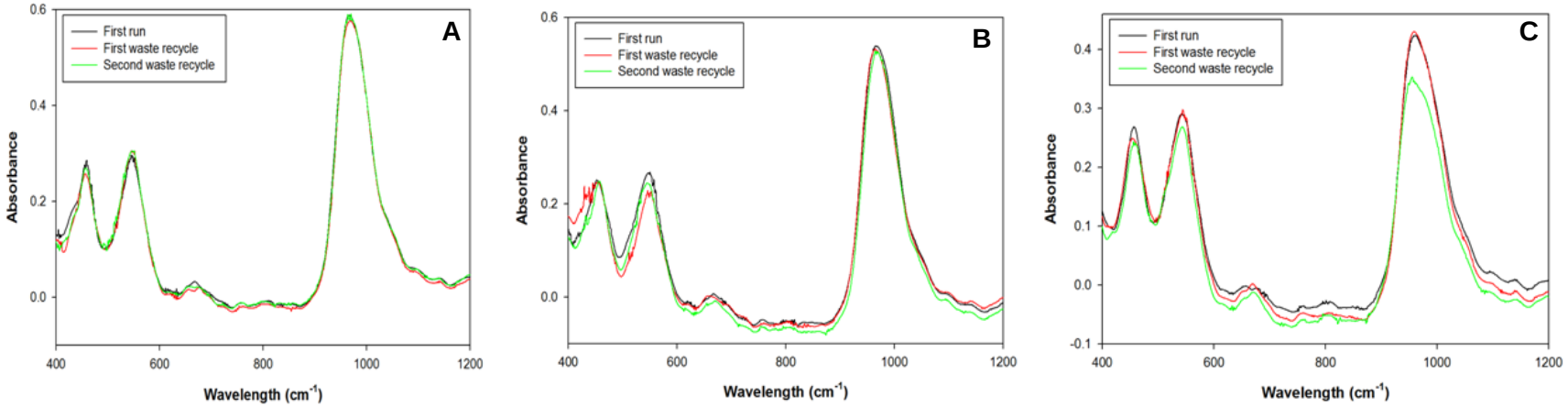

Figure 5-5: ATR-FTIR spectra illustrating reproducibility of results (A) First set of experiments. (B) First repetition of results. (C) Second repetition of results

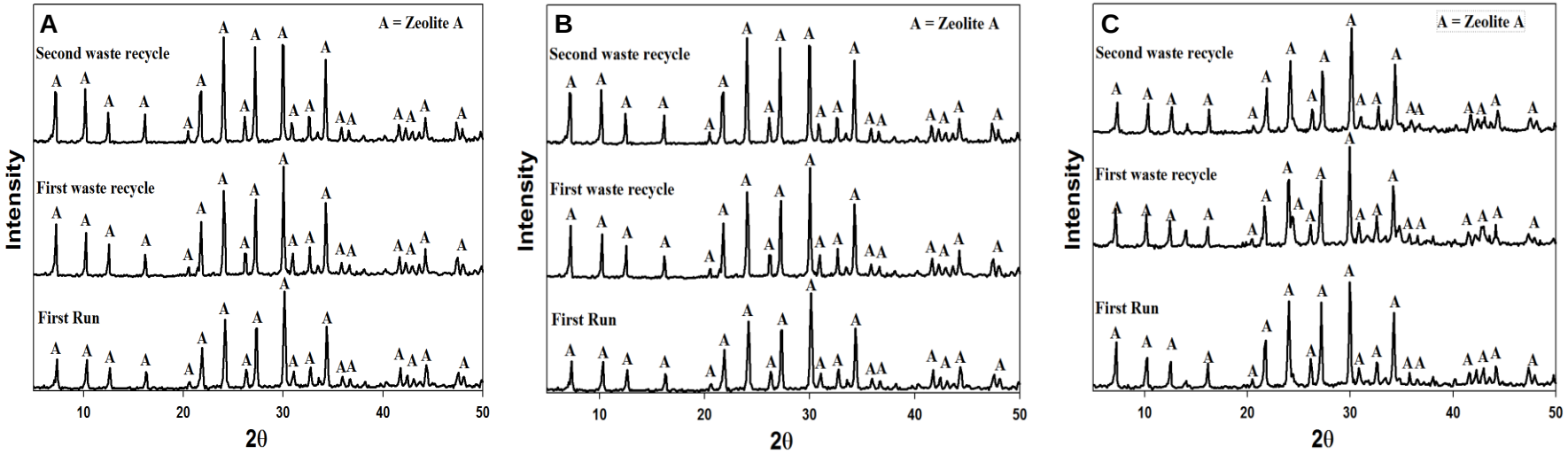

Figure 5-6: XRD patterns illustrating the reproducibility of results (A) First set of experiments. (B) First repetition of results. (C) Second repetition of results

Table 5-2 illustrates the inductively coupled plasma atomic emission spectrometry of the final waste solution collected after the second consecutive waste recycle. Once again, from the results it was clear that the toxic elements from the fly ash do not leach out into the supernatant waste solution after synthesis. Figure 5-7 illustrates the accumulation of Si and Al in the waste solution after each consecutive waste recycles. The levels of Si seemed to remain at a relatively constant average, while the concentrations of Al decreased gradually. This decrease in Al is not problematic since the Si/Al ratio can easily be adjusted. These relatively consistent levels of Si and Al are responsible for the successful product in each case. An abnormally large accumulation or depletion in either Si or Al would have required the waste to be altered before being recycled. The fact that the toxic elements did not accumulate in the liquid waste is a promising incentive for the scale-up of the synthesis of zeolite A from South African coal fly ash. Toxic elements in waste streams complicate its disposal due to South African environmental laws. However, from chapter 3 it was seen that these elements concentrated in the solid waste. Also, the solid waste contains most of the Si and Al originating from the fly ash. It is recommended that alternative, more efficient methods to extract these elements from the fused ash be explored.

Table 5-1: ICP-AES results of the final waste solution generated after recycling the liquid waste for a second consecutive time

Elemental concentrations in final waste solution (ppm)			
Al	929.19	Ba	1.50
Ca	16.61	Ce	0.13
Fe	11.08	Co	0.00
K	268.76	Cu	0.27
Mg	4.10	Nb	0.00
Mn	2.19	Ni	3.36
Na	31766.64	Pb	0.19
P	120.53	Rb	1.12
Si	2532.03	Sr	0.13
Ti	0.98	V	9.69
		Y	0.01
		Zn	2.68

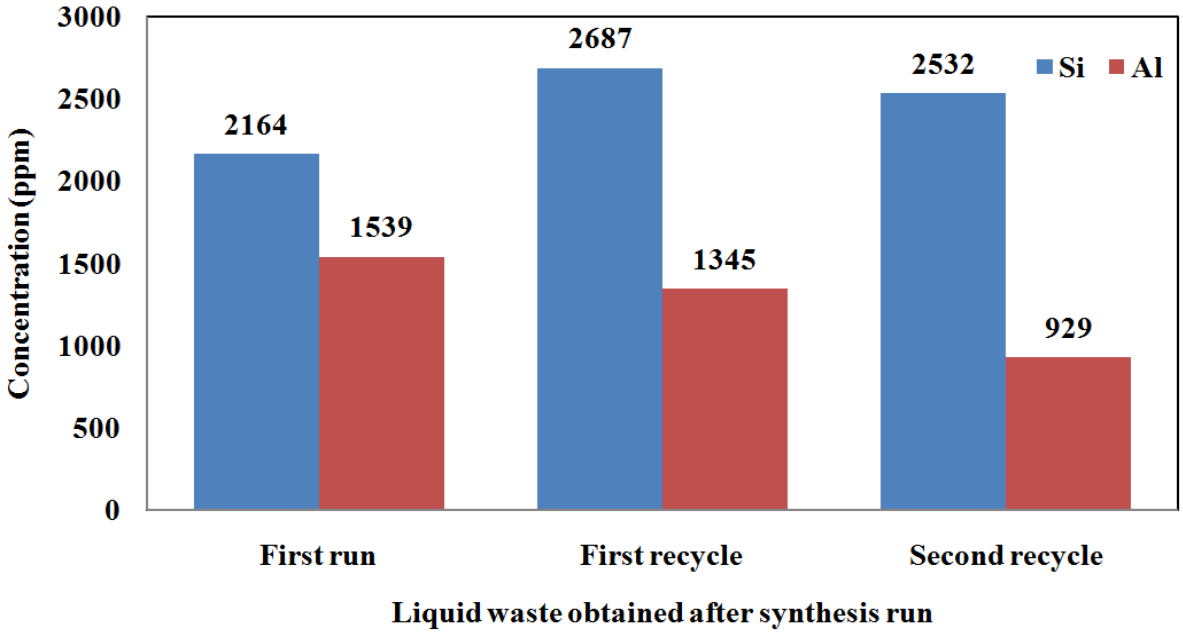

Figure 5-7: ICP-AES results for the waste solutions obtained after each consecutive run illustrating the accumulation of Si and Al

5.4 Chapter summary

The opportunity to minimise the consumption of ultrapure water and production of large quantities of liquid waste; during the synthesis of zeolite A from South African coal fly ash was realised. Protocols were developed whereby liquid waste could be recycled back into the synthesis system to replace the use of ultrapure water, thus serving a dual function. A general waste minimisation approach was developed for the production of zeolite A, by taking into account what lessons learnt from the previous study (chapter 4). High quality zeolite A could repeatedly be synthesized in pure phase when ultrapure water in the system was replaced with liquid waste produced from the system. Critical analysis of final waste solutions proved that toxic elements from the coal fly ash did not leach out into the supernatant waste solution. The study successfully developed a generalized waste minimisation approach which can be applied to similar synthesis systems. Construction of a scale-up synthesis plant is deemed feasible due to the high value of zeolite A in industry as well as the structured approach this study provides for the minimisation of waste and costly ultrapure water consumption.

CHAPTER 6

6 Replacement of hydrothermal treatment with sonochemical treatment during the synthesis of zeolites from South African coal fly ash

6.1 Introduction

In chapter 3 very important lessons were learnt regarding the distribution of elements in the 2-step synthesis approach. This vital data was then used to develop protocols whereby the liquid supernatant waste generated in the process could be minimised (Du Plessis *et al.*, 2013). However, this process still requires further optimisation. The 2-step synthesis process starts off with a time consuming 48 hr aging step (refer to section 3.2.2.1). Before this process can be scale-up to pilot scale the energy consumption and process time of the aging step needs to be optimized. The low temperature which the aging step is operated at (47 ^{o}C) suggested that this step might be replaceable with less time consuming alternatives. In a recent study fly ash was converted into cancrinite by means of sonochemical treatment (Musyoka, 2012). This treatment step involves subjecting fly ash to high intensity sonication in the presence of a strong alkali solution. It was speculated that the time consuming aging step in the synthesis of zeolite Na-P1 and analcime could be replaced with a short high intensity sonochemical treatment step. Ultrasonic waves are sound waves operating at frequencies above the limits of human hearing, generally above 16 kHz (Ensminger and Bond, 2011a). High intensity sonication causes microscopic violent cavitation in liquids (Ensminger and Bond, 2011a). In solid liquid samples the violent cavitation has a destructive effect when the vapour bubbles explode against the solid particles. It is this characteristic effect of elastic wave propagation that has been employed in the synthesis cancrinite from fly ash.

The aim of this study was to investigate the possibility of reducing the processing time of the aging step during the 2-step zeolite synthesis process. The objectives were to attempt replacing the aging step with a short sonochemical treatment step and to investigate the effects of ultrasound on the synthesis process.

6.2 Experimental Section

6.2.1 Experimental approach

In this synthesis approach the aging step, of the 2-step synthesis approach (refer to section 3.2.2.1), was replaced with sonochemical treatment. 20 g of fly ash was mixed with 100 ml 5 M NaOH in a plastic sonication container. The mixture was subjected to sonication at 100% amplitude with a 600 W MISONIX S-4000 sonicator (Figure 6-1).

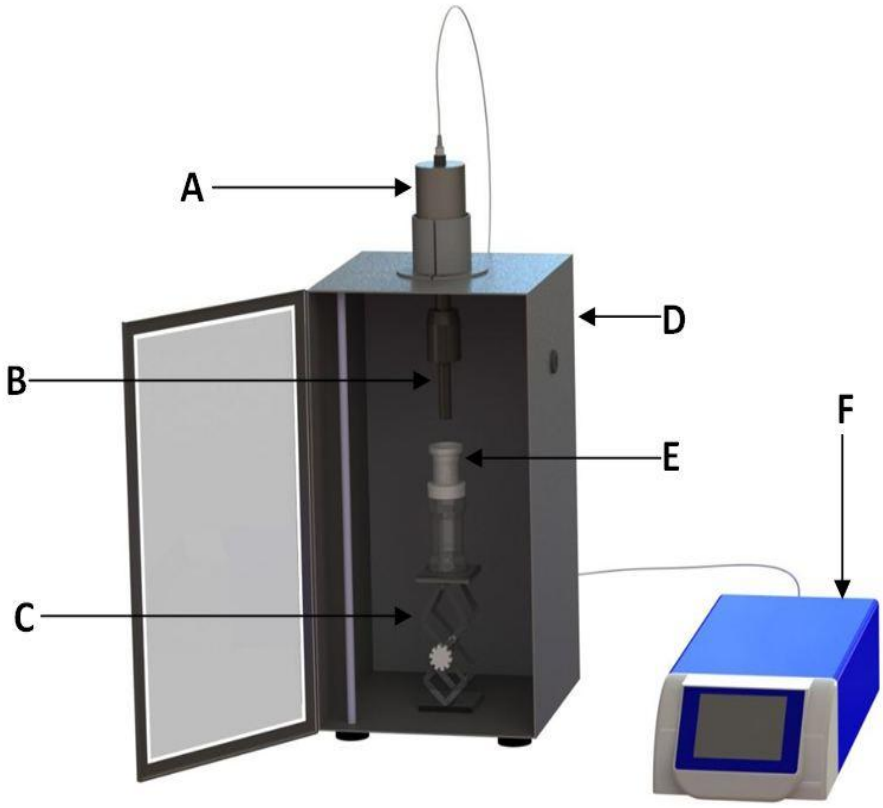

Figure 6-1: (A) Converter transforming electrical inputs into mechanical vibrations through the probe (B) Sonication probe with a removable ¼" tip(C) Height adjustable stand (D) Sound enclosure (E) Plastic 100 ml sonication container (F) 600 W MISONIX S-4000 sonicator

The sonication container was positioned so that the sonicator probe was in the centre of the container. This was done to allow equal radial distribution of the ultrasound waves and to prevent contact of the probe with the container walls. The tip of the sonicator probe was submerged 3 cm below the slurry surface. After sonication was complete the resulting slurry was mixed with 150 ml ultrapure water, transferred into autoclaves and subjected to hydrothermal treatment. All conditions of the hydrothermal treatment step was kept unchanged

(refer to section 3.2.2.1). After 48 hours of hydrothermal treatment the zeolite product was separated from the supernatant, washed with ultrapure water (±5000 ml) and left overnight at 80 ^{o}C to dry. To obtain the optimum sonication time, samples were sonicated for varying time durations before being subjected to hydrothermal treatment. The sonication times were varied from 5 – 30 min in 5 min intervals. The temperature of the slurry being sonicated was monitored but not controlled. The slurry temperature was allowed to increase to allow for better dissolution of amorphous phases. The sample pressure was not controlled since the sonication container is open to the atmosphere. The optimum sonication time was selected as the minimum time that produced zeolites while dissolving most crystalline phases in the coal fly ash. Varies studies illustrated that by using sonication during the zeolite synthesis process the crystallization time is decreased due to a dramatic increase in the rate of crystallization (Andaç *et al.*, 2006; Andaç *et al.*, 2005; Belviso *et al.*, 2011). For this reason, the optimum sonication time was then selected and the hydrothermal treatment time altered in order to determine whether the synthesis time can be lowered even further. The optimum results i.e. optimum sonication/hydrothermal time combination was then reproduced to ensure reliability and accuracy of results.

6.2.2 Materials and characterization techniques

The raw materials used in this chapter were the same used in the original 2-step method (see section 3.2.3). To analyse the quality of the products obtained XRD analysis was employed on all zeolitic products obtained. The changes in the shape of the products produced were observed by means of SEM.

6.3 Results and Discussion

6.3.1 Replacing aging with sonochemical treatment

The first step in replacing the aging step with sonochemical treatment was obtaining the optimum sonication time. Therefore, the aging step was replaced with varying times of sonochemical treatment. After the sonochemical treatment step, in each case, the sonicated slurry was not filtered. All the solids in the system was used throughout the synthesis process like the normal 2-step process. Also, no adjustments were made to the Si/Al ratio of the sonicated slurry before being subjected to normal hydrothermal treatment step (see section 3.2.2.1). Figure 6-2 illustrates the XRD patterns obtained of the products after replacing the aging step with 5 – 30 minutes of sonochemical treatment. With 5 minutes sonication the products contained a small amount of zeolite Na-P1, analcime and a considerable amount of

undissolved mullite. However, by replacing the aging step with 10 min sonication an almost pure phase analcime was obtained.

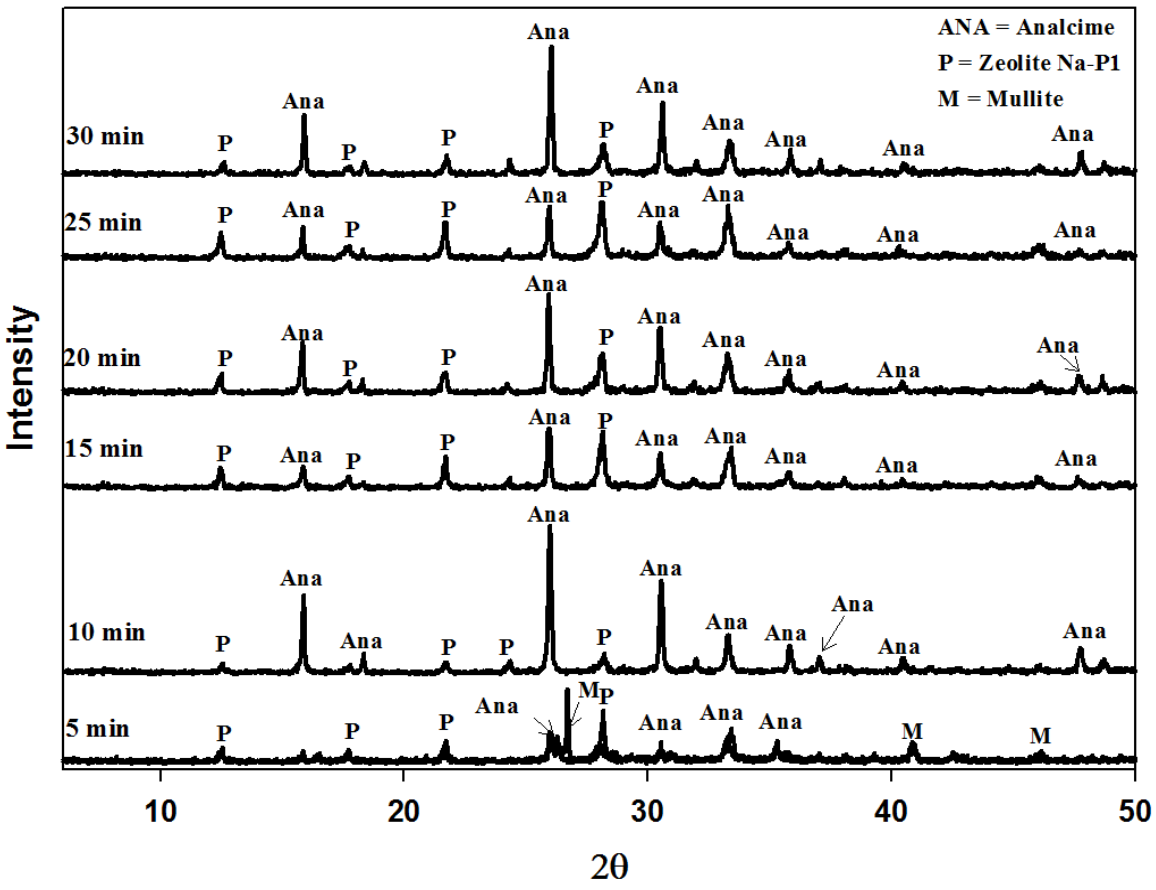

Figure 6-2: X-ray diffraction patterns of zeolite products obtained after replacing the aging step with varying times of sonochemical treatment (5 - 30 min) with constant hydrothermal conditions (static HT for 48 h at 140 ^{o}C).

All the crystalline and amorphous phases in the ash were dissolved and an insignificant amount of zeolite Na-P1 was found in the product. This favouring of analcime over zeolite Na-P1 can be attributed to an increase in the rate of crystallization brought about by the ultrasound waves (Andaç *et al.*, 2005; Belviso *et al.*, 2011). Wu et al. (2006b) found that ultrasound causes the formation of more nucleation sites, consequently increasing the rate of crystallization. An increase in the rate of crystallization then accelerates the effects of Ostwald ripening (Auerbach *et al.*, 2003d). Due to Ostwald ripening (Boistelle and Astier, 1988), the zeolite structural groups were rearranged in zeolite Na-P1 to form analcime (Auerbach *et al.*, 2003a). This phenomenon was illustrated by Mainganye as well (Mainganye, 2012). The author illustrated how zeolite Na-P1 was favoured over analcime, in the 2-step process, when the hydrothermal treatment time

was reduced. With 15 min to 30 min sonication, followed by hydrothermal treatment, a varying mixture of zeolite Na-P1 and analcime was found in the product. These irregularities in the results can be attributed to the nature of the sonication instrument used in this study. A variable power sonicator was used on which the power could not be set. The instrument varied its power output based on the sample temperature. The intensity of sonication affects the cavitation effect in the sample, which is responsible for breaking down the ash (Ensminger and Bond, 2011b). Therefore the inconsistent results after 10 minutes sonication might be attributed to this factor. From the results given in Figure 6-2 it was clear that the optimum sonication time was 10 minutes. Since the sonication resulted in an increase in the rate of crystallization, the opportunity to reduce the hydrothermal treatment (HT) time was explored. By replacing the aging step with a constant10 min sonochemical treatment step, the hydrothermal treatment time was varied from 12 hr to 48 hr in 12 hr increments. Figure 6-3 illustrates the XRD patterns of the products obtained after varying the hydrothermal treatment time.

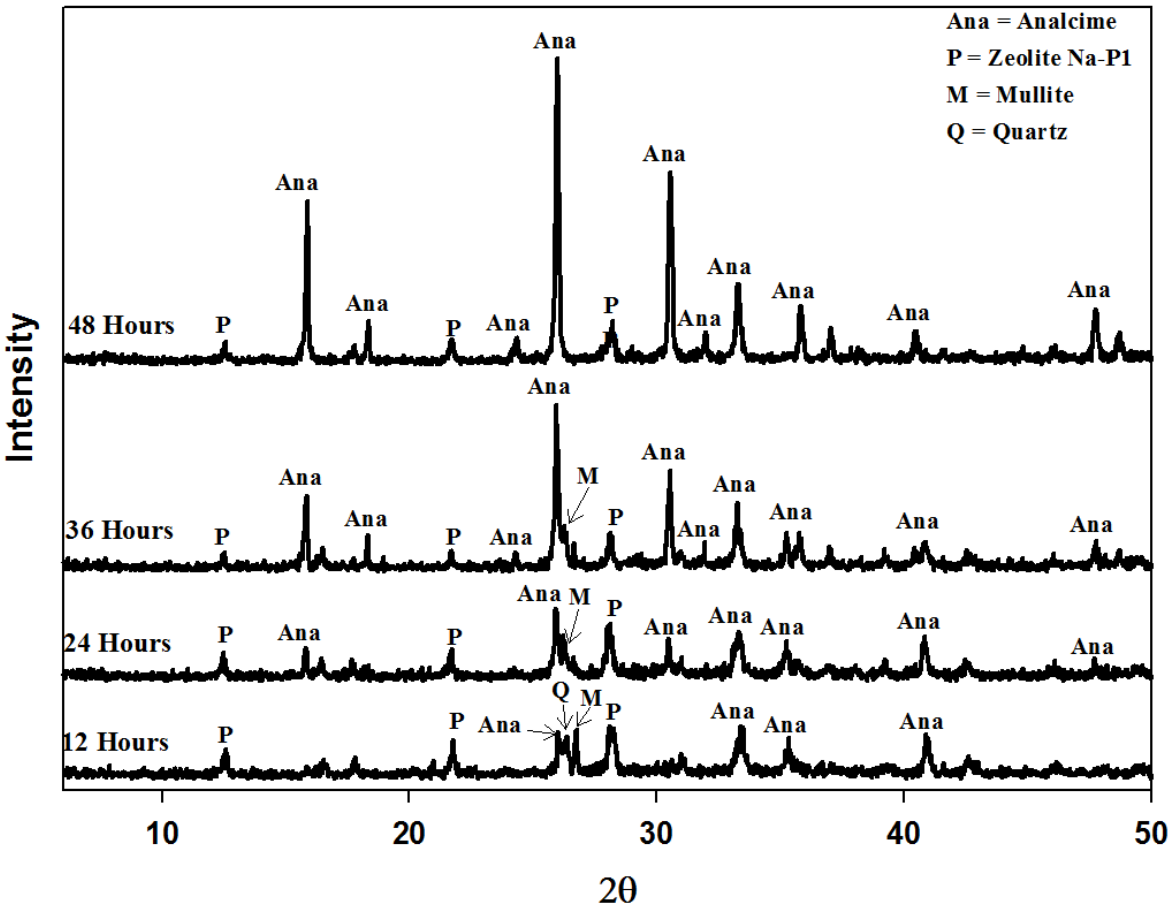

Figure 6-3: X-ray diffraction patterns of zeolite products obtained after varying hydrothermal time from 12 to 48 hr (12 hr increments) with a constant sonochemical treatment time of 10 min

After 12 hours of hydrothermal treatment, most of the crystalline phases originating from the fly ash were still intact. Also, zeolites Na-P1 and analcime crystallised as a mixed phase. After 24 hours hydrothermal treatment, significant quantities of mullite was still present in the product while the crystalline quantities of analcime increased slightly. After 36 hr HT treatment, analcime has become a major crystalline phase in the product while zeolite Na-P1 was found in insignificant quantities. However, even though analcime was the most dominant phase a large amount of undissolved mullite was still present. It is only after 48 hr HT treatment that all the dense crystal phases from the fly ash were dissolved while forming mainly highly crystalline analcime with a residual amount of Na-P1. Thus, it is clear that 48 hours of hydrothermal treatment is required in order to fully dissolve and convert the dense crystal phases present in the fly ash feedstock.

Figure 6-4 illustrates the morphological transformation of the raw fly ash into the two primary zeolitic products.

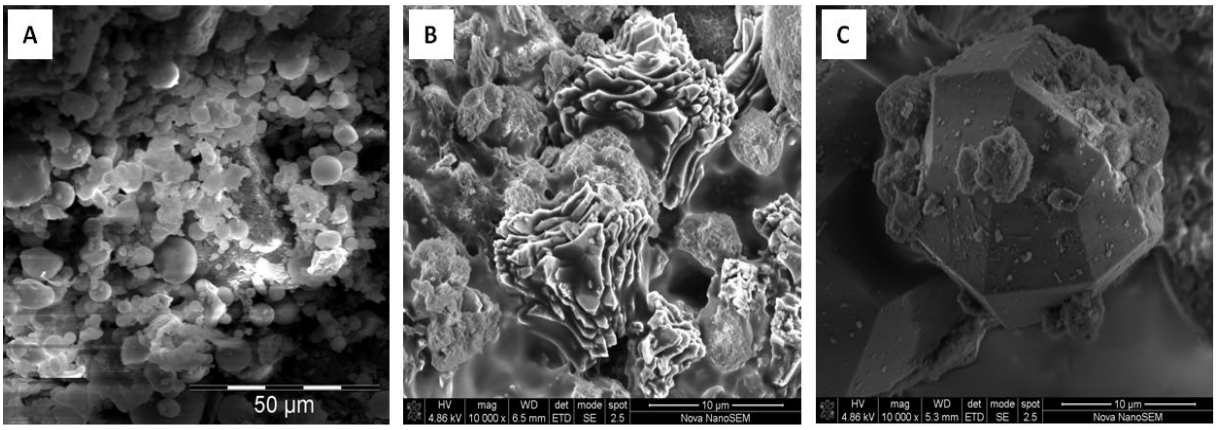

Figure 6-4: SEM micrographs illustrating the morphological transformation of ash into the two zeolite products obtained in this study (A) Raw coal fly ash (B) Zeolite Na-P1 (C) Zeolite analcime

The spherical particles contained in the raw fly ash were broken down during the synthesis process to form crystalline zeolite products. Zeolite Na-P1, synthesized in the base-line study, was found to have a sharp angled flower-like morphology. On the other hand zeolite analcime, synthesized by replacing the aging step with 10 min sonication followed by 48 hr HT, illustrated a well defined trapezohedron shape with a total of 24 faces.

In order to ensure accuracy of results the reproducibility of the optimum conditions was studied. The optimum synthesis conditions were found to be 10 min sonochemical treatment, followed by 48 hr hydrothermal treatment at 140 ^{o}C. The experimental work was repeated by employing

these conditions. Figure 6-5 illustrates the XRD results of this reproducibility study. The experiments were run a total of three times (Run 1 – 3).

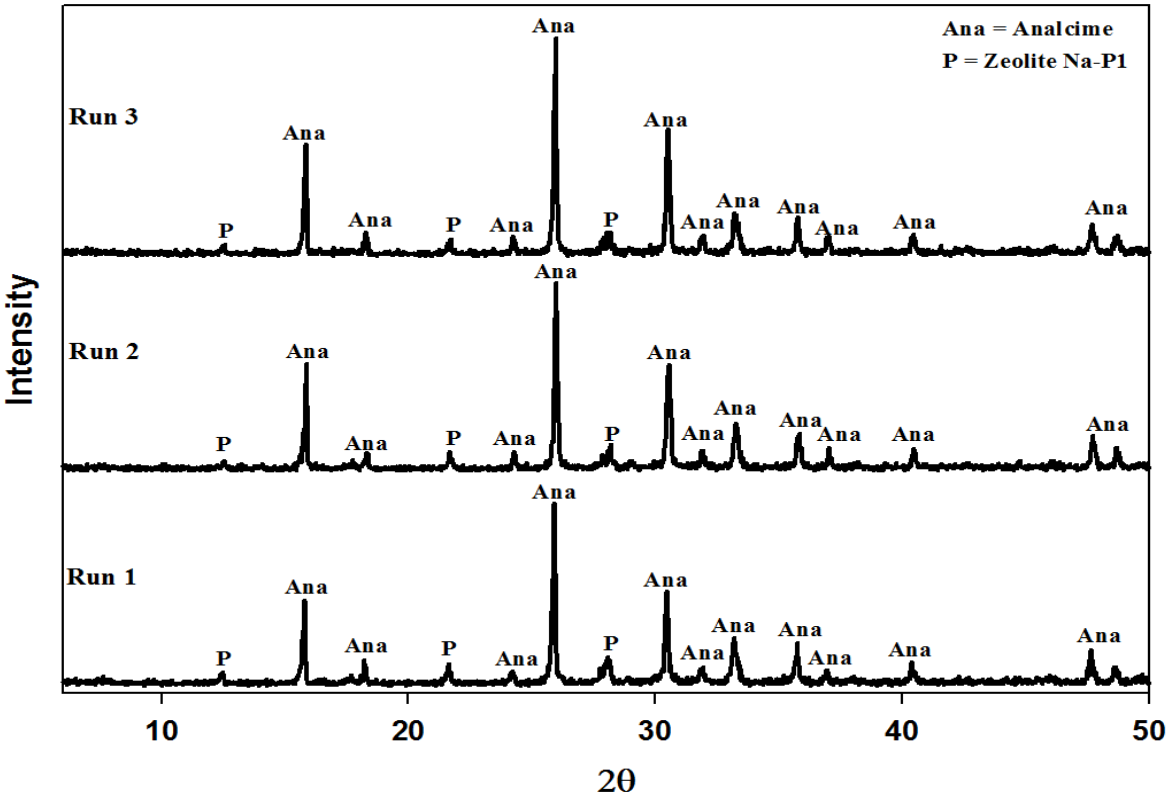

Figure 6-5: X-ray diffraction patterns illustrating the reproducibility of results obtained from optimum synthesis conditions (Aging replaced with 10 min sonochemical treatment followed by static hydrothermal treatment at 140 ^{o}C for 48 hr).

In all cases it was found that zeolite analcime is the major product formed when employing these synthesis conditions. The relative crystallinity of analcime in run 1 – 3 was found to be 92%, 91% and 91% respectively. Therefore the results were found to be highly reproducible which greatly increases its upscale potential. This study effectively replaced the 48 hr aging step, in the 2-step process, with a mere 10 min of sonochemical treatment. This has greatly increased the feasibility of the synthesis process.

6.4 Chapter summary

The opportunity to reduce the synthesis time, and consequently the energy demands, of the 2-step zeolite synthesis process was explored. An attempt was made to replace the 48 hr aging step of this 2-step process with sonochemical treatment. The sonochemical treatment consisted of sonication under alkaline conditions. In the first steps sonication times were varied in order to obtain the optimum sonochemical treatment time. It was found that 10 min of sonochemical

treatment was efficient in order to produce highly crystalline zeolites. The dominating zeolite phase found in the product was analcime. Results indicated that the introduction of ultrasound in the synthesis process dramatically increased the rate of zeolite crystallization. The optimum synthesis conditions were found to be 10 min sonochemical treatment followed by 48 hr hydrothermal treatment at 140 °C. A reproducibility study illustrated that the results obtained from these optimum conditions are highly reproducible. In three repetitions of these experiments the relative crystallinity of analcime was found to be 92%, 91% and 91% respectively. This study effectively reduced the synthesis time of the 2-step process by nearly 50%. By introducing ultrasound in the synthesis process its feasibility could be improved dramatically for scale-up purposes.

CHAPTER 7

7 Replacement of high temperature fusion with sonochemical treatment during the synthesis of zeolite A from South African coal fly ash

7.1 Introduction

In a recent study zeolite A was synthesized from South African coal fly ash by use of the fusion assisted method (Musyoka *et al.*, 2012b). Because of its various important uses in industry; such as its use in detergents, polyvinyl chloride and drying of gasses (Auerbach *et al.*, 2003b); the economical potential of the synthesis of zeolite A on an industrial scale is promising. The mineralogy of fly ash complicates the synthesis of high value metastable phases. This is due to the fact that the various minerals and phases in the ash dissolves at different rates (Fernandez-Jimenez and Palomo, 2005). Complicating this aspect further is the fact that the mineralogy of ash, from the same power plant, varies between batches (Mainganye, 2012). For this reason pre-dissolving the phases using high temperature fusion method appeared to be a robust approach to the synthesis of the zeolite (Chang and Shih, 1998; Molina and Poole, 2004). Although its scale-up potential is promising, the fusion step is energy intensive and thus the operation of purpose-built furnaces on an industrial scale for this process may make it economically unattractive.

In order to scale-up the synthesis process alternative treatment approaches to the fusion step needs to be investigated. One such possible approach is sonochemical treatment which involves exposure to high intensity ultrasonic waves in the presence of a chemical. Under high intensity sonication in liquids, a low pressure in the wave causes the formation of vapour bubbles which collapses violently causing a highly intense cavitation effect (Ensminger and Bond, 2011b). It is the phenomena of cavitation that was speculated could be used in the dissolution of the components in coal fly ash to replace high temperature fusion. With the synthesis of the highly sought after zeolite A, replacing the high temperature fusion step with sonochemical treatment could dramatically increase the process' upscale feasibility.

The aim of this study was to investigate the opportunity to replace the high temperature fusion step, during fusion assisted zeolite synthesis, with a less energy intensive alternative. The objectives of this study were: to investigate the degree of fly ash dissolution possible through

sonochemical treatment, replace the high temperature fusion with the sonochemical treatment and to optimise process conditions to synthesise a pure phase zeolite A product.

7.2 Experimental Section

7.2.1 Experimental approach

The synthesis of zeolite A, by replacing high temperature fusion with sonochemical treatment, was investigated. 20 g of fly ash was mixed with 100 ml 5 M NaOH in a plastic sonication container. The mixture was subjected to sonication at 100% amplitude with a 600 W MISONIX S-4000 sonicator (Figure 7-1).As in chapter 6, in all cases the temperature of the slurry being sonicated was not controlled and allowed to increase. The first step in replacing fusion with sonochemical treatment was to obtain the optimum sonication time that would dissolve maximum amounts of Si and Al species from the ash in a minimum amount of time. The ash was sonicated for varying amounts of time from 5 min to 30 min in 5 min increments. The solid waste and clear solution obtained after sonication was analysed in order to determine the degree of dissolution. After the best sonication time was obtained, attempts were made to synthesise zeolite A from the sonicated slurry.

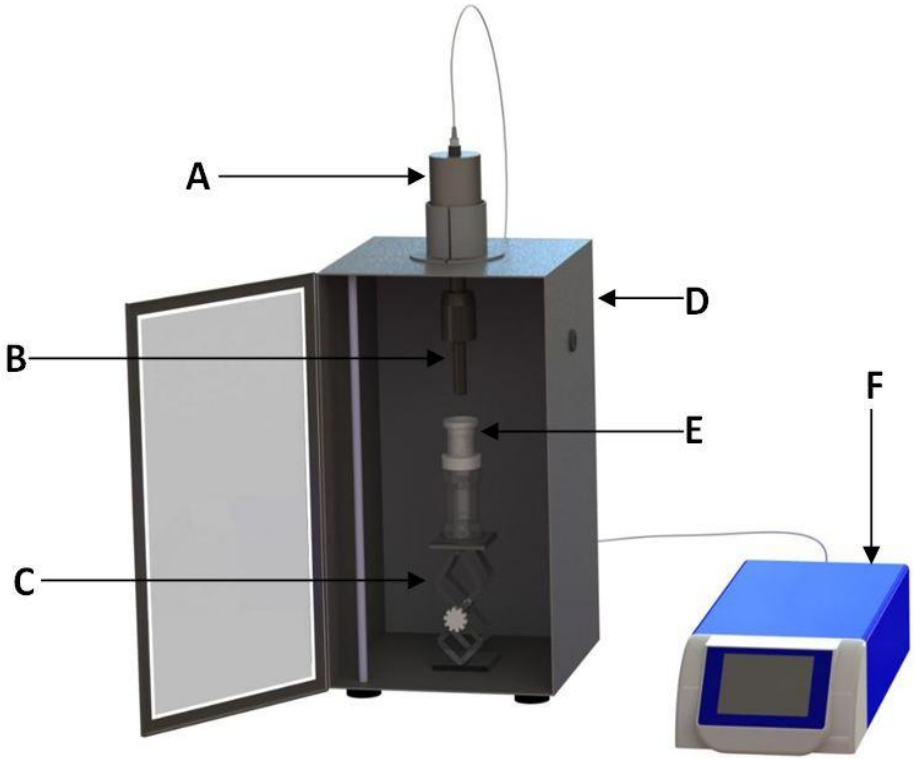

Figure 7-1: (A) Converter transforming electrical inputs into mechanical vibrations through the probe (B) Sonication probe with a removable ¼" tip(C) Height adjustable stand (D) Sound enclosure (E) Plastic 100 ml sonication container (F) 600 W MISONIX S-4000 sonicator

After sonication, the sonicated slurry was filtered, the clear filtrate's Si/Al ratio was adjusted by following the steps described in section 3.2.2.2. No additional water was added to the sonicated slurry before filtration and the solid residues, resulting from filtration, were kept for XRD analysis. The solid residues were not re-sonicated or recycled during this study, but discarded after analysis. The adjusted filtrate was then transferred into glass bottles and subjected to a static hydrothermal treatment in a hot air oven as described in section 3.2.2.2. During the first attempts the hydrothermal conditions were kept the same as the baseline synthesis run i.e. 2 hours at 100 °C (see section 3.2.2.2 for details). In order to obtain a pure phase zeolite A the hydrothermal conditions were then altered in a series of runs. The hydrothermal temperature was decreased to 80 °C or 90 °C and for each temperature the time was varied between 1.5 h and 6 h in order to obtain the optimum temperature/time combination for the synthesis of a pure phase zeolite A.

7.2.2 Materials and characterization techniques

The raw materials used in this study was the same used in the original fusion assisted method, refer to section 3.2.3. The mineralogical changes in the sonicated fly ash and zeolite products

was observed through XRD analysis (refer to section 3.2.3) while morphological changes was observed by SEM. By means of ICP-AES analysis on liquid products the degree of dissolution of fly ash was determined. The power output and slurry sample temperature data was gathered with the MISONIX S-4000 sonicator's built-in software.

7.3 Results and Discussion

7.3.1 Replacing fusion with sonochemical treatment

As discussed in section 7.2.1, the first step in replacing the high temperature fusion step with sonochemical treatment is to find the optimum time of sonication which the fly ash needs to be subjected to. Therefore the fly ash was subjected to sonication for varying amounts of time. The sonicated slurry was then filtered and the residual solid waste analysed. Figure 7-2 illustrates the XRD patterns of the solid waste obtained after subjecting the fly ash to sonication for varying time durations. From these results it became clear that the crystalline mullite and quartz phases in the ash did not dissolve, however the amorphous phases which constitutes a larger part of the ash did indeed dissolve. This can be seen by the disappearance of the amorphous region (20 - 30 2θ) in the XRD spectra (see section 3.3.1).

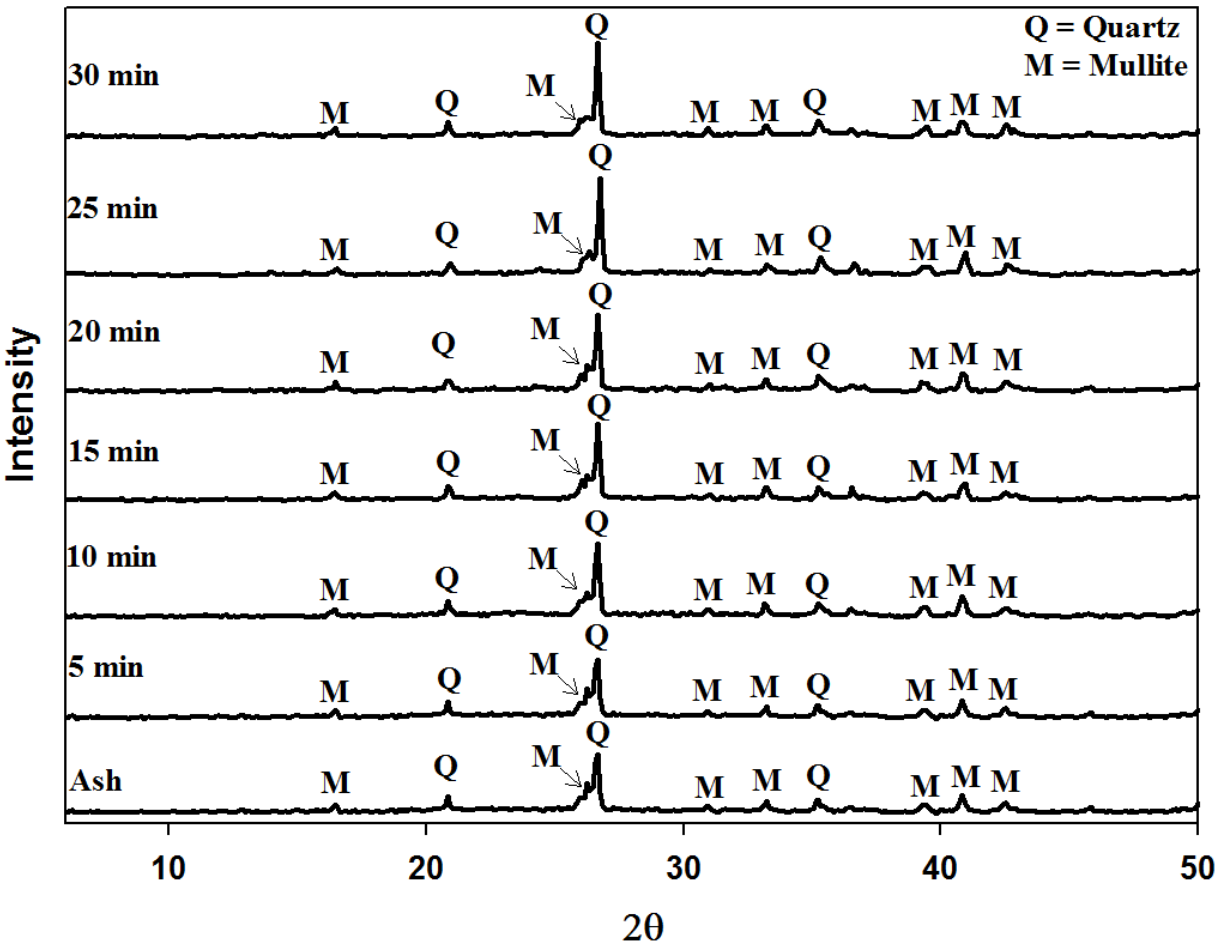

Figure 7-2: XRD results of the solid waste obtained after subjecting fly ash to sonication for varying durations of time (5-30 min at 100% amplitude).

The reason for the poor dissolution of the crystal phases in the fly ash is due to the fact that the MISONIX S-4000 sonicator is a variable power instrument. The sonicator varies its power output based on the sample temperature and cannot be altered manually. Figure 7-3 illustrates the decrease in power output over time and temperature. The power decreases from 170 W to 30 W after 20 minutes of operation. The temperature increases from 40 °C to 100 °C within the first 7 min of sonication and remained within 100 °C ±2 °C thereafter. After the first 10 min of sonication, no measureable amount of water have evaporated. However, after 30 min of sonication, on average, about 15 ml of water evaporated. In cases where a the liquid level decreased due to evaporation, the levels were topped up to 100 ml with ultrapure water before filtering the slurry. The reason why the starting temperature of the samples being sonicated is 40 °C is due to the exothermic nature of the dissolution of NaOH in water, which increased the sample temperature. By means of AES-ICP the amounts of Si and Al dissolved from the fly ash

could be calculated and is expressed in Figure 7-3 as a weight % over time. During the first 5 min of sonication, only 11% Si and 5% Al dissolved from the fly ash. The amount of Si dissolved increased to 24% over 10 minutes, after 10 min it remained relatively constant. Al on the other hand increased to 6% over a 10 min period after which it remained within this range up to 25 minutes and beyond. From Figure 7-3, taking into account the dissolution of Si/Al and the power output over time, the optimum sonication time was found to be 10 min.

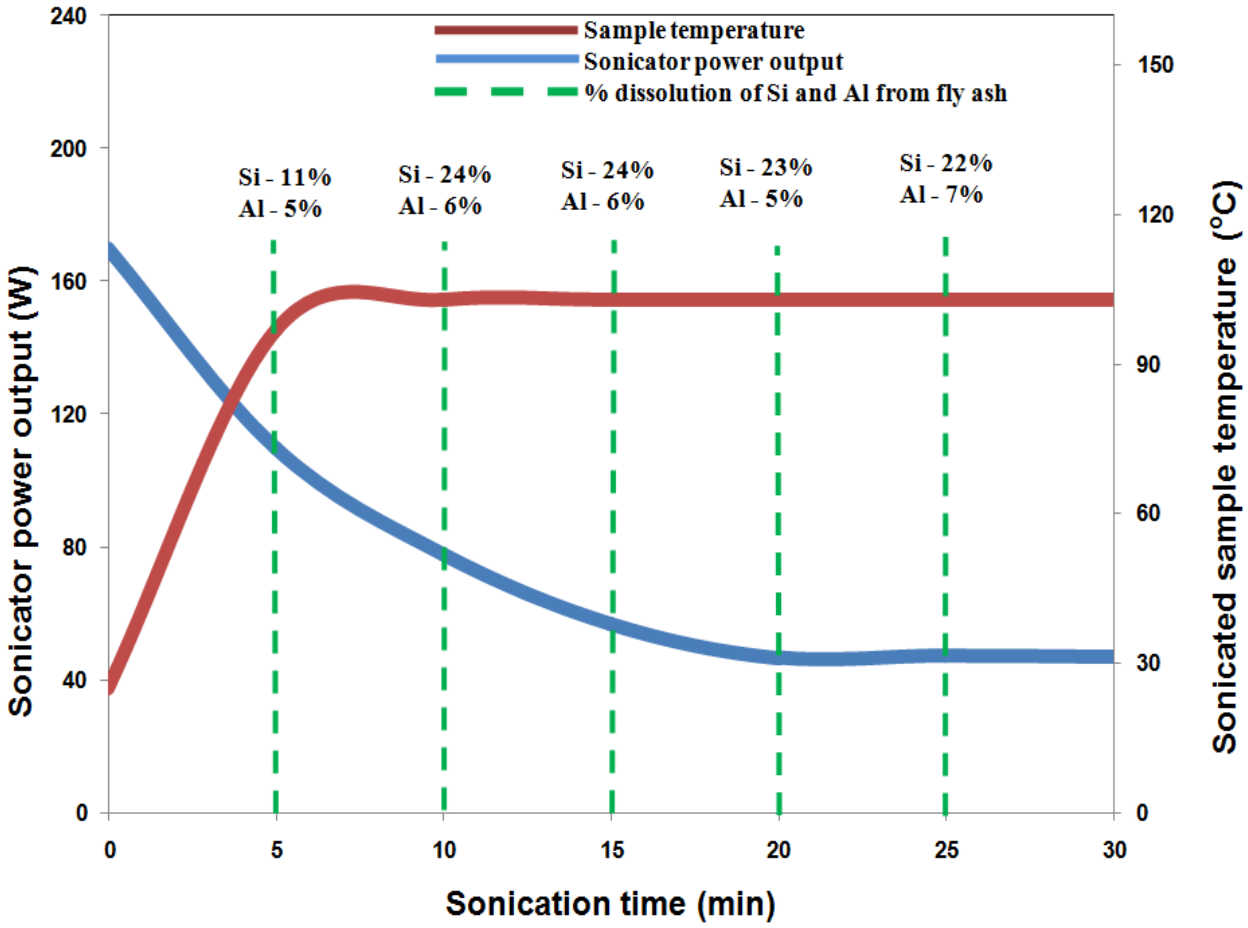

Figure 7-3: Figure illustrating the drop in sonicator power output, increase in sample temperature weight % dissolution of Si/Al as a function of time

Figure 7-4 illustrates SEM micrographs taken of raw coal fly ash, and the solid waste obtained after 10 min or 30 min sonication. Coal fly ash has a spherical glassy morphology and by applying ultrasound irradiation the spherical shape of the particulates was broken down to irregular agglomerated material. The crystalline forms of quartz and mullite still existed unaffected, as XRD showed, even though the morphology changed.

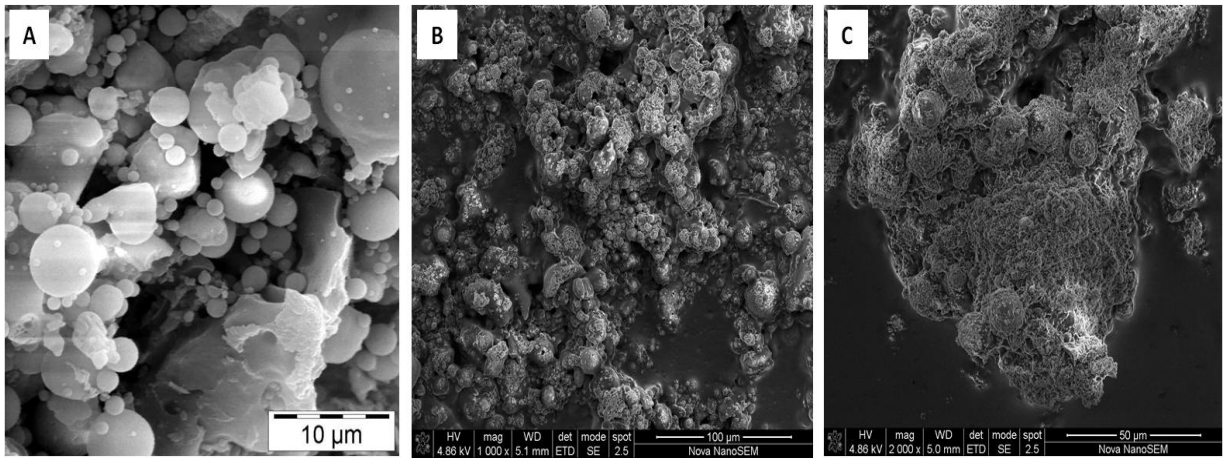

Figure 7-4: SEM micrographs illustrating the change in fly ash morphology after sonication (A) Raw coal fly ash (B) Solid waste after 10 min sonication (C) Solid waste after 30 min sonication

With the sonication time optimised, zeolite A was synthesized from the clear filtrate obtained after filtering the sonicated slurry. The clear filtrate was left to cool to room temperature after which its Si/Al ratio was adjusted with the addition of a sodium aluminate solution (see section 3.2.2.2). The adjusted filtrate solution was then subjected to static hydrothermal treatment using the conditions described in section 3.2.2.2 i.e. 2 hours at 100 °C. Figure 7-5 illustrates the XRD patterns of the zeolite product obtained by applying these synthesis conditions.

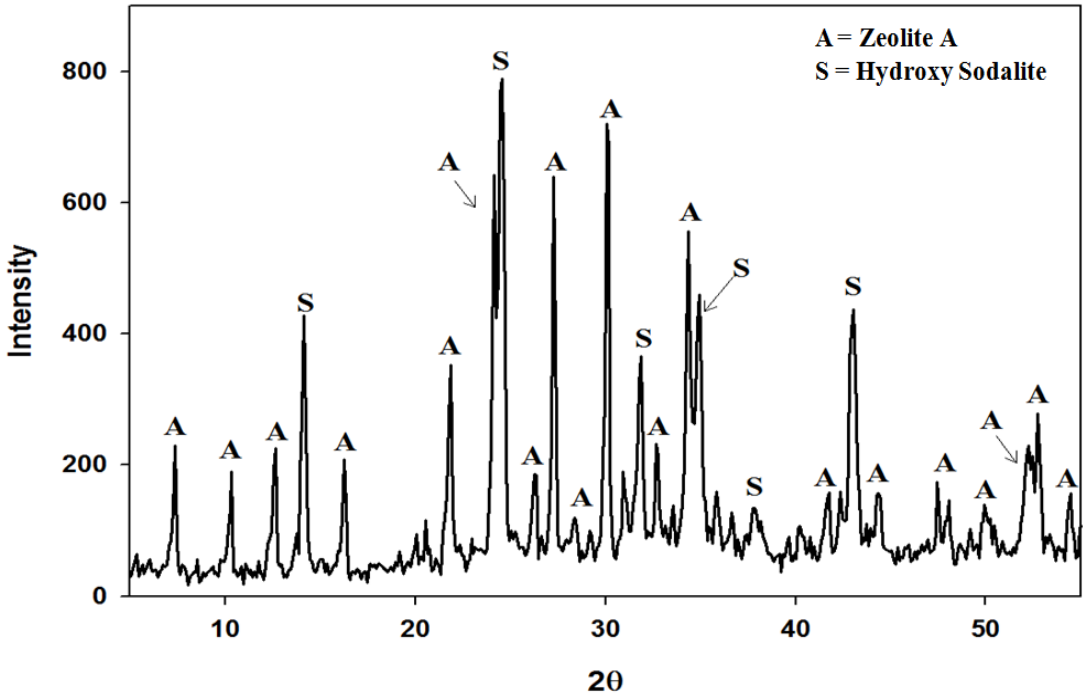

Figure 7-5: XRD results of zeolite A synthesized after replacing high temperature fusion with 10 min sonication

Two zeolite phases developed over the 2 hour crystallization period namely hydroxysodalite and zeolite A. According to the phenomena of Ostwald ripening (Boistelle and Astier, 1988), metastable phases such as zeolite A will continually transform into a more stable denser phase. It has been shown that zeolite A, which is a more useful and desired metastable phase, will transform into hydroxysodalite (Tassopoulos and Thompson, 1987) which has limited uses due to its small pore sizes of 2.8 Å. Belviso et al. (2011) showed that the use of ultrasound during the hydrothermal synthesis of zeolite X decreased the hydrothermal treatment temperature and subsequently increased the rate of crystallization. In all instances of zeolite synthesis the rate of crystallization is increased by an increase in temperature (Auerbach *et al.*, 2003d). For this reason it was clear that in order to retard the crystallization process in order to prevent the transformation of zeolite A into hydroxysodalite, the crystallization temperature would have to be decreased. To attempt the synthesis of a pure phase zeolite A the crystallization temperature was decreased to 80 and 90 °C and the crystallization time was varied between 1.5 h and 6 h. Figure 7-6 illustrates the XRD patterns for the zeolite products after varying the hydrothermal treatment time at a temperature of 90 °C.

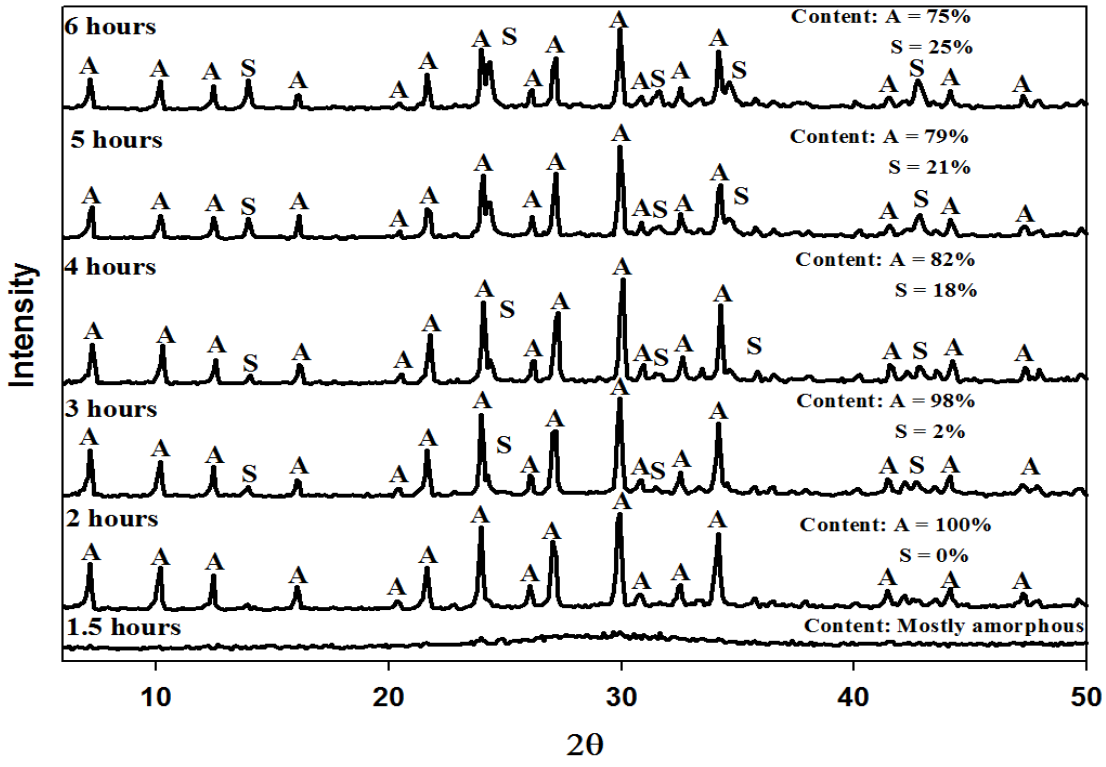

Figure 7-6: XRD results of the zeolite products obtained after replacing fusion with 10 min sonochemical treatment and varying the hydrothermal treatment time at a temperature of 90°C (A = zeolite A, S = hydroxysodalite).

At a crystallization time of 2 h a pure phase of zeolite A was obtained. From 3 hours to 6 hours zeolite hydroxysodalite started to form and its relative crystallinity increased to 25%. Figure 7-6 illustrates the phenomena of Ostwald ripening as the metastable zeolite A was transformed into the more stable hydroxysodalite by increasing the crystallization time.

Figure 7-7 represents the XRD patterns obtained from zeolite products after replacing fusion with 10 min sonochemical treatment and reducing the hydrothermal treatment temperature even further to 80 °C.

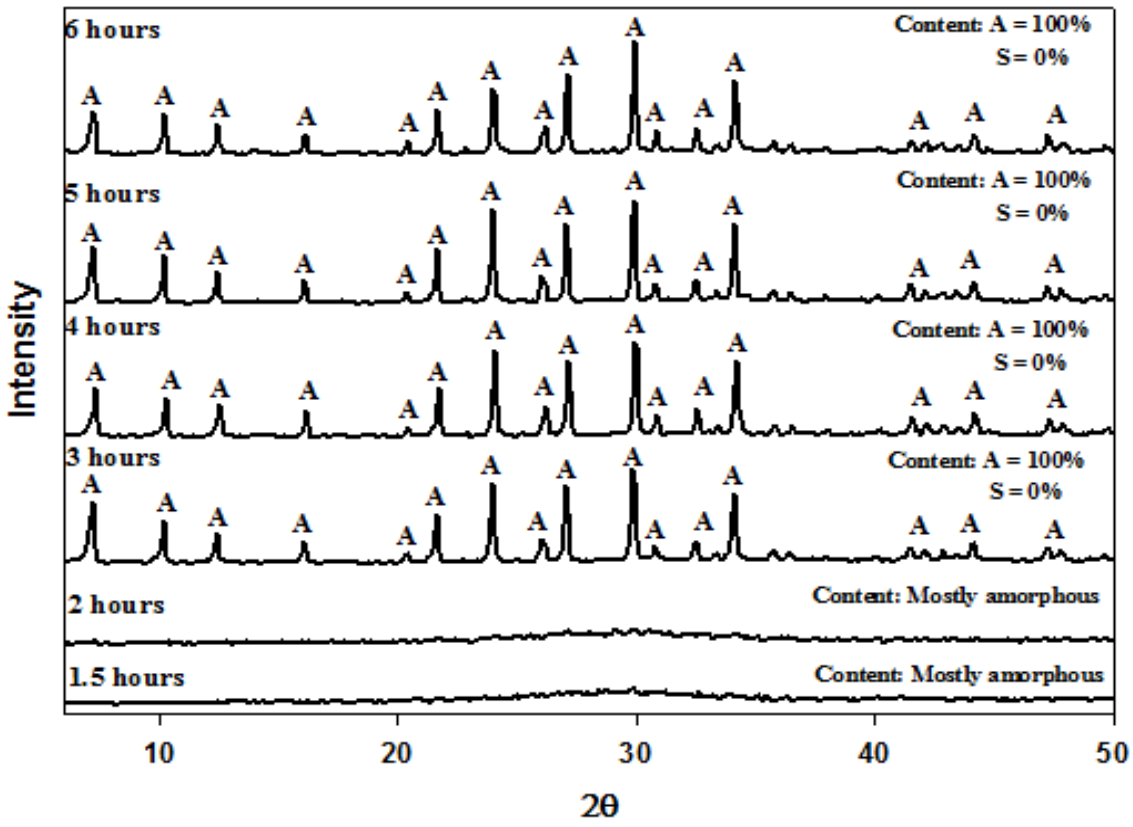

Figure 7-7: XRD XRD results of the zeolite products obtained after replacing fusion with 10 min sonochemical treatment and varying the hydrothermal treatment time at a temperature of 80°C (A = zeolite A, S = hydroxysodalite).

The hydrothermal treatment time was once again varied from 1.5 hours to 6 hours. After 2 hours of hydrothermal treatment the product still contained mostly amorphous phases. From 3 hours till 6 hours crystallization of a pure phase zeolite A was obtained. In accordance with synthesis at 90 °C and Ostwald ripening a further increase in time at 80 °C will eventually also yield zeolite hydroxysodalite.

From these results the optimum hydrothermal treatment conditions, when replacing high temperature fusion with 10 min sonochemical treatment, were found to be HT at 90 °C for 2 hours. Figure 7-8 illustrates the change in morphology of the zeolite products obtained from using the conventional crystallization conditions and the optimized synthesis conditions.

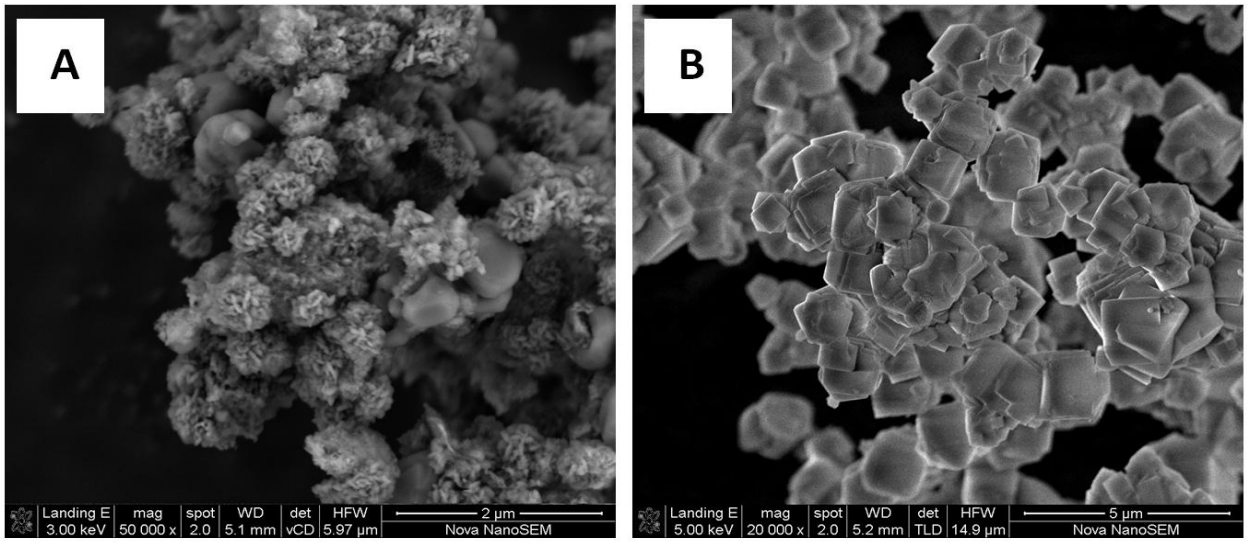

Figure 7-8: SEM micrographs of resulting zeolite products (A) sodalite and zeolite A mixture obtained when using conventional crystallization conditions i.e. 2 h at 100 °C (B) pure phase zeolite A synthesized from optimized crystallization conditions i.e. 2 h at 90 °C

In order to secure accuracy of results the reproducibility of the optimum results were tested. Figure 7-9 illustrates the XRD results of this study. The optimum results i.e. sonication for 10 minutes followed by hydrothermal treatment for 2 hours at 90 °C, were reproduced twice. Run 1 refers to the first experiment where the relative crystallinity of zeolite was 100%. Run 2 and 3 represent the 2 repeating runs which resulted in a relative crystallinity of 97% and 98% respectively. Results were found to be highly reproducible and this synthesis route proved to be a feasible procedure for up-scale operation.

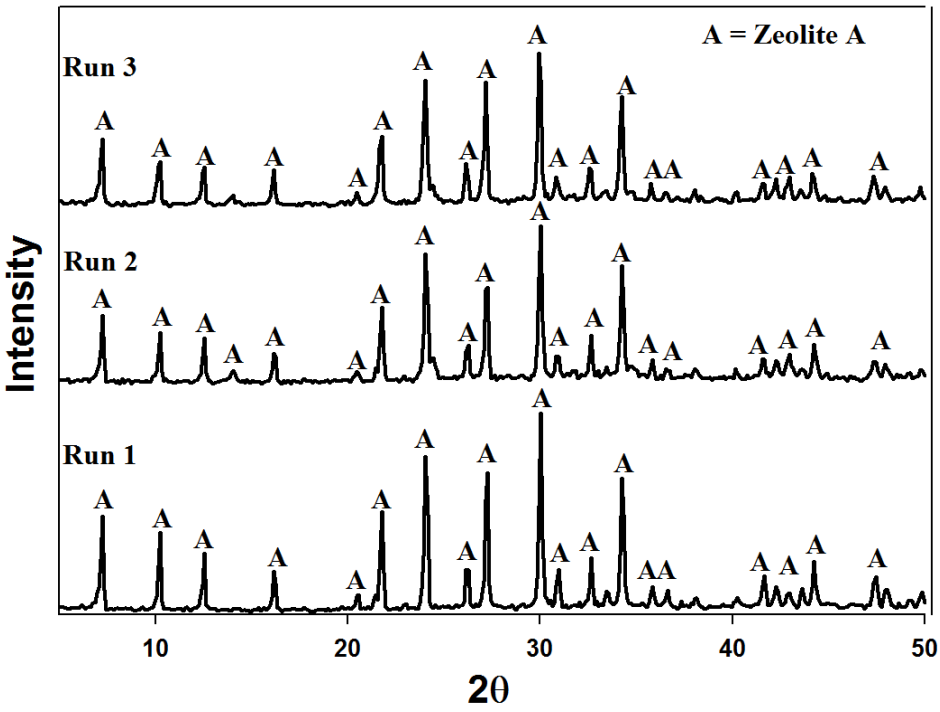

Figure 7-9: XRD patterns illustrating the reproducibility of optimum results i.e. 10 minutes sonication followed by 2 hours hydrothermal treatment at 90 °C

7.4 Chapter summary

The opportunity to replace high temperature (550 °C) fusion with sonochemical treatment during the synthesis of zeolite A from South African coal fly ash was investigated. It was proved that 10 min of high intensity ultrasound irradiation could successfully replace the conventional 90 min energy intensive fusion step which is operated at 550 °C. It was found that during sonication only amorphous phases from the ash could be dissolved. By replacing the fusion step with sonochemical treatment, 24% of the Si originating from fly ash could be extracted into solution, before being used in hydrothermal treatment. The use of ultrasound instead of fusion also reduced the required crystallization temperature of zeolite A during hydrothermal treatment considerably. This improved the energy efficiency of the overall process even further. Hydrothermal treatment conditions could be successfully optimized in order to produce a high quality pure phase zeolite A. Optimum hydrothermal treatment conditions were found to be 2 hours at 90 °C. This is a 10°C reduction from the conventional HT temperature when fusion assistance was used. This study developed a novel, economically viable, approach to the synthesis of zeolite A from coal fly ash. By replacing high temperature fusion with a short sonochemical treatment step, in order to release Al and Si pre-cursors, makes this process a feasible scale-up option.

CHAPTER 8

8 HAZOP study of principal bench scale reactor design

8.1 Introduction

In an attempt to scale up the process of synthesising zeolites from coal fly ash a structured process engineering approach was followed. Before the process can be scaled up to a pilot and full scale operation, an intermediate scale needs to be designed and tested. A bench scale reactor was designed which would fill this scale design gap. This reactor was designed to handle 1 kg of fly ash. However, before this design can be advanced to an implementation stage, the risks and hazards regarding the design need to be identified and minimised. Identifying risks in an operations environment is a crucial activity to ensure safe and reliable production. Operations staff should be constantly aware of the possible risks affecting their safety, the safety of the environment and the reliability of production. In this section the principal bench scale reactor design, capable of handling 1 kg synthesis medium at a time, is discussed and a HAZOP study performed on this design.

8.2 Reactor design

Figure 8-1 illustrates the principal reactor design proposed for bench scale operations. The reactor consists of a stainless vessel with a Teflon lining. In the centre of the reactor lid is a hole, 10 mm in diameter, through which the impeller shaft will pass. Four other holes in the reactor lid, 6 mm in diameter, will be used to attach miscellaneous fittings if needed. These access holes can be used for temperature probes, pressure gauges, sampling points etc. When not in use, these holes will be blinded off. Hold-down clamps on the reactor body ensure that the reactor lid is clamped down securely onto the reactor body. The heat source for this reactor will come from a UniTemp - Mica® band heater. These band heaters can be made to specification by UniTemp, to suite any reactor requirements. This reactor design can be used for both the 2-step method and fusion assisted process. In the 2-step process it can be used for both aging and hydrothermal treatment. However, with the incorporation of ultrasound in the synthesis of zeolites, this reactor will be used only for the hydrothermal step. To date, no investigations have studied agitation during hydrothermal treatment. With this reactor design, mechanical agitation will be made possible during hydrothermal treatment. Also, with the specialized heating equipment from UniTemp it will be possible to closely monitor system

energy requirements and perform energy balances. On this larger scale, with larger impeller shaft diameters, it will be possible to determine mixing power requirements.

One of the fundamental flaws with this design though is that it is still an open system. The impeller shaft hole in the lid of the reactor has a diameter of 10 mm. The impeller shaft diameter used will be maximum 8 mm. Section 8.1 describes the HAZOP study that was performed in the hope of eliminating design flaws like this.

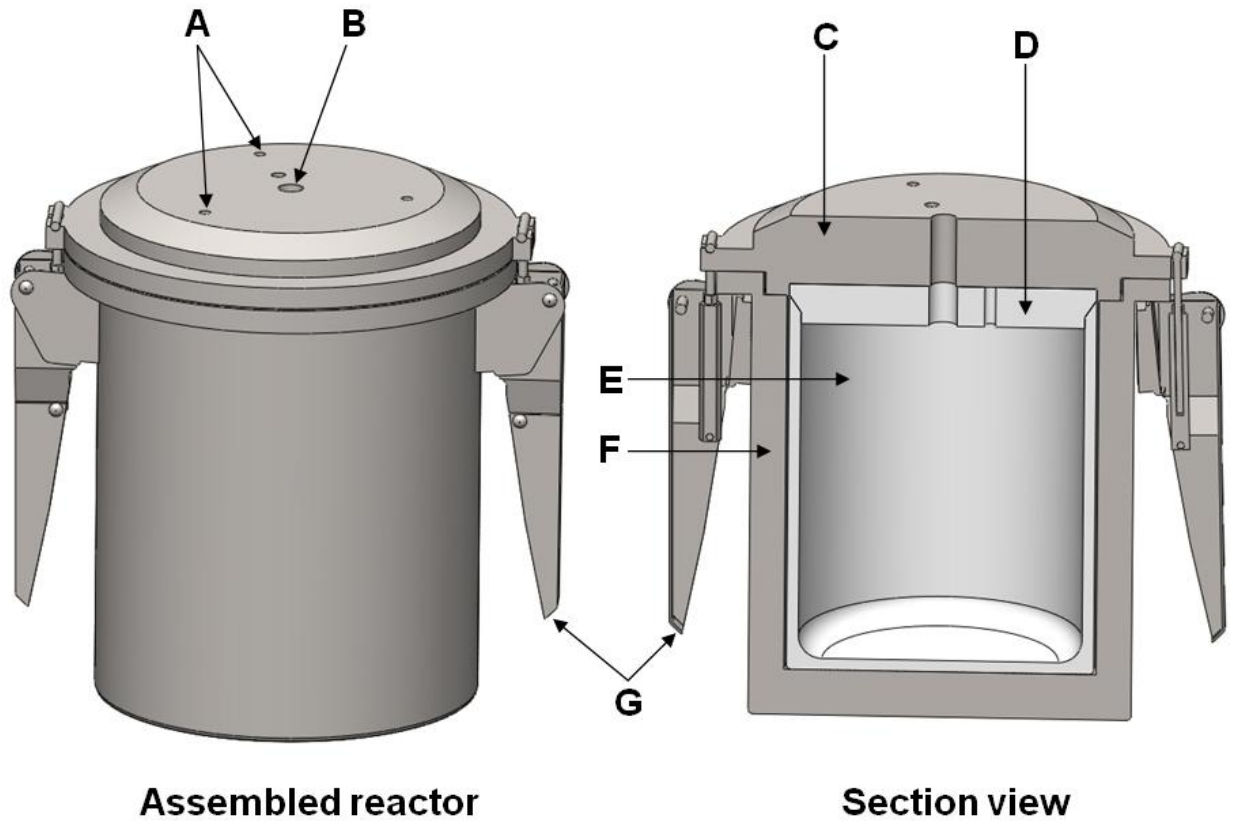

Figure 8-1: Proposed reactor design of bench scale (1 kg) zeolite synthesis. (A) Miscellaneous access holes in reactor lid (B) Impeller shaft hole (C) Stainless steel reactor lid (D) Reactor lid Teflon lining (E) Reactor vessel Teflon lining (F) Stainless steel reactor vessel (G) Hold-down clams.

8.3 HAZOP study

Table 8-1 illustrates the tabulated summary of the HAZOP study performed on the principal reactor design. The table illustrates a process deviation, its consequence, the action required to remedy the deviation and also an assigned action item number. In order to remedy the fundamental problem with the seal surrounding the impeller shaft, it was recommended that a

hydraulic seal be installed in the reactor lid (recommended by industry specialist). If the reactor is not sealed the NaOH solution will reach its boiling point and will remain at that temperature. This means that the crystallization temperature of 140 °C will not be reached in the 2-step method. This in turn will result in poor dissolution of crystal phases in the fly ash and formation of unwanted phases in the product. In order to control the pressure and temperature inside the reactor it is recommended that an accurate temperature and pressure control system from UniTemp® be installed once the reactor has been fabricated.

Table 8-1: Tabulated HAZOP study of principal bench scale reactor design.

Process unit: Zeolite synthesis reactor unit					
Guide word	**Deviation**	**Cause**	**Consequence**	**Action**	**Ref No.**
None of	No temperature rise	System not closed off to atmosphere	Required crystallization temperature not reached	Install hydraulic seal around impeller shaft	1
More of	More Pressure	Rise in temperature due to incorrect control	Zeolite quality and yield affected	Install an accurate UniTemp® temperature controller	2
Less of	Less Pressure	Vapour leak through hydraulic seal	Teflon lining implode due to vacuum after reactor has cooled. Zeolite quality and yield affected.	Install vacuum relief valve and pressure gauge. Install secondary hydraulic seal.	3 4
More of	High shaft vibrations	Excessive shaft length	Damage hydraulic seal and bend impeller shaft	Install brass bush to stabilize shaft	5
Less of	Less agitation speed	Increase in reactants viscosity	Improper mixing yielding impure zeolite phases	Include in operations manual the monitoring and adjusting of mixer speed	6

In the case of a vapour leak, the pressure inside the reactor will drop to below atmospheric levels after its contents have cooled. If the reactor is opened with a strong vacuum in the vessel, the Teflon lining may implode damaging the lining beyond repair. For this reason a vacuum relief valve and pressure gauge needs to be installed on the miscellaneous openings on the reactor lid (action item 3). To ensure that water vapour does not leak through the hydraulic seal, it was recommended that a secondary seal be installed (recommendation by Mr. G van Heerden from GS Tool and Die Maker*scc*). Due to the length of the impeller shaft, high shaft vibrations might damage the hydraulic seal or allow passage of water vapour pass the seal. To ensure this does not happen it was decided to install a brash bush in the reactor lid to stabilize the shaft (action item 5). Lastly, during the synthesis of zeolites the viscosity of the reacting medium might change. This will cause a change in the mixing patterns in the reactor and cause improper mixing. In the operations manual of the reactor a section should be including on adjusting the mixer power to compensate for changes in viscosity. However, this will be the result of a hydrothermal mixing study that can be performed only after the commissioning of the bench scale reactor. From all the action items listed in table 8-1 (No. 1-6), the only actions requiring a change in the rector design are 1/4 and 5. Figure 8-2 illustrates a section view of the new designed reactor lid. Item C in figure 8-1 illustrates the double hydraulic seal system. The inside diameter of the hydraulic seal should be less than 8 mm to ensure a proper seal around the impeller shaft. The double seal consists of two separate seals, as depicted by action items 1 and 4. Item D the in the figure indicates the brash bush that will be installed to stabilize the impeller shaft (action item 5). The only design changes to the stainless steel lid were cut-outs in which the brash bush and seals will fit. Also, a lip on top of the lid surface, above the double seal, was suggested (Mr. G van Heerden) to ensure mechanical integrity of the lid. Detailed mechanical drawings of the four main components of the reactor are illustrated in Appendix C. The hold down clamps used on the reactor vessel will be latch type toggle clamps from Good Hand Inc., model number GH-43110.

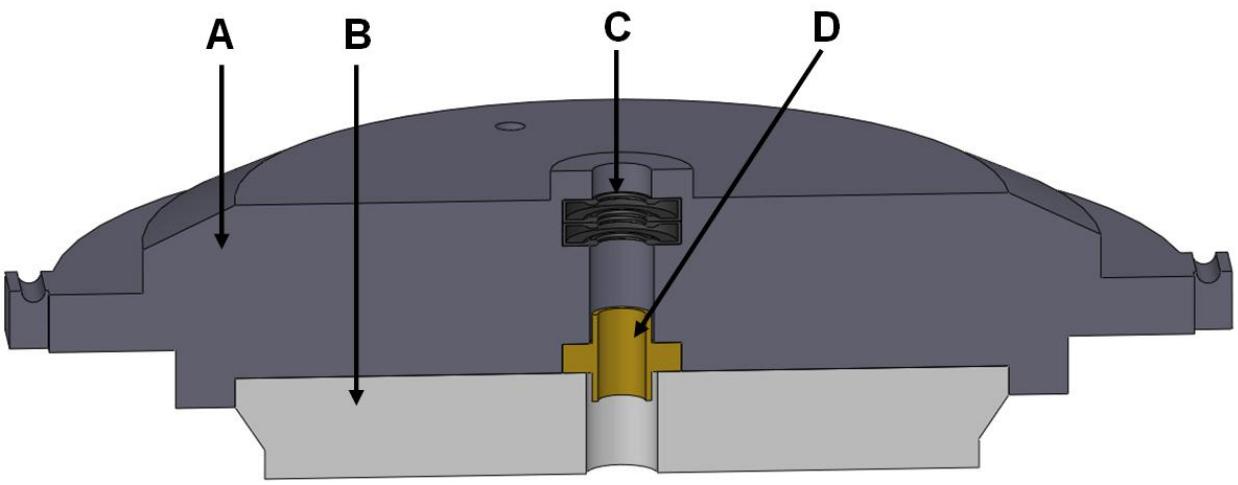

Figure 8-2: Sectioned view illustration of optimize reactor lid design based on the outcome of a HAZOP study. (A) Stainless steel reactor lid (B) Reactor lid Teflon lining (C) Double hydraulic seal system (D) Brash bushing stabilizing impeller shaft.

8.4 Chapter summary

To facilitate the design of a pilot scale zeolite synthesis system, a bench scale (1 kg) reactor was designed. A HAZOP study was performed on this reactor design to identify possible operational and safety risks in the design. It was found that the reactor will have to be fitted with a double hydraulic seal to prevent vapour to escape between the lid and impeller shaft. In order for the double hydraulic seal system to operate effectively a brass bush needs to be installed on the impeller shaft inside the lid of the reactor. Also, to prevent damage to the reactor, it needs to be fitted with a safety relief valve. The HAZOP study should be revised regularly once the reactor is commissioned. HAZOP studies will form a crucial part in nearly every design phase of both the pilot scale and full scale designs of this process.

CHAPTER 9

9 Conclusions and recommendations

9.1 Conclusions

An overall and elemental balance around both the synthesis approaches successfully revealed the fate of elements during the synthesis. In the 2-step process, most elements originating from the coal fly ash (Fe, Mn, Mg, Ca, Ti, Ba, Ce, Co, Cu, Nb, Ni, Pb, Rb, Sr, Y and Zn) were found in the solid zeolite product except for phosphorous and vanadium. In both synthesis processes these two elements were found in the supernatant waste and recovered zeolite washing water. In the fusion assisted process it was found that most elements concentrated in the solid residue waste. The solid residue waste is the solids resulting from filtering the fused ash slurry after the extraction step. It was found that the fate of these elements was not a result of the synthesis mechanisms involved. Due to the low mobility of these elements, due to the presence of CaO in coal fly ash, they do not leach out into solution. For this reason, whenever all the solids in the system is used to synthesize the zeolite product, these elements form part of the overall zeolite product, but not the zeolite crystal structure. However, if the Si and Al is extracted into solution and only the clear solution used in the synthesis process, then these elements do not form part of the zeolite product. In the fusion assisted process, where the clear solution is used to synthesize zeolite A, the only elements found in the zeolite product were Na, K, S, Ba and Zn. Also, in the fusion assisted process most of the Si (66.2%) and Al (68.7%) were found in the solid residue waste, illustrating the poor yield efficiency of this process. In the 2-step process on the other hand, most of the Si (72.2%) and Al (81.5%) were found in the zeolite product. However, the 2-step process generated an impure product while the fusion assisted process resulted in a pure phase zeolite A product. Therefore there is a trade-off in these two process between yield efficiency and product purity. Various elements were found in the supernatant waste from both these process (Al, As, Si, Na, Fe, K, Hg, P, Ni, Pb, Rb and V). The most problematic elements in the liquid supernatant waste were As, Hg, Pb and Al. These elements were found in the recovered washing water as well but in much lower concentrations. From these results it was clear that minimisation of the liquid supernatant waste would be critical.

A waste minimisation study on the 2-step process dramatically reduced the liquid supernatant waste produced by the process. Protocols were developed whereby the liquid supernatant waste was successfully recycled as a source of NaOH. The 2-step process consisted of an

aging step operated at 47 °C for 48 hr, followed by a hydrothermal treatment step operated at 140 °C for another 48 hr. The supernatant waste was recycle 2 consecutive times after adjusting its alkalinity in between runs. The recycled liquid waste replaced the starting 5 M NaOH solution used in the aging step. It was found that with this approach 40% of the supernatant waste could be recycled. Design changes were made to the process and protocols developed whereby 100% of the supernatant waste could be recycled. It was found that by starting the process with a 2 M NaOH solution, and still keeping the mass ratio of ash to NaOH as 1:1, highly crystalline analcime could be synthesised. This also allowed 100% of the supernatant waste to be recycled. The results for this approach were found to be highly reproducible. It was found that by recycling the supernatant waste the relative crystallinity of analcime increased. This was found to be due to the accumulation of Si in solution which favoured analcime formation.

The supernatant waste resulting from the fusion assisted process could also be minimised successfully. Protocols were developed whereby 100% of the supernatant waste could be recycled back into the synthesis system while simultaneously reducing the consumption of ultrapure water. This was achieved by replacing the ultrapure water, used in the extraction step of this process, with the supernatant waste resulting from the process. It was found that recycling the supernatant waste did not affect the quality of zeolite A produced from the process. A reproducibility study illustrated that the results were highly reproducible making this approach environmentally feasible for scale-up purposes.

The synthesis time of the 2-step process was successfully reduced by replacing the aging step with a short sonochemical treatment step. Sonochemical treatment consisted of sonication of the raw fly ash in an alkali medium (5 M NaOH solution). The 48 hr aging step in this process was replaced with 10 min sonochemical treatment. The introduction of ultrasound increased the rate of crystallization during the hydrothermal treatment step. However, even though the crystallisation rate increased, the processing time of HT could not be reduced. Therefore, optimum HT conditions were found to be the same as the normal HT conditions i.e. 140 °C for 48 hr. With the introduction of sonochemical treatment, the overall reduction of synthesis time was found to be nearly 50%. This reduction in synthesis time also reduced the energy demands of the process.

A successful replacement of the high temperature fusion, in the fusion assisted process, with sonochemical treatment was achieved. Results illustrated that the fusion step could be

effectively replaced with a mere 10 min of sonochemical treatment step. It was also found that the introduction of ultrasound increased the rate of zeolite A crystallization. Ultrasound also decreased the crystallization temperature of zeolite A in this process from 100 °C to 90 °C. Optimum synthesis conditions were found to be 10 min sonochemical treatment followed by hydrothermal treatment at 90 °C for 2 hr. With the introduction of ultrasound in this process the energy demands was reduced and the overall synthesis time reduced with more than 50%. This process design change improved the process' upscale feasibility.

A HAZOP study on the principal bench scale reactor design effectively highlighted the design's shortcomings. It was found that an improper seal around the impeller shaft seal would result in impure zeolitic phases being formed. Also, the length of the impeller shaft would cause instability resulting in the breaking of the installed hydraulic seal. An optimised design was suggested in which a double hydraulic seal system would prevent vapour leaks around the impeller shaft. Also, the incorporation of a brass bush would stabilize the impeller shaft. These design changes could have greatly reduce the risk of equipment and process failure when operating this larger scale reactor.

The investigations in this study have successfully prepared the process of synthesizing zeolites from South African fly ash for scale-up operation. Critical design changes were made to remedy the fundamental process design flaws which restricted the processes' upscale feasibility. With these new optimized processes, the aim to reduce the vast amounts of coal fly ash disposed in South Africa can be pursued. This will greatly relieve the environmental and economical stress caused by the disposal of fly ash in the country.

9.2 Recommendations

Currently zeolite products obtained from the two principal synthesis routes are washed with ultrapure water. This generates large volumes of washing water waste. Although not as serious as the supernatant waste, it would still require treatment before disposal. It is recommended that alternative approaches be explored to clean the zeolite products.

The fusion assisted process produces a solid waste. This waste contains most of the SI and Al from the coal fly ash. This is the reason for the low yield efficiency of this process. It is recommended that this solid waste be recycled back into the synthesis system to extract more of the Si and Al into solution. This is expected to greatly improve the yield efficiency in this process. It is recommended that future work be continued with all the process design changes made in this study.

Due to the scale of the process used in this study, a detailed energy balance study could not be performed. The energy demands of the processes will be required in order to design the pilot and full scale processes. It is recommended that a detailed energy balance should be performed on the bench (1 kg) scale process to determine the energy demands of the varies unit operations involved in the process.

Lastly, it is recommended that a new product separation method be explored. Currently the zeolite products are recovered by means of filtration with filter paper. This causes loss of the product and is very time consuming.

Bibliography

Adriano, D., Page, A., Elseewi, A., Chang, A. & Straughan, I. 1980. Utilization and disposal of fly ash and other coal residues in terrestrial ecosystems: A review. *Journal of Environmental Quality,* 9**,** 333-344.

Ahmaruzzaman, M. 2010. A review on the utilization of fly ash. *Progress in Energy and Combustion Science* 36**,** 327–363.

Akar, G., Polat, M., Galecki, G. & Ipekoglu, U. 2012. Leaching behavior of selected trace elements in coal fly ash samples from Yenikoy coal-fired power plants. *Fuel processing technology,* 104**,** 50-56.

Al-Anber, M. & Al-Anber, Z. A. 2008. Utilization of natural zeolite as ion-exchange and sorbent material in the removal of iron. *Desalination,* 225**,** 70-81.

Alexander, L. & Klug, H. P. 1948. Basic aspects of X-ray absorption. *Analytical Chemistry,* 20**,** 886-889.

Alonso, J. L. & Wesche, K. 1991. Characterization of fly ash. *In:* WESCHE, K. (ed.) *Fly Ash in Concrete: Properties and Performance.* London: E & FN Spon.

Ames, L. L. 1991. Cation Sieve Properties of the Open Zeolites Chabazite, Mordenite, Erionite and Clinoptilolite. *The American Mineralogist* 46**,** 1120-1131.

Andaç, Ö., Murat Telli, Ş., Tatlier, M. & Erdem-Şenatalar, A. 2006. Effects of ultrasound on the preparation of zeolite A coatings. *Microporous and Mesoporous Materials,* 88**,** 72-76.

Andaç, Ö., Tatlıer, M., Sirkecioğlu, A., Ece, I. & Erdem-Şenatalar, A. 2005. Effects of ultrasound on zeolite A synthesis. *Microporous and Mesoporous Materials,* 79**,** 225-233.

Andrés, J. M., Ferrer, P., Querol, X., Plana, F. & Umaña, J. C. Year. Zeolitisation of coal fly ashes using microwaves. Process optimization. *In:* International Ash Utilization Symposium, 1999.

Athanasiadis, K. & Helmreich, B. 2005. Influence of chemical conditioning on the ion exchange capacity and on kinetic of zinc uptake by clinoptilolite. *Water Research,* 39**,** 1527-1532.

Auerbach, S. M., Carrado, K. A. & Dutta, P. K. 2003a. Introduction to the Structural Chemistry of Zeolites. *In:* LOBO, R. F. (ed.) *Handbook of Zeolite Science and Technology.* New York: Marcel Dekker Inc.

Auerbach, S. M., Carrado, K. A. & Dutta, P. K. 2003b. *Handbook of Zeolite Science and Technology,* New York, Marcel Dekker Inc.

Auerbach, S. M., Carrado, K. A. & Dutta, P. K. 2003c. Zeolites: A Primer. *In:* PARYA, P. & DUTTA, P. K. (eds.) *Handbook of Zeolite Science and Technology.* New York: Marcel Dekker Inc.

Auerbach, S. M., Carrado, K. A. & Dutta, P. K. 2003d. Theoretical and Practical Aspects of Zeolite Crystal Growth. *In:* SUBOTIC´, B. & BRONIC´, J. (eds.) *Handbook of Zeolite Science and Technology.* New York: Marcel Dekker Inc.

Auerbach, S. M., Carrado, K. A. & Dutta, P. K. 2003e. Gas Separation by Zeolites. *In:* SIRCAR, S. & MYERS, A. L. (eds.) *Handbook of Zeolite Science and Technology.* New York: Marcel Dekker Inc.

Azizi, S. N. & Yousefpour, M. 2009. Synthesis of Aluminum-Rich Analcime Using an Ethylene Diamine Derivative as Template. *Zeitschrift fur Anorganische und Allgemeine Chemie,* 635**,** 1654-1658.

Baerlocher, C. H., Meier, W. M. & Holson, D. 2001. Atlas of Zeolite Framework Types. Amsterdam: Elsevier.

Barrer, R. M. 1982. *Hydrothermal chemistry of zeolites*, Academic Press London.

Bartelmehs, K. L., Downs, R. T., Gibbs, G. V., Boisen, M. B. & Birch, J. B. 1995. Tetrahedral rigid-body motion in silicates. *American Mineralogist,* 80**,** 680-690.

Basaldella, E. I., Kikot, A. & Tara, J. C. 1997. Effect of aluminum concentration on crystal size and morphology in the synthesis of a NaAl zeolite. *Materials Letters,* 31**,** 83-86.

Baur, W. 1978. Variation of mean Si-O bond lengths in silicon-oxygen tetrahedra. *Acta Crystallographica Section B,* 34**,** 1751-1756.

Bebon, C., Colson, D., Marrot, B., Klein, J. P. & Di Renzo, F. 2002. Synthesis of zeolites: study and application of a new process of homogenous shaking out of the medium to minimize the shear rate during the crystallization. *Microporous and Mesoporous Materials,* 53**,** 13-20.

Belviso, C., Cavalcante, F. & Fiore, S. 2010. Synthesis of zeolite from Italian coal fly ash: Differences in crystallization temperature using seawater instead of distilled water. *Waste management,* 30**,** 839-847.

Belviso, C., Cavalcante, F., Lettino, A. & Fiore, S. 2011. Effects of ultrasonic treatment on zeolite synthesized from coal fly ash. *Ultrasonics Sonochemistry,* 18**,** 661-668.

Berkgaut, V. & Singer, A. 1996. High capacity cation exchanger by hydrothermal zeolitization of coal fly ash. *Applied Clay Science,* 10**,** 369-378.

Bhanarkar, A. D., Gavane, A. G., Tajne, D. S., Tamhane, S. N. & Nema, P. 2008. Composition and size distribution of particules emissions from a coal-fired power plant in India. *Fuel,* 87**,** 2095-2101.

Biškup, B. & Subotić, B. 2004. Kinetic analysis of the exchange processes between sodium ions from zeolite A and cadmium, copper and nickel ions from solutions. *Separation and Purification Technology,* 37**,** 17-31.

Boistelle, R. & Astier, J. P. 1988. Crystallization mechanisms in solution. *Journal of Crystal Growth,* 90**,** 14-30.

Bosnar, S., Antonić, T., Bronić, J. & Subotić, B. 2004. Mechanism and kinetics of the growth of zeolite microcrystals. Part 2: Influence of sodium ions concentration in the liquid phase on the growth kinetics of zeolite A microcrystals. *Microporous and Mesoporous Materials,* 76**,** 157-165.

Bosnar, S. & Subotic, B. 1999. Mechanism and kinetics of the growth of zeolite microcrystals: Part 1: Influence of the alkalinity of the system on the growth kinetics of zeolite A microcrystals. *Microporous and Mesoporous Materials,* 28**,** 483-493.

Breck, D. W. 1974. *Zeolite Molecular Sieves,* New York, John Wiley & Sons

Bregolato, M., Bolis, V., Busco, C., Ugliengo, P., Bordiga, S., Cavani, F., Ballarini, N., Maselli, L., Passeri, S., Rossetti, I. & Forni, L. 2007. Methylation of phenol over high-silica beta zeolite: Effect of zeolite acidity and crystal size on catalyst behaviour. *Journal of Catalysis,* 245**,** 285-300.

Byrappa, K. & Yoshimura, M. 2001. *Handbook of hydrothermal technology: a technology for crystal growth and materials processing,* Norwich, Noyes Publications/William Andrew Publishing.

Cao, G. & Shah, M. J. 2007. In situ monitoring of zeolite crystallization by electrical conductivity measurement: New insight into zeolite crystallization mechanism. *Microporous and Mesoporous Materials,* 101**,** 19-23.

Carlson, C. L. & Adriano, D. C. 1993. Environmental Impacts of Coal Combustion Residues. *Journal of Environmental Quality,* 22**,** 227-247.

Casci, J. L. 2005. Zeolite molecular sieves: preparation and scale-up. *Microporous and Mesoporous Materials,* 82**,** 217-226.

Catalfamo, P., Corigliano, F., Primerano, P. & Di Pasquale, S. 1993. Study of the pre-crystallization stage of hydrothermally treated amorphous aluminosilicates through the composition of the aqueous phase. *Journal of the Chemical Society, Faraday Transactions,* 89**,** 171-175.

Ccsd. 2009. *Power Station Emission Handbook* [Online]. Available: http://www.ccsd.biz/PSE_Handbook/5/8/index.cfm [Accessed 19 December 2012].

Chang, H. & Shih, W. 1998. A General Method for the Conversion of Fly Ash into Zeolites as Ion Exchangers for Cesium. *Industrial and Engineering Chemistry Research,* 37**,** 71-78.

Choi, J., Kimoto, K. & Ichikawa, Y. 2011. Quartz dissolution experiments at various pH, temperature and stress conditions: CLSM and ICP-AES investigations. *Environmental Earth Sciences***,** 1-10.

Corma, A., Corell, C., Fornés, V., Kolodziejski, W. & Pérez-Pariente, J. 1995. Infrared spectroscopy, thermoprogrammed desorption, and nuclear magnetic resonance study of the acidity, structure, and stability of zeolite MCM-22. *Zeolites,* 15**,** 576-582.

Covarrubias, C., García, R., Arriagada, R., Yánez, J. & Garland, M. T. 2006. Cr(III) exchange on zeolites obtained from kaolin and natural mordenite. *Microporous and Mesoporous Materials,* 88**,** 220-231.

Criado, M., Fernandez-Jimenez, A. & Palomo, A. 2010. Alkali activation of fly ash. Part III: Effect of curing conditions on reaction and its graphical description. *Fuel***,** 1-8.

Cruciani, G. 2006. Zeolites upon heating: Factors governing their thermal stability and structural changes. *Journal of Physics and Chemistry of Solids,* 67**,** 1973-1994.

Cullity, B. D. 1956. *Elements of X Ray Diffraction,* Massachusetts, Addison-Wesley.

Cundy, C. S. & Cox, P. A. 2005. The hydrothermal synthesis of zeolites: Precursors, intermediates and reaction mechanism. *Microporous and Mesoporous Materials,* 82**,** 1-78.

Ćurković, L., Cerjan-Stefanović, Š. & Filipan, T. 1997. Metal ion exchange by natural and modified zeolites. *Water Research,* 31**,** 1379-1382.

Davis, M. E. & Lobo, R. F. 1992. Zeolite and molecular sieve synthesis. *Chemistry of Materials,* 4**,** 756-768.

Ding, L., Zheng, Y., Zhang, Z., Ring, Z. & Chen, J. 2006. Effect of agitation on the synthesis of zeolite beta and its synthesis mechanism in absence of alkali cations. *Microporous and Mesoporous Materials,* 94**,** 1-8.

Dosskey, M. G. & Adriano, D. C. 1993. Trace element toxicity in va mycorrhizal cucumber grown on weathered coal fly ash. *Soil Biology and Biochemistry,* 25**,** 1547-1552.

Dove, M. T., Heine, V. & Hammonds, K. D. 1995. Rigid unit modes in framework silicates. *Mineralogical Magazine,* 59**,** 629-640.

Držaj, B. 1985. *Zeolites: synthesis, structure, technology, and application: proceedings of an international symposium*, Elsevier Science Ltd.

Du Plessis, P. W., Ojumu, T. V. & Petrik, L. F. 2013. Waste minimisation protocols for the process of synthesizing zeolites from South African coal fly ash. *Materials,* 6**,** 1688-1703.

Dwivedi, S., Saquib, Q., Al-Khedhairy, A. A., Ali, A.-Y. S. & Musarrat, J. 2012. Characterization of coal fly ash nanoparticles and induced oxidative DNA damage in human peripheral blood mononuclear cells. *Science of The Total Environment,* 437**,** 331-338.

Elliot, A. D. & Zhang, D. Year. Controlled Release Zeolite Fertilisers: A Value Added Product Produced from Fly Ash. *In:* International Ash Utilization Symposium (IAUS) and World of Coal Ash (WOCA), 2005.

Ensminger, D. & Bond, L. J. 2011a. Ultrasonics A Broad Field. *In:* L.L, F. (ed.) *Ultrasonics: Fundamentals, Technologies, and Applications.* Third ed. Boca Raton: CRC Press.

Ensminger, D. & Bond, L. J. 2011b. Elastic Wave Propagation and Associated Phenomena. *In:* L.L, F. (ed.) *Ultrasonics: Fundamentals, Technologies, and Applications.* Third ed. Boca Raton: CRC Press.

Epping, J. D. & Chmelka, B. F. 2006. Nucleation and growth of zeolites and inorganic mesoporous solids: Molecular insights from magnetic resonance spectroscopy. *Current Opinion in Colloid & Interface Science,* 11**,** 81-117.

Erol, M., Küçükbayrak, S. & Ersoy-Meriçboyu, A. 2007. Characterization of coal fly ash for possible utilization in glass production. *Fuel,* 86**,** 706-714.

Erten-Kaya, Y. & Cakicioglu-Ozkan, F. 2012. Effect of ultrasound on the kinetics of cation exchange in NaX zeolite. *Ultrasonics Sonochemistry,* 19**,** 701-706.

Eskom. 2011a. *Integrated Report 2011* [Online]. Available: www.eskom.co.za/annreport11/ [Accessed 18 July 2011 2011].

Eskom. 2011b. *Coal Power* [Online]. Available: http://www.eskom.co.za/live/content.php?Category_ID=121 [Accessed 11 April 2011 2011].

Eskom. 2010. *Annual Review 2010:Generation Business* [Online]. Available: http://financialresults.co.za/2011/eskom_ar2011/downloads/eskom-ar2011.pdf [Accessed 23 July 2011 2011].

Fan, F., Feng, Z., Li, G., Sun, K., Ying, P. & Li, C. 2008. In Situ UV Raman Spectroscopic Studies on the Synthesis Mechanism of Zeolite X. *Chemistry – A European Journal,* 14**,** 5125-5129.

Fei. 2010. *An Introduction to Electron Microscopy* [Online]. Available: http://www.fei.com/uploadedfiles/documents/content/introduction_to_em_booklet_july_10.pdf [Accessed 5 January 2012].

Feijen, E. J. P., Martens, J. A. & Jacobs, P. A. 1994. Zeolites and their mechanism of synthesis. *In:* WEITKAMP, J., KARGE, H. G., PFEIFER, H. & HÖLDERICH, W. (eds.) *Zeolites and Related Microporous Materials: state of the art.* AMsterdam: Elsevier.

Fernandez-Jimenez, A. & Palomo, A. 2005. Composition and microstructure of alkali activated fly ash binder: Effect of the activator. *Cement and Concrete Research* 35**,** 1984 – 1992.

Fisher, G. L., Chang, D. & Brummer, M. 1976. Fly ash collected from electrostatic precipitators: microcrystalline structures and the mystery of the spheres. *Science,* 192**,** 553-555.

Fisher, G. L., Mcneill, K. L., Prentice, B. A. & Mcfarland, A. R. 1983. Physical and biological studies of coal and oil fly ash. *Environmental health perspectives,* 51**,** 181.

Fisher, G. L., Prentice, B. A., Silberman, D., Ondov, J. M., Biermann, A. H., Ragaini, R. C. & Mcfarland, A. R. 1978. Physical and morphological studies of size-classified coal fly ash. *Environmental Science & Technology,* 12**,** 447-451.

Flanigen, E. M., Khatami, H. & Seymenski, H. A. 1971. *In:* E.M, F. & L.B, S. (eds.) *Advances in Chemistry 101.* Wasgington DC: AMERICAN CHEMICAL SOCIETY.

Fogler, H. S. 2006. *Elements of Chemical Reaction Engineering,* Massachusetts, Pearson Education Inc.

Frising, T. & Leflaive, P. 2008. Extraframework cation distributions in X and Y faujasite zeolites: A review. *Microporous and Mesoporous Materials,* 114**,** 27-63.

García-Trenco, A. & Martínez, A. 2012. Direct synthesis of DME from syngas on hybrid CuZnAl/ZSM-5 catalysts: New insights into the role of zeolite acidity. *Applied Catalysis A: General,* 411–412**,** 170-179.

Gitari, W. M., Petrik, L. F., Etchebers, O., Key, D. L. & Okujeni, C. 2008. Utilization of fly ash for treatment of coal mines wastewater: Solubility controls on major inorganic contaminants. *Fuel,* 87**,** 2450–2462.

Goodarzi, F. 2006. Morphology and chemistry of fine particles emitted from a Canadian coal-fired power plant. *Fuel,* 85**,** 273-280.

Grande, C. A., Cavenati, S., Barcia, P., Hammer, J., Fritz, H. G. & Rodrigues, A. E. 2006. Adsorption of propane and propylene in zeolite 4A honeycomb monolith. *Chemical Engineering Science,* 61**,** 3053-3067.

Gupta, G. & Torres, N. 1998. Use of fly ash in reducing toxicity of and heavy metals in wastewater effluent. *Journal of Hazardous Materials,* 57**,** 243-248.

Gutiérrez, B., Pazos, C. & Coca, J. 1993. Characterization and leaching of coal fly ash. *Waste management & research,* 11**,** 279-286.

Hawkins, D. B. 1981. Kinetics of Glass Dissolution and Zeolite Formation Under Hydrothermal Conditions. *Clays and Clay Minerals,* 29**,** 331-340.

Haynes, R. J. 2009. Reclamation and revegetation of fly ash disposal sites – Challenges and research needs. *Journal of Environmental Management,* 90**,** 43-53.

Helble, J. 1994. Trace element behavior during coal combustion: results of a laboratory study. *Fuel processing technology,* 39**,** 159-172.

Hendricks, N. R. 2005. *The application of high capacity ion exchange adsorbent material, synthesized from fly ash and acid mine drainage, for the removal of heavy and trace metals from secondary co-disposed process waters.* Megastar Scientiae Unpublished, University of the Western Cape.

Hill, R. J. & Gibbs, G. V. 1979. Variation in d(T-O),d(T...T) and /_TOT in silica and silicate minerals, phosphates and aluminates. *Acta Crystallographica Section B,* 35**,** 25-30.

Himmelblau, D. M. & Riggs, J. B. 2004. *Basic Principals and Calculations in Chemical Eingineering,* New Jersey, Prentice-Hall.

Höller, H. & Wirsching, U. 1985. Zeolite formation from fly ash. *Fortschritte der Mineralogie,* 63(1)**,** 21-43.

Hollman, G., Steenbruggen, G. & Janssen-Jurkovičová, M. 1999. A two-step process for the synthesis of zeolites from coal fly ash. *Fuel,* 78**,** 1225-1230.

Hould, N. D., Foster, A. & Lobo, R. F. 2011. Zeolite beta mechanisms of nucleation and growth. *Microporous and Mesoporous Materials,* 142**,** 104-115.

Hower, J. C., Robertson, J. D., Thomas, G. A., Wong, A. S., Schram, W. H., Graham, U. M., Rathbone, R. F. & Robl, T. L. 1996. Characterization of fly ash from Kentucky power stations. *Fuel,* 75**,** 403-411.

Hsu, T.-C., Yu, C.-C. & Yeh, C.-M. 2008. Adsorption of Cu^{2+} from water using raw and modified coal fly ashes. *Fuel,* 87**,** 1355-1359.

Hu, Y., Liu, C., Zhang, Y., Ren, N. & Tang, Y. 2009. Microwave-assisted hydrothermal synthesis of nanozeolites with controllable size. *Microporous and Mesoporous Materials,* 119**,** 306-314.

Hurley, J. P. & Schobert, H. H. 1992. Ash formation during pulverized subbituminous coal combustion. 1. Characterization of coals, and inorganic transformations during early stages of burnout. *Energy & fuels,* 6**,** 47-58.

Inada, M., Eguchi, Y., Enomoto, N. & Hojo, J. 2005a. Synthesis of zeolite from coal fly ashes with different silica–alumina composition. *Fuel,* 84**,** 299-304.

Inada, M. & Hojo, J. Year. Microwave Processing for Fly-Ash Zeolite Production. *In:* International Symposium on EcoTopia Science, 2007. 739-741.

Inada, M., Tsujimoto, H., Eguchi, Y., Enomoto, N. & Hojo, J. 2005b. Microwave-assisted zeolite synthesis from coal fly ash in hydrothermal process. *Fuel,* 84**,** 1482-1486.

Inglezakis, V. J. & Loizidou, M. D. 2007. Ion exchange of some heavy metal ions from polar organicsolvents into zeolite. *Desalination,* 211**,** 238-248.

Iwasaki, A., Hirata, M., Kudo, I. & Sano, T. 1996. Behavior of the (010) face of silicalite crystal. *Zeolites,* 16**,** 35-41.

Iwasaki, A., Kudo, I. & Sano, T. 1997. Three-dimensional real-time observation of growth and dissolution of silicalite crystal. *In:* HAKZE CHON, S.-K. I. & YOUNG SUN, U. (eds.) *Studies in Surface Science and Catalysis.* Elsevier.

Iyer, R. 2002. The surface chemistry of leaching coal fly ash. *Journal of Hazardous Materials,* 93**,** 321-329.

Iza. 2013. *Synthesis Commission* [Online]. Available: http://www.iza-online.org/synthesis/default.htm [Accessed 2 January 2013].

Iza. 2012. *The Structure Commission* [Online]. Available: http://www.iza-structure.org [Accessed 21 December 2012].

Izquierdo, M. & Querol, X. 2012. Leaching behaviour of elements from coal combustion fly ash: An overview. *International Journal of Coal Geology,* 94**,** 54-66.

Jegadeesan, G., Al-Abed, S. R. & Pinto, P. 2008. Influence of trace metal distribution on its leachability from coal fly ash. *Fuel,* 87**,** 1887-1893.

Jha, V. K. & Hayashi, S. 2009. Modification on natural clinoptilolite zeolite for its NH4+ retention capacity. *Journal of Hazardous Materials,* 169**,** 29-35.

Jones, K. B., Ruppert, L. F. & Swanson, S. M. 2012. Leaching of elements from bottom ash, economizer fly ash, and fly ash from two coal-fired power plants. *International Journal of Coal Geology,* 94**,** 337-348.

Joshi, U. D., Joshi, P. N., Tamhankar, S. S., Joshi, V. P., Idage, B. B., Joshi, V. V. & Shiralkar, V. P. 2002. Influence of the size of extraframework monovalent cations in X-type zeolite on their thermal behavior. *Thermochimica Acta,* 387**,** 121-130.

Juan, R., Hernandez, S., Andres, J. M. & Ruiz, C. 2008. Ion exchange uptake of ammonium in wastewater from a Sewage Treatment Plant by zeolitic materials from fly ash. *Journal of Hazardous Materials*.

Kang, S.-J. & Egashira, K. 1997. Modification of different grades of Korean natural zeolites for increasing cation exchange capacity. *Applied Clay Science,* 12**,** 131-144.

Kang, S.-J., Egashira, K. & Yoshida, A. 1998. Transformation of a low-grade Korean natural zeolite to high cation exchanger by hydrothermal reaction with or without fusion with sodium hydroxide. *Applied Clay Science,* 13**,** 117-135.

Keane, M. A. 1996. The role of the alkali metal co-cation in the ion exchange of Y zeolites IV. Cerium ion exchange equilibria. *Microporous Materials,* 7**,** 51-59.

Keane, M. A. 1995a. Role of the alkali metal co-cation in the ion exchange of Y zeolites II. Copper ion-exchange equilibria. *Microporous Materials,* 3**,** 385-394.

Keane, M. A. 1995b. Role of the alkali metal co-cation in the ion exchange of Y zeolites III. Equilibrium properties of the Ni/Cu/Na 瑕 Y and Ni/Cu/K 瑕 Y zeolite systems. *Microporous Materials,* 4**,** 359-368.

Kletz, T. 1999. *HAZOP and HAZAN,* Eastbourne, Institution of Chemical Engineers.

Kokotailo, G. T., Fyfe, C. A., Feng, Y., Grondey, H., Gies, H., Marler, B. & Cox, D. E. 1995. Powder X-ray diffraction and solid state NMR techniques forzeolite structure determination. *In:* H.K. BEYER, H. G. K. I. K. & NAGY, J. B. (eds.) *Studies in Surface Science and Catalysis.* Elsevier.

Kosanović, C., Havancsák, K., Subotić, B., Svetličić, V., Radić, T. M., Cziráki, Á., Huhn, G., Buljan, I. & Smrečki, V. 2011. Study of the mechanism of formation of nano-crystalline zeolite X in heterogeneous system. *Microporous and Mesoporous Materials,* 142**,** 139-146.

Koukouzas, N., Hamalainen, J., Papanikolaou, D., Tourunen, A. & Jantti, T. 2007. Mineralogical and elemental composition of fly ash from pilot scale fluidized bed combustion of lignite, bituminous coal, wood chips and their blends. *Fuel,* 86**,** 2186-2193.

Kruger, R. A. 1997. Fly ash beneficiation in South Africa: creating new opportunities in the market-place. *Fuel,* 76**,** 777-779.

Kubota, M., Nakabayashi, T., Matsumoto, Y., Shiomi, T., Yamada, Y., Ino, K., Yamanokuchi, H., Matsui, M., Tsunoda, T., Mizukami, F. & Sakaguchi, K. 2008. Selective adsorption of bacterial cells onto zeolites. *Colloids and Surfaces B: Biointerfaces,* 64**,** 88-97.

Kutchko, B. G. & Kim, A. G. 2006. Fly ash characterization by SEM-EDS. *Fuel,* 85**,** 2537-2544.

Langmi, H. W., Walton, A., Al-Mamouri, M. M., Johnson, S. R., Book, D., Speight, J. D., Edwards, P. P., Gameson, I., Anderson, P. A. & Harris, I. R. 2003. Hydrogen adsorption in zeolites A, X, Y and RHO. *Journal of Alloys and Compounds,* 356–357**,** 710-715.

Lee, S. H., Sakai, E., Daimon, M. & Bang, W. K. 1999. Characterization of fly ash directly collected from electrostatic precipitator. *Cement and Concrete Research,* 29**,** 1791-1797.

Levenspiel, O. 1999. *Chemical Reaction Engineering,* New York, John Wiley & Sons.

Li, C., Li, Y., Sun, H. & Li, L. 2011. The Composition of Fly Ash Glass Phase and Its Dissolution Properties Applying to Geopolymeric Materials. *Journal of the American Ceramic Society,* 94**,** 1773-1778.

Li, Y., Liu, J. & Yang, W. 2006. Formation mechanism of microwave synthesized LTA zeolite membranes. *Journal of Membrane Science,* 281**,** 646-657.

Li, Y. & Yang, W. 2008. Microwave synthesis of zeolite membranes: A review. *Journal of Membrane Science,* 316**,** 3-17.

Lin, L., Lei, Z., Wang, L., Liu, X., Zhang, Y., Wan, C., Lee, D.-J. & Tay, J. H. 2013. Adsorption mechanisms of high-levels of ammonium onto natural and NaCl-modified zeolites. *Separation and Purification Technology,* 103**,** 15-20.

Liu, G., Zhang, H., Gao, L., Zheng, L. & Peng, Z. 2004. Petrological and mineralogical characterizations and chemical composition of coal ashes from power plants in Yanzhou mining district, China. *Fuel processing technology,* 85**,** 1635-1646.

Lyer, R. S. & Scott, J. A. 2001. Power station fly ash - a review of value-added utilization outside of the construction industry. *Resources, Conservation and Recycling,* 31**,** 217-228.

Madzivire, G., Gitari, W. M., Vadapalli, V. R. K., Ojumu, T. V. & Petrik, L. F. 2011. Fate of sulphate removed during the treatment of circumneutral mine water and acid mine drainage with coal fly ash: Modelling and experimental approach. *Minerals Engineering,* 24**,** 1467-1477.

Madzivire, G., Petrik, L. F., Gitari, W. M., Ojumu, T. V. & Balfour, G. 2010. Application of coal fly ash to circumneutral mine waters for the removal of sulphates as gypsum and ettringite. *Minerals Engineering,* 23**,** 252-257.

Mainganye, D. 2012. *Synthesis of zeolites from South African coal fly ash: Investigation of scale-up conditions.* MTECH: Chemical Engineering Unpublished Thesis, Cape Peninsula University of Technology.

Mainganye, D., Ojumu, T. V. & Petrik, L. F. 2013. Scale-up synthesis of zeolites Na-P1 from South African coal fly ash: effect of impeller design and agitation on the ageing step. *Materials,* 6**,** 2074-2089.

Malekian, R., Abedi-Koupai, J., Eslamian, S. S., Mousavi, S. F., Abbaspour, K. C. & Afyuni, M. 2011. Ion-exchange process for ammonium removal and release using natural Iranian zeolite. *Applied Clay Science,* 51**,** 323-329.

Manning, T. & Grow, W. 1997. Inductively Coupled Plasma - Atomic Emission Spectrometry. *The Chemical Educator,* 2**,** 1-19.

Mantler, M. & Schreiner, M. 2000. X-ray fluorescence spectrometry in art and archaeology. *X-Ray Spectrometry,* 29**,** 3-17.

Marrot, B., Bebon, C., Colson, D. & Klein, J. P. 2001. Influence of the Shear Rate During the Synthesis of Zeolites. *Cryst. Res. Technol,* 36**,** 269-281.

Maxwell, I. E. & Stork, W. H. J. 1991. Chapter 15 Hydrocarbon Processing with Zeolites. *In:* H. VAN BEKKUM, E. M. F. & JANSEN, J. C. (eds.) *Studies in Surface Science and Catalysis.* Elsevier.

Mccusker, L. B., Baerlocher, C., Grosse-Kunstleve, R., Brenner, S. & Wessels, T. 2001. Solving Complex Zeolite Structures from Powder Diffraction Data. *CHIMIA International Journal for Chemistry,* 55**,** 497-504.

Mekatel, H., Amokrane, S., Benturki, A. & Nibou, D. 2012. Treatment of Polluted Aqueous Solutions by Ni2+, Pb2+, Zn2+, Cr+6,Cd+2 and Co+2 Ions by Ion Exchange Process Using Faujasite Zeolite. *Procedia Engineering,* 33**,** 52-57.

Miano, F. 1996. Adsorption of hydrocarbon vapour mixtures onto zeolite 5A. *Colloids and Surfaces A: Physicochemical and Engineering Aspects,* 110**,** 95-104.

Milan, Z., Sánchez, E., Weiland, P., De Las Pozas, C., Borja, R., Mayari, R. & Rovirosa, N. 1997. Ammonia removal from anaerobically treated piggery manure by ion exchange in columns packed with homoionic zeolite. *Chemical Engineering Journal,* 66**,** 65-71.

Molina, A. & Poole, C. 2004. A comparative study using two methods to produce zeolites from fly ash. *Minerals Engineering,* 17**,** 167-173.

Mondale, K. D., Carland, R. M. & Aplan, F. F. 1995. The comparative ion exchange capacities of natural sedimentary and synthetic zeolites. *Minerals Engineering,* 8**,** 535-548.

Moreno, N., Querol, X., Ayora, C., Alastuey, A. & Fernandez-Pereira, C. 2001. Potential Environmental Applications of Pure Zeolitic Material Synthesised from Fly Ash. *Journal of Environmental Engineering,* 127**,** 994-1002.

Mortier, W. J. 1982. *Compilation of Extra Framework Sites in Zeolites,* Guildford, Butterworth & Co.

Murayama, N., Yamamoto, H. & Shibata, J. 2002. Mechanism of zeolite synthesis from coal fly ash by alkali hydrothermal reaction. *International Journal of Mineral Processing,* 64**,** 1-17.

Musyoka, N., Petrik, L., Balfour, G., Ndungu, P., Gitari, W. & Hums, E. 2012a. Synthesis of zeolites from coal fly ash: application of a statistical experimental design. *Research on Chemical Intermediates,* 38**,** 471-486.

Musyoka, N. M. 2012. Zeolite A, X and Cancrinite from South African coal fly ash: mechanism of crystallization, routes to rapid synthesis and new morphology. *Unpublished PhD Thesis.* Cape Town: University of the Western Cape.

Musyoka, N. M. 2009. Hydrothermal synthesis and optimisation of zeolite Na-P1 from South African coal fly ash. *Unpublished MSc Thesis.* Cape Town: University of the Western Cape.

Musyoka, N. M., Petrik, L. & Hums, E. 2012b. Synthesis of Zeolite A, X and P from a South African Coal Fly Ash. *Advanced Materials Research,* 512**,** 1757-1762.

Musyoka, N. M., Petrik, L. F., Balfour, G., Gitari, W. M. & Hums, E. 2011a. Synthesis of hydroxy sodalite from coal fly ash using waste industrial brine solution. *Journal of Environmental Science and Health, Part A,* 46**,** 1699-1707.

Musyoka, N. M., Petrik, L. F., Gitari, W. M., Balfour, G. & Hums, E. 2012c. Optimization of hydrothermal synthesis of pure phase zeolite Na-P1 from South African coal fly ashes. *Journal of Environmental Science and Health, Part A,* 47**,** 337-350.

Musyoka, N. M., Petrik, L. F. & Hums, E. Year. Ultrasonic assisted synthesis of zeolite A from coal fly ash using mine waters (acid mine drainage and circumneutral mine water) as a substitute for ultra pure water. *In:* RÜDE, T. R., FREUND, A. & WOLKERSDORFER, C., eds. Mine Water – Managing the Challenges, 2011b Aachen, Germany International Mine Water Association, 423-428.

Musyoka, N. M., Petrik, L. F., Hums, E., Baser, H. & Schwieger, W. 2012d. In situ ultrasonic monitoring of zeolite A crystallization from coal fly ash. *Catalysis Today,* 190**,** 38-46.

Nagy, J. B., Bodart, P., Hannus, I. & Kiricsi, I. 1998. *Synthesis, Characterization and Use of Zeolitic Microporous Materials,* Szeged, Deca Gen Ltd.

Nathan, Y., Dvorachek, M., Pelly, I. & Mimran, U. 1999. Characterization of coal fly ash from Israel. *Fuel,* 78**,** 205-213.

Nationmaster. 2011. *South Africa Energy Stats* [Online]. Available: http://www.nationmaster.com/country/sf-south-africa/ene-energy [Accessed 11 April 2011 2011].

Navarrete-Casas, R., Navarrete-Guijosa, A., Valenzuela-Calahorro, C., López-González, J. D. & García-Rodríguez, A. 2007. Study of lithium ion exchange by two synthetic zeolites: Kinetics and equilibrium. *Journal of Colloid and Interface Science,* 306**,** 345-353.

Newsam, J. M. 1992. *In:* CHEETHAM, A. K. & DAY, P. (eds.) *Solid State Chemistry: Compounds.* New York: Oxford University Press.

Ojha, K., Pradhan, N. C. & Samanta, A. N. 2004. Zeolite from fly ash: synthesis and characterization. *Bulletin of Material Science,* 27**,** 555–564.

Ören, A. H. & Kaya, A. 2006. Factors affecting adsorption characteristics of Zn2+ on two natural zeolites. *Journal of Hazardous Materials,* 131**,** 59-65.

Ostroski, I. C., Barros, M. a. S. D., Silva, E. A., Dantas, J. H., Arroyo, P. A. & Lima, O. C. M. 2009. A comparative study for the ion exchange of Fe(III) and Zn(II) on zeolite NaY. *Journal of Hazardous Materials,* 161**,** 1404-1412.

Palomo, A., Alonso, S., Fernandez-Jiménez, A., Sobrados, I. & Sanz, J. 2008. Alkaline activation of fly ashes: NMR study of the reaction products. *Journal of the American Ceramic Society,* 87**,** 1141-1145.

Pandey, V. C., Singh, J. S., Singh, R. P., Singh, N. & Yunus, M. 2011. Arsenic hazards in coal fly ash and its fate in Indian scenario. *Resources, Conservation and Recycling,* 55**,** 819-835.

Papaioannou, C., Petroutsos, G. & Gunβer, W. 1997. Examination of the adsorption of hydrocarbons at low coverage on faujasite zeolites. *Solid State Ionics,* 101–103, Part 2**,** 799-805.

Park, J. S., Taniguchi, S. & Park, Y. J. 2009. Alkali borosilicate glass by fly ash from a coal-fired power plant. *Chemosphere,* 74**,** 320-324.

Paul, E. L., Atiemo-Obeng, V. A. & Kresta, S. M. 2004a. *Handbook of Industrial Mixing,* New Jersey, John Wiley & Sons.

Paul, E. L., Atiemo-Obeng, V. A. & Kresta, S. M. 2004b. Mechanically Stirred Vessels *In:* HEMRAJANI, R. R. & TATTERSON, G. B. (eds.) *Hanbook of Industrial Mixing.* New Jersey: John Wiley & Sons.

Petrik, L. F., White, R., Klink, M., Somerset, V., Key, D. L., Iwuoha, E., Burgers, C. & Fey, M. V. 2005. Utilization of Fly Ash for Acid Mine Drainage remediation. Water Research Commission Report No. 1242/1/05.

Petrik, L. F., White, R. A., Richard, A., Klink, M. J., Michael, J., Somerset, V. S., Burgers, C. L., Colleen, L. & Fey, M. V. Year. Utilisation of South African fly ash to treat acid coal mine drainage and production of high quality zeolites from the residual solids. *In:* International Ash Utilisation symposium, October 20-22 2003 Lexington, Kentucky, USA.

Pfenninger, A. 1999. Manufacture and Use of Zeolites for Adsorption Process. *Molecular Sieves,* 2**,** 164-197.

Querol, X., Alastuey, A., Fernandez-Turiel, J. L. & Lopez-Soler, A. 1995. Synthesis of zeolites by alkaline activation of ferro-aluminous fly ash. *Fuel,* 74**,** 1226-1231.

Querol, X., Moreno, N., Alastuey, A., Juan, R., Andres, J. M., Lopez-Soler, A., Ayora, C., Medinaceli, A. & Valero, A. 2007. Synthesis of high ion exchange zeolites from coal fly ash. *Geologica Acta,* 5**,** 49-57.

Querol, X., Moreno, N., Umana, J. C., Alastuey, A., Hernandez, E., Lopez-Soler, A. & Plana, F. 2002. Synthesis of zeolites from coal fly ash: an overview. *International Journal of Coal Geology,* 50**,** 413-423.

Querol, X., Plana, F., Alastuey, A. & Lopez-Soler, A. 1997. Synthesis of Na-zeolites from fly ash. *Fuel,* 76**,** 793-799.

Querol, X., Umana, J. C., Plana, F., Alastuey, A., Lopez-Soler, A., Medinaceli, A., Valero, A., Domingo, M. J. & Garcia-Rojo, E. 2001. Synthesis of zeolites from fly ash at pilot plant scale. Examples of potential applications. *Fuel,* 80**,** 857-865.

Rafey, W. & Sovacool, B. K. 2011. Competing discourses of energy development: The implications of the Medupi coal-fired power plant in South Africa. *Global Environmental Change,* 21**,** 1141-1151.

Ram, L. C. & Masto, R. E. 2010. An appraisal of the potential use of fly ash for reclaiming coal mine spoil. *Journal of Environmental Management,* 91**,** 603-617.

Rayalu, S., Meshram, S. U. & Hasan, M. Z. 2000. Highly crystalline faujasitic zeolites from flyash. *Journal of Harardous Materials,* 77**,** 123-131.

Ren, L., Li, C., Fan, F., Guo, Q., Liang, D., Feng, Z., Li, C., Li, S. & Xiao, F.-S. 2011. UV–Raman and NMR Spectroscopic Studies on the Crystallization of Zeolite A and a New Synthetic Route. *Chemistry – A European Journal,* 17**,** 6162-6169.

Reto, G., Carleton, L. E. & Lumpkin, G. R. 2003. Micro- and nanochemistry of fly ash from a coal-fired power plant. *Mineralogical Society of America,* 88**,** 1853-1865.

Ribeiro, F. R., Alvarez, F., Henriques, C., Lemos, F., Lopes, J. M. & Ribeiro, M. F. 1995. Structure-activity relationship in zeolites. *Journal of Molecular Catalysis A: Chemical,* 96**,** 245-270.

Ribeiro, F. R., Rodrigues, A. E., Rollmann, L. D. & Naccache, C. 1984. *Zeolites: Science and Technology,* Lancaster, Martinus Nijhoff Publishers.

Rios R, C. A., Williams, G. D. & Roberts, C. L. 2009. A comparative study of two methods for the synthesis of fly ash-based sodium and potassium type zeolites. *Fuel,* 88**,** 1403-1416.

Ríos, R., Carlos, A., Williams, C. D. & Roberts, C. L. 2009. A comparative study of two methods for the synthesis of fly ash-based sodium and potassium type zeolites. *Fuel,* 88**,** 1403-1416.

Robb, G. M., Zhang, W. & Smirniotis, P. G. 1998. Acidity of dealuminated β-zeolites via coupled nh3-stepwise temperature programmed desorption (STPD) and FT-IR spectroscopy. *Microporous and Mesoporous Materials,* 20**,** 307-316.

Robson, H. & Lillerud, K. P. 2001. *Verified Syntheses of Zeolitic Materials,* Amsterdam, Elsevier.

Sarioglu, M. 2005. Removal of ammonium from municipal wastewater using natural Turkish (Dogantepe) zeolite. *Separation and Purification Technology,* 41**,** 1-11.

Sathupunya, M., Gulari, E., Jamieson, A. & Wongkasemjit, S. 2004. Microwave-assisted preparation of zeolite K–H from alumatrane and silatrane. *Microporous and Mesoporous Materials,* 69**,** 157-164.

Sawic. 2012. *Waste Policy and Regulation* [Online]. Available: http://www.sawic.org.za/?menu=13 [Accessed 20 December 2012].

Scheetz, B. E. & Earle, R. 1998. Utilization of fly ash. *Current Opinion in Solid State and Materials Science,* 3**,** 510-520.

Shende, A., Juwarkar, A. S. & Dara, S. S. 1994. Use of fly ash in reducing heavy metal toxicity to plants. *Resources, Conservation and Recycling,* 12**,** 221-228.

Sheng, J., Huang, B. X., Zhang, J., Zhang, H., Sheng, J., Yu, S. & Zhang, M. 2003. Production of glass from coal fly ash. *Fuel,* 82**,** 181-185.

Sherry, H. S. 1979. Ion-Exchange Properties of the Natural Zeolite Erionite. *Clays and Clay Minerals,* 27**,** 231-237.

Shigemoto, N., Hayashi, H. & Miyaura, K. 1993. Selective formation of Na-X zeolite from coal fly ash by fusion with sodium hydroxide prior to hydrothermal reaction. *Journal of Materials Science,* 28**,** 4781-4786.

Silva, L. F. O., Daboit, K., Sampaio, C. H., Jasper, A., Andrade, M. L., Kostova, I. J., Waanders, F. B., Henke, K. R. & Hower, J. C. 2012. The occurrence of hazardous volatile elements and nanoparticles in Bulgarian coal fly ashes and the effect on human health exposure. *Science of The Total Environment,* 416**,** 513-526.

Singer, A. & Berkgaut, V. 1995. Cation Exchange Properties of Hydrothermally Treated Coal Fly Ash. *Environmental Science & Technology,* 29**,** 1748-1753.

Sistani, S., Ehsani, M. R., Kazemian, H. & Didari, M. 2010. Microwave Assisted Synthesis of Nano Zeolite Seed for Synthesis Membrane and Investigation of its Permeation Properties for H2 Separation. *Iran. J. Chem. Chem. Eng. Research Note Vol,* 29.

Skubas, N. 2003. Principals of echocardiography for the anesthesiologist. *The Greek E-Journal of Perioperative Medicine* 1**,** 26-39

Smith, K. R., Veranth, J. M., Lighty, J. a. S. & Ann, E. 1998. Mobilization of iron from coal fly ash was dependent upon the particle size and the source of coal. *Chemical research in toxicology,* 11**,** 1494-1500.

Sočo, E. & Kalembkiewicz, J. 2009. Investigations on Cr mobility from coal fly ash. *Fuel,* 88**,** 1513-1519.

Somerset, V., Petrik, L. & Iwouha, E. 2005a. Alkaline Hydrothermal Conversion of Fly Ash Filtrates Into Zeolites 2: Utilization in Wastewater Treatment. *Journal of Environmental Science and Health,* 40**,** 1627-1636.

Somerset, V. S., Petrik, L. F., White, R. A., Klink, M. J., Key, D. & Iwouha, E. I. 2005b. Alkaline hydrothermal zeolites synthesized from high SiO2 and Al2O3 co-disposal fly ash filtrates. *Fuel,* 84**,** 2324-2329.

Somerset, V. S., Petrik, L. F., White, R. A., Klink, M. J., Key, D. & Iwuoha, I. 2004. The use of X-ray fluorescence (XRF) analysis in predicting the alkaline hydrothermal conversion of fly ash precipitates into zeolites. *Talanta,* 64**,** 109-114.

Steenbruggen, G. & Hollman, G. G. 1998. The synthesis of zeolites from fly ash and the properties of the zeolite products. *Journal of Geochemical Exploration,* 62**,** 305-309.

Steijns, M. & Mars, P. 1976. The adsorption of sulfur by microporous materials. *Journal of Colloid and Interface Science,* 57**,** 175-180.

Stuart, B. 2005. *Infrared spectroscopy,* New Jersey, Wiley Online Library.

Szostak, R. 1997. *Molecular sieves: principals of synthesis and identification,* New York, Springer.

Taffarel, S. R. & Rubio, J. 2009. On the removal of Mn2+ ions by adsorption onto natural and activated Chilean zeolites. *Minerals Engineering,* 22**,** 336-343.

Tassopoulos, M. & Thompson, R. W. 1987. Transformation behaviour of zeolite A to hydroxysodalite in batch and semi-batch crystallizers. *Zeolites,* 7**,** 243-248.

Tatlier, M., Barış Cigizoglu, K., Tokay, B. & Erdem-Şenatalar, A. 2007. Microwave vs. conventional synthesis of analcime from clear solutions. *Journal of Crystal Growth,* 306**,** 146-151.

Termuehlen, H. & Emsperger, W. 2003. *Evolutionary Development of Coal-Fired Power Plants*, ASME Press.

Tsiridis, V., Petala, M., Samaras, P., Kungolos, A. & Sakellaropoulos, G. P. 2012. Environmental hazard assessment of coal fly ashes using leaching and ecotoxicity tests. *Ecotoxicology and Environmental Safety,* 84**,** 212-220.

Ursini, O., Lilla, E. & Montanari, R. 2006. The investigation on cationic exchange capacity of zeolites: The use as selective ion trappers in the electrokinetic soil technique. *Journal of Hazardous Materials,* 137**,** 1079-1088.

Vadapalli, V. R. K., Klink, M. J., Etchebers, O., Petrik, L. F., Gitari, W., White, R. A., Key, D. & Iwuoha, E. 2008. Neutralization of acid mine drainage using fly ash, and strength development of the resulting solid residues. *South African Journal of Science,* 108**,** 317-325.

Vassilev, S. V., Kitano, K. & Vassileva, C. G. 1997. Relations between ash yield and chemical and mineral composition of coals. *Fuel,* 76**,** 3-8.

Vassilev, S. V., Kitano, K. & Vassileva, C. G. 1996. Some relationships between coal rank and chemical and mineral composition. *Fuel,* 75**,** 1537-1542.

Vassilev, S. V. & Vassileva, C. G. 2007. A new approach for the classification of coal fly ashes based on their origin, composition, properties, and behaviour. *Fuel,* 86**,** 1490-1512.

Vassilev, S. V., Vassileva, C. G., Karayigit, A. I., Bulut, Y., Alastuey, A. & Querol, X. 2005. Phase–mineral and chemical composition of composite samples from feed coals, bottom ashes and fly ashes at the Soma power station, Turkey. *International Journal of Coal Geology,* 61**,** 35-63.

Vuthaluru, H. B. & French, D. 2008. Ash chemistry and mineralogy of an Indonesian coal during combustion: Part II — Pilot scale observations. *Fuel Processing Technology,* 89**,** 6 0 8 – 6 2 1.

Wagner, N. J. & Hlatshwayo, B. 2005. The occurrence of potentially hazardous trace elements in five Highveld coals, South Africa. *International Journal of Coal Geology,* 63**,** 228-246.

Walton, K. S., Abney, M. B. & Douglas Levan, M. 2006. CO2 adsorption in Y and X zeolites modified by alkali metal cation exchange. *Microporous and Mesoporous Materials,* 91**,** 78-84.

Wang, S. & Wu, H. 2006. Environmental-benign utilisation of fly ash as low-cost adsorbents. *Journal of Hazardous Materials,* 136**,** 482-501.

Wang, Y. & Lin, F. 2009. Synthesis of high capacity cation exchangers from a low-grade Chinese natural zeolite. *Journal of Hazardous Materials,* 166**,** 1014-1019.

Wang, Y., Lin, F. & Pang, W. 2008. Ion exchange of ammonium in natural and synthesized zeolites. *Journal of Harardous Materials*.

Wang, Y. F., Lin, F. & Pang, W. Q. 2007. Ammonium exchange in aqueous solution using Chinese natural clinoptilolite and modified zeolite. *Journal of Hazardous Materials,* 142**,** 160-164.

Warzywoda, J. & Thompson, R. W. 1991. Synthesis of zeolite A in the Na/K system and the effect of seeding. *Zeolites,* 11**,** 577-582.

Weitkamp, J. & Puppe, L. 1999. *Catalysis and zeolites: fundamentals and applications*, Springer.

Wernert, V., Schäf, O., Ghobarkar, H. & Denoyel, R. 2005. Adsorption properties of zeolites for artificial kidney applications. *Microporous and Mesoporous Materials,* 83**,** 101-113.

Woinarski, A. Z., Snape, I., Stevens, G. W. & Stark, S. C. 2003. The effects of cold temperature on copper ion exchange by natural zeolite for use in a permeable reactive barrier in Antarctica. *Cold Regions Science and Technology,* 37**,** 159-168.

Woolard, C. D., Petrus, K. & Horst, M. V. D. 2000. The use of a modified fly ash as an adsorbent for lead. *Water SA,* 26**,** 531-536.

Wu, D., Sui, Y., Chen, X., He, S., Wang, X. & Kong, H. 2008. Changes of mineralogical–chemical composition, cation exchange capacity, and phosphate immobilization capacity during the hydrothermal conversion process of coal fly ash into zeolite. *Fuel,* 87**,** 2194-2200.

Wu, D., Zhang, B., Yan, L., Kong, H. & Wang, X. 2006a. Effect of some additives on synthesis of zeolite from coal fly ash. *International Journal of Mineral Processing,* 80**,** 266 –272.

Wu, J., Wang, B., Li, N. & Xiang, S. 2006b. Effect of Aging with Ultrasound on the Synthesis of MCM-49 Zeolite. *Chinese Journal of Catalysis,* 27**,** 375-377.

Xiong, G., Yu, Y., Feng, Z.-C., Xin, Q., Xiao, F.-S. & Li, C. 2001. UV Raman spectroscopic study on the synthesis mechanism of zeolite X. *Microporous and Mesoporous Materials,* 42**,** 317-323.

Yang, G. C. C. & Yang, T. 1998. Synthesis of zeolites from municipal incinerator fly ash. *Journal of Harardous Materials,* 62**,** 75-76.

Yao, Y. & Sun, H. 2012. A novel silica alumina-based backfill material composed of coal refuse and fly ash. *Journal of Hazardous Materials,* 213–214**,** 71-82.

Yin, X., Zhu, G., Wang, Z., Yue, N. & Qiu, S. 2007. Zeolite P/NaX composite membrane for gas separation. *Microporous and Mesoporous Materials,* 105**,** 156-162.

Yossifova, M. G. 2007. Mineral and inorganic chemical composition of the Pernik coal, Bulgaria. *International Journal of Coal Geology,* 72**,** 268-292.

Zhang, J., Dong, W., Li, J., Qiao, L., Zheng, J. & Sheng, J. 2007. Utilization of coal fly ash in the glass–ceramic production. *Journal of Hazardous Materials,* 149**,** 523-526.

Zheng, L., Liu, G., Wang, L. & Chou, C.-L. 2008. Composition and quality of coals in the Huaibei Coalfield, Anhui, China. *Journal of Geochemical Exploration,* 97**,** 59-68.

Zhu, Z., Chen, Q., Xie, Z., Yang, W. & Li, C. 2006. The roles of acidity and structure of zeolite for catalyzing toluene alkylation with methanol to xylene. *Microporous and Mesoporous Materials,* 88**,** 16-21.

Žilková, N., Bejblová, M., Gil, B., Zones, S. I., Burton, A. W., Chen, C.-Y., Musilová-Pavlačková, Z., Košová, G. & Čejka, J. 2009. The role of the zeolite channel architecture and acidity on the activity and selectivity in aromatic transformations: The effect of zeolite cages in SSZ-35 zeolite. *Journal of Catalysis,* 266**,** 79-91.

South African Government. 2008. National Environmental Management: Waste Act 59 of 2008. http://www.sawic.org.za/documents/384.pdf

Appendix A: Chapter 3 supporting data and calculations

Table A-1 to A-5 illustrates the data utilized to determine the compositions of all solid and liquid products in the material balance study discussed in chapter 3. It is good practice to produce at least 3 sets of ICP-AES data. Therefore each experiment was run 3 times to ensure accuracy and reproducibility of results.

Where XRF data illustrates mass fractions of oxides (Table A-1, A-3 and A4) a simple conversion calculation was performed in order to obtain the elemental mass fraction in the sample. Illustrated below is a sample calculation for Si.

$$Weight\ fraction\ of\ Si = Oxide\ weight\ fraction \times \left(\frac{Molar\ mass\ of\ Si}{Molar\ mass\ of\ oxide}\right)$$

$$= 0.4128 \times \left(\frac{28\ \frac{g}{mole}}{60\ \frac{g}{mole}}\right)$$

$$= 0.1926$$

Table A- 1: XRF results illustrating the composition of the zeolite product obtained from the 2-step synthesis method.

Major oxides (mean wt%)		Trace elemental concentrations (ppm)	
SiO_2	41.28	As	4.16
TiO_2	1.49	Cu	35.54
Al_2O_3	26.47	Nb	30.77
Fe_2O_3	4.41	Ni	83.09
MnO	0.05	Pb	30.72
MgO	1.33	Rb	11.79
CaO	4.06	Sr	781.18
Na_2O	9.94	Th	39.43
K_2O	0.24	Y	76.49
P_2O_5	0.06	Zn	66.81
Cr_2O_3	0.03	Zr	401.70
NiO	0.01	Co	34.15
V_2O_5	0.01	Cr	192.14
ZrO_2	0.05	S	194.84
CuO	*<0.01*	V	41.37
LOI	10.48	Ba	1079.01
		Ce	307.15

Table A- 2: ICP-AES data of all liquid products obtained from the 2 step synthesis method.

Elemental concentrations in liquid products (ppm)						
Element	**Supernatant waste**			**Washing water**		
	Run 1	Run 2	Run 3	Run 1	Run 2	Run 3
Al	49.8	38.5	59.6	0.8	-0.4	-0.4
As	-0.3	0.0	0.9	-0.2	0.5	-1.1
B	41.4	35.7	32.4	131.0	77.4	44.9
Ba	0.0	0.1	0.0	0.0	0.0	0.0
Be	0.0	0.0	0.1	0.0	0.0	0.0
Ca	-7.6	-6.1	-5.9	0.8	-5.5	-5.4
Cd	0.0	0.0	0.0	0.0	-0.1	0.0
Ce	-0.1	0.2	0.1	-0.1	0.0	0.0
Co	0.0	-0.1	0.0	0.0	-0.1	-0.1
Cr	1.3	0.6	0.5	0.6	0.6	0.5
Cu	-0.3	-0.4	-0.2	-0.3	-0.4	-0.4
Fe	4.5	7.3	3.7	3.1	3.0	2.7
Hg	0.3	0.1	0.2	0.3	0.5	0.4
K	243.3	272.9	281.7	-18.5	-19.1	-18.4
Li	0.2	0.3	0.3	-0.1	-0.1	-0.1
Mg	-0.7	-0.6	-0.6	-0.4	-0.3	-0.4
Mn	-0.1	-0.1	-0.1	-0.1	-0.1	-0.1
Mo	0.3	0.2	0.3	0.0	0.2	0.1
Na	22866.7	24282.4	23820.7	380.7	324.4	245.2
Nb	0.1	0.1	0.0	0.1	0.1	0.1
Ni	3.3	6.4	5.5	0.0	0.0	-0.1
P	105.7	112.8	119.6	0.7	1.9	0.9
Pb	1.6	2.0	1.6	0.4	-0.2	0.0
Rb	0.7	1.1	1.0	0.0	0.0	0.0
Se	-0.2	0.0	-1.1	-2.4	-0.8	-1.0
Si	5252.3	5554.8	5917.6	32.8	37.8	31.2
Sr	-0.1	0.0	-0.1	0.0	-0.1	-0.1
Th	0.7	0.1	1.2	0.6	0.0	0.9
Ti	1.1	5.5	0.8	0.0	0.0	0.0
V	6.8	6.9	7.8	0.1	0.0	0.0
Y	0.0	0.0	0.0	0.0	0.0	0.0
Zn	-1.4	-1.4	-1.2	-1.8	-1.8	-1.8
Zr	0.0	0.1	0.0	0.0	0.0	0.0

Table A- 3: XRF results illustrating the composition of the zeolite product obtained from the fusion assisted synthesis method.

Major oxides (mean wt%)		Trace elemental concentrations (ppm)	
Al_2O_3	29.08	As	3.00
CaO	*<0.01*	Ba	37.69
Cr_2O_3	0.00	Ce	7.54
CuO	*<0.01*	Co	2.36
Fe_2O_3	0.04	Cr	6.84
K_2O	0.32	Cu	2.29
LOI	16.39	Nb	2.00
MgO	*<0.01*	Ni	17.90
MnO	0.01	Pb	3.00
Na_2O	19.19	Rb	2.00
NiO	0.01	S	576.33
P_2O_5	*<0.01*	Sr	3.00
SiO_2	35.35	Th	3.00
TiO_2	0.01	V	16.81
V_2O_5	*<0.01*	Y	3.00
ZrO_2	0.01	Zn	15.63
		Zr	10.00

Table A- 4: XRF results illustrating the composition of the solid waste product obtained from the fusion assisted synthesis method.

Major oxides (mean wt%)		Trace elemental concentrations (ppm)	
SiO_2	36.90318	As	3
TiO_2	1.0831	Cu	28.88256
Al_2O_3	25.17317	Nb	21.26347
Fe_2O_3	3.49982	Ni	57.93
MnO	0.03211	Pb	41.50922
MgO	0.85043	Rb	6.15231
CaO	2.76137	Sr	544.1067
Na_2O	14.44901	Th	22.39246
K_2O	0.35858	Y	55.34371
P_2O_5	0.0551	Zn	44.63686
Cr_2O_3	0.01026	Zr	286.7671
NiO	0.01464	Co	27.93201
V_2O_5	0.00611	Cr	43.994
ZrO_2	0.03765	S	1018.115
CuO	<0.01	V	46.55
LOI	14.55381	Ba	888.9278
		Ce	241.9367

Table A- 5: ICP-AES data of all liquid products obtained from the fusion assisted synthesis method.

Elemental concentrations in liquid products (ppm)						
Element	Supernatant waste			Washing water		
	Run 1	Run 2	Run 3	Run 1	Run 2	Run 3
Al	1712.8	1512.6	1393.1	79.5	69.6	70.4
As	0.9	1.5	0.2	0.5	0.3	0.6
Ba	1.5	1.8	0.9	0.5	0.4	0.4
Be	0.0	0.0	0.0	-0.1	-0.1	-0.1
Ca	19.0	16.3	12.8	10.4	11.2	10.6
Cd	0.0	0.0	0.0	0.0	0.0	0.0
Ce	0.1	0.2	-0.6	-0.2	-0.5	-0.5
Co	-0.2	-0.2	0.0	0.0	0.1	0.0
Cr	8.4	6.6	9.7	1.7	1.6	1.7
Cu	0.0	0.1	0.8	0.2	0.0	0.0
Fe	6.0	5.5	7.3	4.8	4.7	4.6
Hg	13.7	1.8	2.4	0.5	0.3	0.6
K	160.9	136.7	121.9	9.9	11.0	10.6
Li	1.0	0.9	1.8	0.3	0.3	0.3
Mg	4.3	4.1	2.9	2.8	2.8	2.8
Mn	1.9	1.7	2.2	0.1	0.1	0.1
Mo	0.4	0.2	0.3	0.0	-0.1	0.0
Na	27710.7	25548.4	29456.2	6548.9	5883.2	5290.9
Nb	0.1	0.1	0.2	0.3	0.2	0.4
Ni	1.7	2.6	4.8	5.5	5.8	5.6
P	76.7	60.1	85.1	3.2	3.1	2.1
Pb	0.4	0.3	1.0	0.6	0.8	0.7
Rb	0.8	0.6	0.2	0.0	-0.1	0.0
Se	0.1	-1.2	2.9	-0.3	0.2	-1.4
Si	2275.0	1928.8	2286.8	239.5	230.0	199.3
Sr	0.1	0.1	0.1	0.1	0.1	0.1
Th	0.3	0.2	-0.6	-0.4	-1.0	0.2
Ti	0.5	0.4	0.4	0.2	0.2	0.2
V	6.1	5.0	6.2	0.6	0.5	0.4
Y	0.0	0.0	0.0	0.0	0.0	0.0
Zn	1.1	0.9	2.2	0.7	0.8	0.8
Zr	0.0	0.0	-0.1	0.0	0.0	0.0

For publication purposes only the weight% distribution of elements were shown in the article portrayed in chapter 3. The stream compositions from which these percentages were calculated are tabulated in Tables A-6 and A-7.

Table A- 6: Tabulated material balance illustrating the elemental composition of each stream crossing the system boundary in the 2-step synthesis process.

Elemental composition of raw feed and products (g)				
Element	**Fly ash**	**Zeolite product**	**Supernatant waste**	**Washing water**
Al	1.7E+00	1.4E+00	2.6E-01	4.6E-02
Ba	4.9E-03	4.9E-03	0.0E+00	0.0E+00
Ca	2.7E-01	2.7E-01	0.0E+00	0.0E+00
Ce	2.5E-03	2.5E-03	0.0E+00	0.0E+00
Co	3.0E-04	3.0E-04	0.0E+00	0.0E+00
Cu	1.1E-03	1.1E-03	0.0E+00	0.0E+00
Fe	3.5E-01	3.0E-01	3.9E-02	7.4E-03
K	3.9E-02	1.9E-02	2.0E-02	0.0E+00
Mg	7.1E-02	7.1E-02	0.0E+00	0.0E+00
Mn	2.3E-03	2.3E-03	0.0E+00	0.0E+00
Na	3.0E-03	7.2E-01	2.6E+00	2.4E+00
Nb	3.7E-04	3.0E-04	1.2E-05	6.0E-05
Ni	1.3E-03	8.1E-04	4.4E-04	0.0E+00
P	1.3E-02	4.2E-04	1.0E-02	2.3E-03
Pb	9.0E-04	5.7E-04	1.9E-04	1.4E-04
Rb	5.6E-04	4.4E-04	1.0E-04	2.2E-05
S	2.4E-03	2.4E-03	0.0E+00	0.0E+00
Si	2.6E+00	1.9E+00	6.1E-01	1.1E-01
Sr	9.9E-03	9.9E-03	0.0E+00	0.0E+00
Ti	6.7E-02	6.7E-02	0.0E+00	0.0E+00
V	7.9E-04	4.0E-04	3.9E-04	0.0E+00
Y	9.4E-04	9.4E-04	0.0E+00	0.0E+00
Zn	1.4E-03	1.4E-03	0.0E+00	0.0E+00

Table A- 7: Tabulated material balance illustrating the elemental composition of each stream crossing the system boundary in the fusion assisted synthesis process.

Elemental composition of raw feed and products (g)					
Element	**Fly ash**	**Solid Waste**	**Zeolite product**	**Supernatant waste**	**Washing water**
Al	3.79E+00	3.43E+00	1.08E+00	3.96E-01	9.08E-02
Ba	1.10E-02	9.87E-03	2.64E-04	3.58E-04	5.53E-04
Ca	6.10E-01	5.93E-01	0.00E+00	4.11E-03	1.33E-02
Ce	5.77E-03	5.77E-03	0.00E+00	0.00E+00	0.00E+00
Co	6.82E-04	6.82E-04	0.00E+00	0.00E+00	0.00E+00
Cu	2.50E-03	2.50E-03	0.00E+00	0.00E+00	0.00E+00
Fe	7.86E-01	7.76E-01	2.13E-03	1.61E-03	5.86E-03
K	8.86E-02	2.08E-02	1.88E-02	3.59E-02	1.31E-02
Mg	1.61E-01	1.56E-01	0.00E+00	9.66E-04	3.49E-03
Mn	5.28E-03	4.64E-03	0.00E+00	4.93E-04	1.45E-04
Na	6.75E-03	5.50E+00	9.97E-01	7.09E+00	7.33E+00
Nb	8.41E-04	4.56E-04	0.00E+00	3.26E-05	3.52E-04
Ni	2.84E-03	2.23E-03	0.00E+00	6.11E-04	0.00E+00
P	2.98E-02	7.30E-03	0.00E+00	1.90E-02	3.46E-03
Pb	2.05E-03	1.04E-03	0.00E+00	1.39E-04	8.62E-04
Rb	1.27E-03	1.14E-03	0.00E+00	1.36E-04	0.00E+00
S	5.46E-03	1.42E-03	4.03E-03	0.00E+00	0.00E+00
Si	5.88E+00	3.89E+00	1.15E+00	5.56E-01	2.76E-01
Sr	2.25E-02	2.24E-02	0.00E+00	0.00E+00	1.00E-04
Ti	1.51E-01	1.51E-01	2.44E-04	1.09E-04	2.40E-04
V	1.80E-03	8.11E-04	0.00E+00	7.10E-04	2.74E-04
Y	2.14E-03	2.14E-03	0.00E+00	0.00E+00	0.00E+00
Zn	3.07E-03	1.65E-03	1.09E-04	3.65E-04	9.44E-04

Appendix B: Chapter 6 supporting data and reproducibility of best results

Table B-1 below illustrates the power and temperature data used to construct Figure 6-7 in section 6-4-3. These readings were measured and displayed automatically by the MISONIX S-4000 sonicator used in the study.

Table B- 1: Power and temperature data taken in 5 minute increments during sonication of fly ash samples.

Time (Min)	Power (W)	Temperature (°C)
0	170	25
5	110	97
10	78	103
15	57	103
20	47	103
25	47	103
30	47	103

Table B-2 on pages 168-170 illustrates the ICP-AES data used to determine the Si and Al weight fractions dissolved, as illustrated in Figure 6-7. Also included in the table are the concentrations of the full list of elements found in the extracted clear solutions after varying times of sonication (5 – 30 min). For each time set, the experiments were run 3 times (Run 1- 3) to ensure accuracy and reproducibility of data.

Table B- 2:ICP-AES data illustrating concentrations of elements in clear solution extracted after sonicating fly ash for varying amounts of time.

Elemental concentrations in clear solution after fly ash sonication (ppm)						
Element	**5 min**			**10 min**		
	Run 1	Run 2	Run 3	Run 1	Run 2	Run 3
Al	1,404.9	1,396.9	1,495.5	1,838.1	1,921.7	1,863.2
As	0.9	1.2	1.4	0.8	2.0	2.1
B	21.0	19.8	18.9	18.3	17.4	17.3
Ba	2.9	3.7	3.0	2.3	1.8	2.2
Be	0.1	0.1	0.1	0.1	0.1	0.1
Ca	22.2	22.6	21.8	17.7	17.4	18.3
Cd	-0.1	-0.1	-0.2	-0.1	-0.1	-0.2
Co	0.0	0.0	0.0	0.1	0.1	0.1
Cr	3.5	3.5	3.5	2.6	2.5	2.4
Cu	-0.1	-0.1	-0.1	-0.3	-0.2	-0.3
Fe	17.2	16.6	16.8	41.9	40.3	42.9
Hg	5.7	3.5	2.7	2.0	1.9	2.0
K	2.5	3.1	1.7	25.3	23.9	29.0
Li	0.4	0.4	0.4	0.6	0.6	0.6
Mg	2.9	2.9	2.8	3.6	3.6	3.9
Mn	4.7	4.6	4.6	6.0	6.0	6.0
Mo	0.8	0.6	0.6	0.7	0.7	0.7
Na	39,664.6	40,239.4	40,129.1	40,444.7	39,712.0	41,353.0
Nb	-0.3	-0.4	-0.3	0.0	-0.2	-0.2
Ni	2.5	2.8	2.6	2.7	2.9	2.9
P	90.8	93.5	94.4	127.1	122.0	132.0
Pb	0.7	0.7	0.7	1.6	0.8	1.4
Se	-2.7	-3.2	-2.3	-3.3	-0.3	2.4
Si	6,901.4	6,590.8	6,589.9	14,352.3	13,396.8	14,535.4
Sr	2.6	2.7	2.7	1.5	1.4	1.5
Th	-0.2	-0.3	-0.2	-0.5	0.0	-0.2
Ti	1.3	1.2	1.2	4.9	4.7	5.0
U	0.4	-12.0	-7.7	-4.5	-8.0	-12.0
V	5.3	5.6	5.5	6.6	6.5	6.9
Y	0.0	0.0	0.0	0.0	0.0	0.0
Zn	0.4	0.4	0.4	1.3	1.1	1.3
Zr	0.4	0.4	0.3	0.5	0.6	0.6

Elemental concentrations in clear solution after fly ash sonication (ppm)						
Element	**15 min**			**20 min**		
	Run 1	Run 2	Run 3	Run 1	Run 2	Run 3
Al	1,980.3	1,994.4	1,802.7	1,579.5	1,620.9	1,675.3
As	0.9	0.8	0.4	1.8	1.6	0.5
B	17.1	16.9	16.5	15.5	15.0	14.9
Ba	-0.1	-0.1	-0.1	-0.2	-0.4	-0.4
Be	0.2	0.2	0.2	0.3	0.3	0.3
Ca	14.0	13.9	14.2	4.6	9.0	8.6
Cd	-0.1	-0.1	-0.1	-0.1	-0.1	-0.1
Co	0.4	0.3	0.4	0.5	0.5	0.5
Cr	2.5	2.5	2.4	-1.3	0.8	0.5
Cu	-0.3	-0.2	-0.2	-0.4	-0.2	-0.2
Fe	54.3	55.3	56.5	33.7	39.4	40.4
Hg	1.7	1.3	1.5	0.8	1.0	0.7
K	88.4	92.2	91.8	197.4	205.2	214.3
Li	1.3	1.3	1.3	2.0	2.1	2.2
Mg	5.2	5.3	5.5	5.6	5.7	6.0
Mn	5.6	5.7	5.6	4.0	4.2	4.2
Mo	0.6	0.7	0.7	0.5	0.6	0.6
Na	40,924.2	41,132.0	41,530.5	40,652.5	41,115.6	41,720.3
Nb	0.2	0.5	0.3	0.7	0.8	0.8
Ni	2.9	3.0	2.9	-0.3	1.5	1.2
P	163.8	168.7	170.7	184.4	185.7	195.4
Pb	2.8	3.0	2.6	3.9	3.8	3.8
Se	-1.6	-0.2	0.6	-2.9	2.1	-1.9
Si	14,056.2	14,085.2	14,146.5	13,928.5	14,163.9	13,519.1
Sr	0.6	0.6	0.6	0.3	0.4	0.4
Th	0.3	-0.7	-0.6	0.2	0.0	-0.5
Ti	7.8	8.0	8.1	10.8	10.7	11.3
U	-12.7	-3.0	-14.1	8.8	-19.9	-1.3
V	8.0	8.2	8.4	9.1	9.1	9.6
Y	0.0	0.0	0.0	0.0	0.0	0.0
Zn	2.6	2.8	2.8	3.2	3.8	3.9
Zr	0.7	0.7	0.8	0.6	0.7	1.0

Elemental concentrations in clear solution after fly ash sonication (ppm)						
Element	**25 min**			**30 min**		
	Run 1	Run 2	Run 3	Run 1	Run 2	Run 3
Al	1,914.7	2,036.0	1,994.3	1,900.6	1,992.2	1,969.7
As	1.5	1.7	1.6	0.9	1.5	1.6
B	14.5	14.4	13.5	8.5	9.7	9.5
Ba	-0.3	-0.3	-0.3	-0.6	-0.7	-0.6
Be	0.3	0.3	0.3	0.2	0.2	0.2
Ca	14.8	5.1	4.8	4.4	4.1	4.3
Cd	-0.1	-0.1	-0.1	-0.1	-0.1	-0.1
Co	0.4	0.6	0.6	0.4	0.4	0.4
Cr	-1.3	-1.3	-1.3	-1.3	-1.3	-1.3
Cu	0.8	-0.3	-0.2	-0.1	-0.3	-0.3
Fe	30.0	31.4	30.6	21.5	22.5	21.7
Hg	0.9	0.7	0.9	0.6	0.2	0.5
K	284.6	302.4	295.9	348.9	367.1	356.2
Li	2.6	2.7	2.7	2.8	2.9	2.8
Mg	6.5	6.2	6.2	4.8	4.9	5.0
Mn	3.7	3.7	3.7	3.3	3.3	3.3
Mo	0.4	0.4	0.5	0.3	0.4	0.4
Na	40,626.5	41,647.6	40,977.4	39,458.0	40,722.2	39,973.3
Nb	1.4	1.3	1.4	1.3	1.4	1.4
Ni	0.6	0.3	0.6	0.2	-0.1	0.4
P	198.1	210.3	207.4	184.1	193.9	187.9
Pb	4.5	4.5	4.9	4.4	4.4	4.3
Se	-3.7	0.0	-0.6	-0.2	1.2	0.3
Si	12,595.1	13,317.8	12,974.9	14,657.4	12,727.3	13,832.9
Sr	0.3	0.3	0.3	0.2	0.2	0.2
Th	-0.3	-0.3	-0.2	0.0	-1.2	-0.6
Ti	14.9	15.5	15.2	15.1	15.7	15.2
U	-2.6	-7.1	-14.4	-34.9	-17.8	-14.2
V	9.9	10.4	10.4	10.0	10.4	10.1
Y	0.0	0.0	0.0	0.0	0.0	0.0
Zn	5.0	4.4	4.4	4.7	4.8	4.6
Zr	1.2	0.7	0.8	1.8	1.8	2.3

Appendix C: Mechanical drawings of principal bench scale reactor design

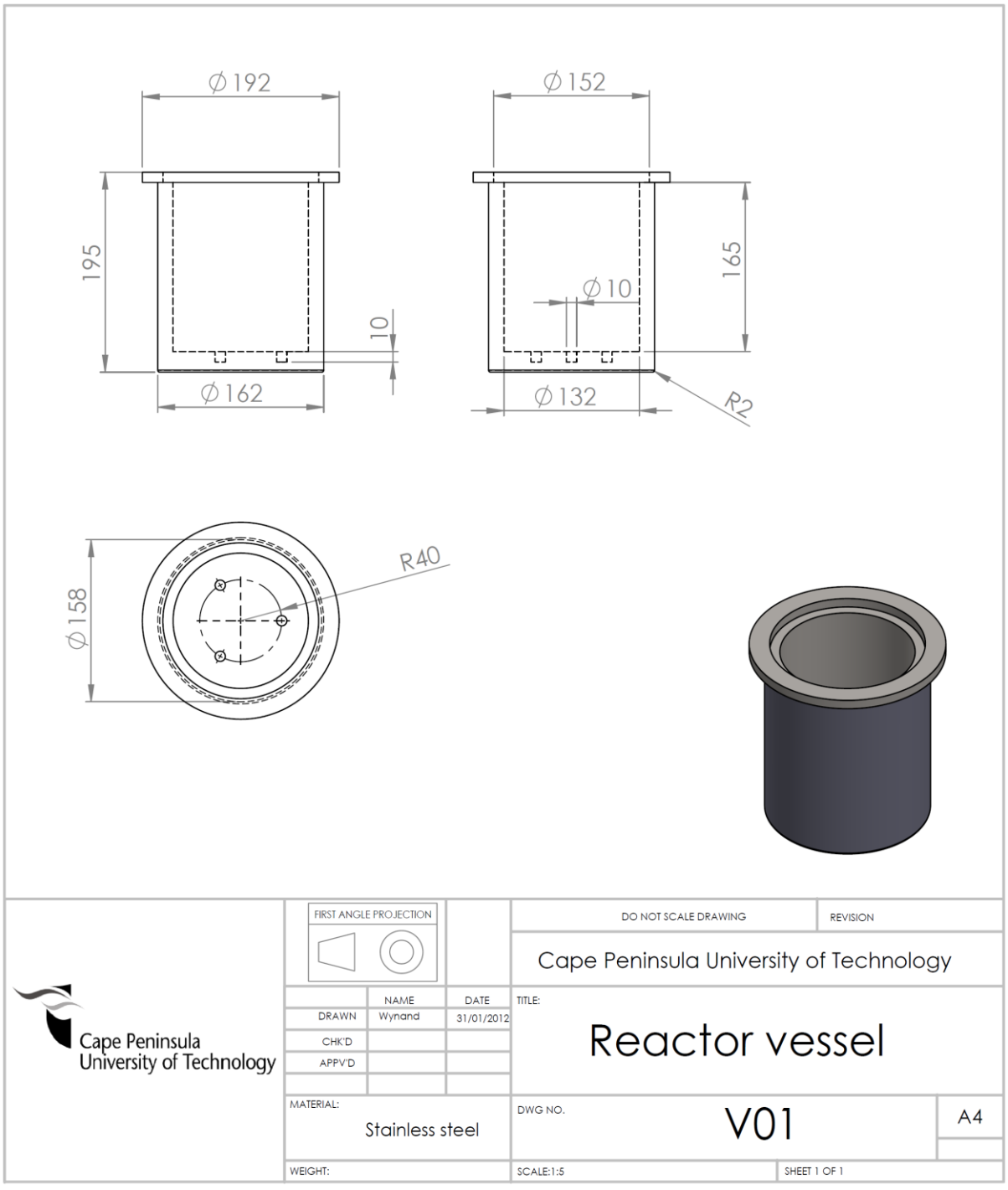

Figure C- 1: Mechanical detailed drawing of bench scale reactor vessel.

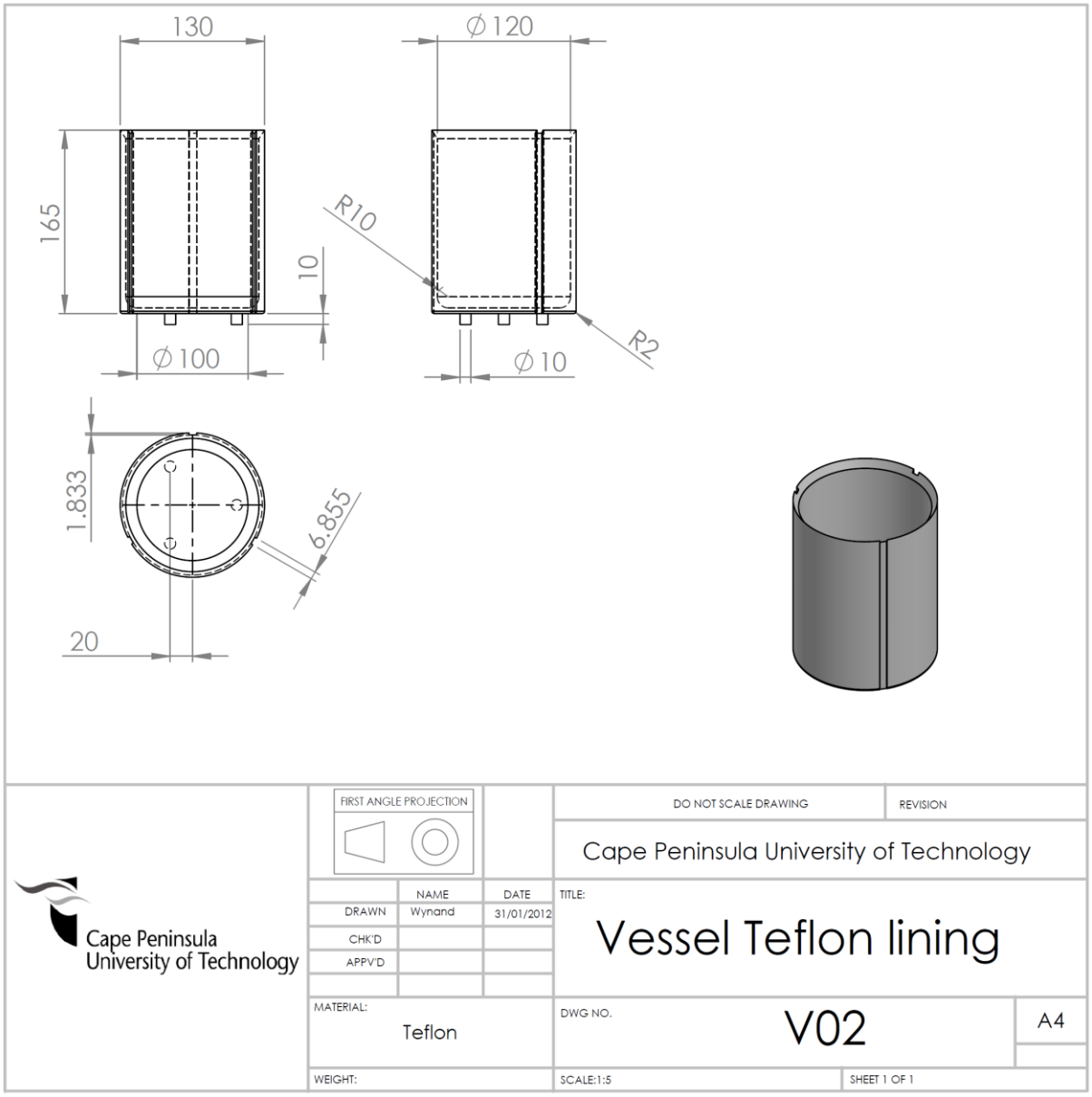

Figure C- 2: Mechanical detailed drawing of bench scale reactor Teflon lining.

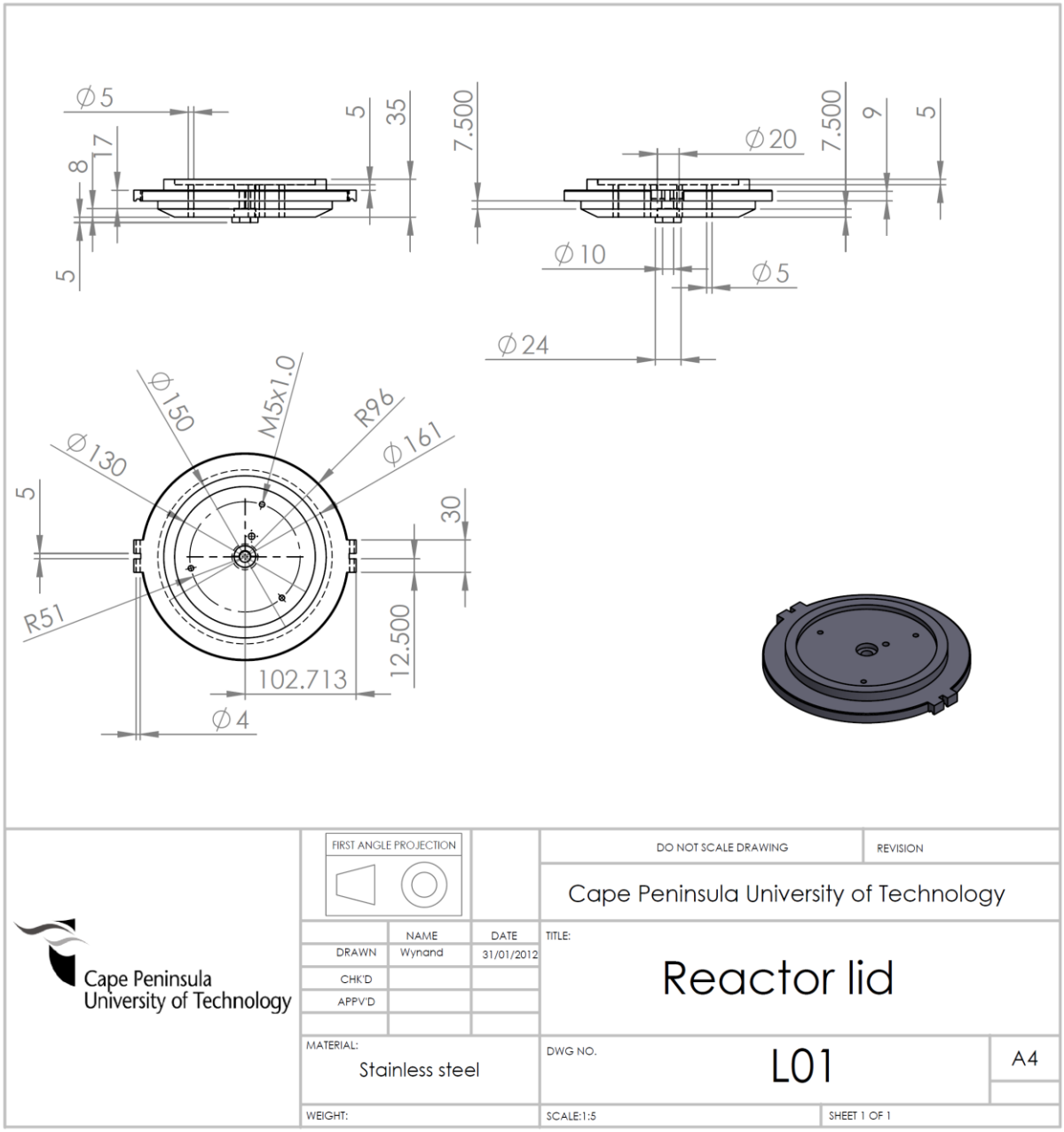

Figure C- 3: Mechanical detailed drawing of bench scale reactor lid.

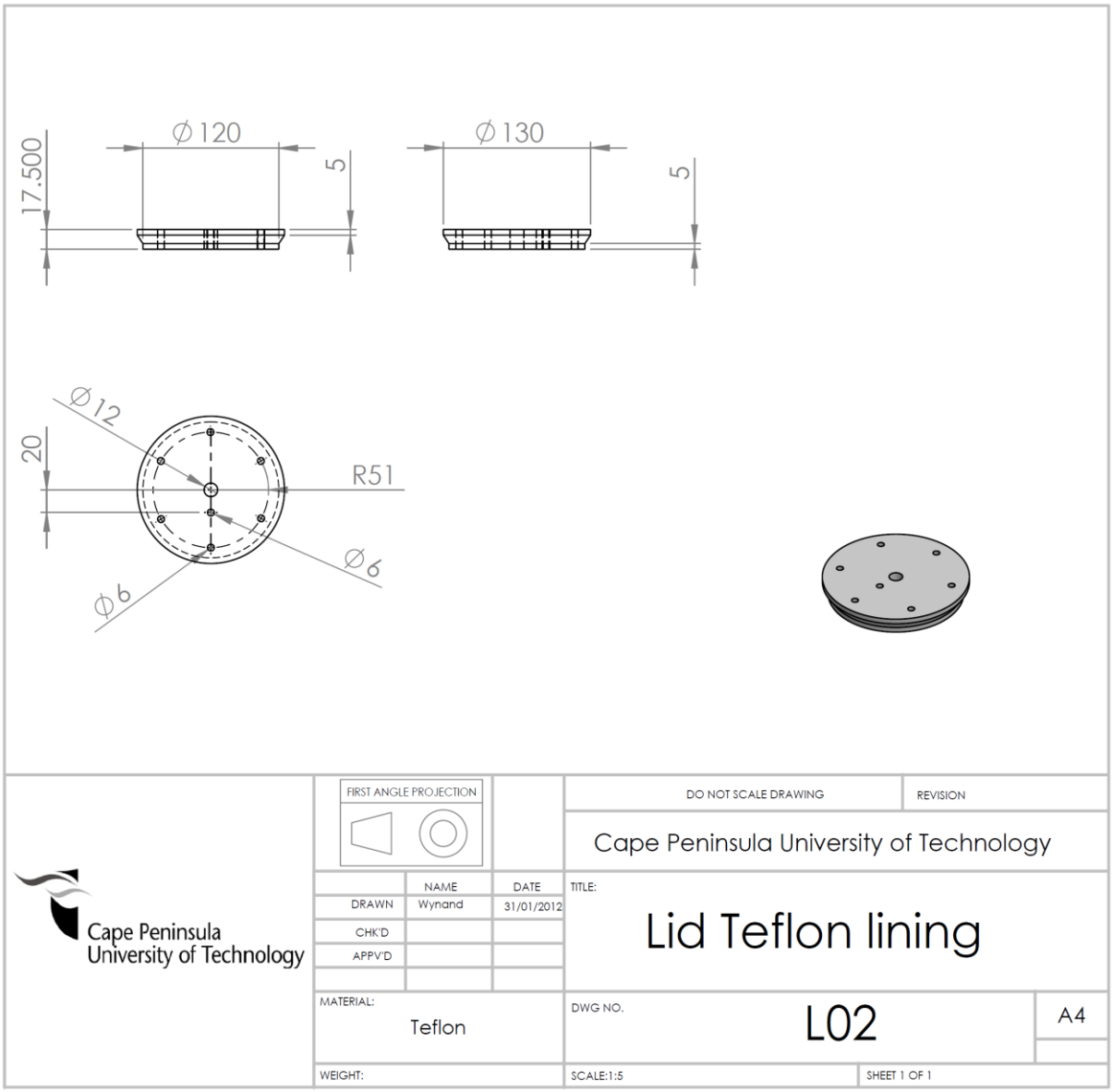

Figure C- 4: Mechanical detailed drawing of bench scale reactor lid Teflon lining.